Coordination Chemistry Reviews, 114 (1992) 107–167
Elsevier Science Publishers B.V., Amsterdam

Coordination chemistry of soluble metal oxides of molybdenum and vanadium

Qin Chen and Jon Zubieta[1]
Department of Chemistry, Syracuse University, Syracuse, NY13244-4100 (USA)

(Received 11 April 1991)

CONTENTS

A. INTRODUCTION AND SCOPE OF THE REVIEW

Oxides are known for all the elements of the periodic table except the lighter noble gases. Furthermore, most elements form more than one binary compound with oxygen [1]. Structural classifications of oxides span the range from discrete binuclear molecular species to polymeric species, exhibiting chain, layer, and three-dimensional network structures. The metal oxides adopt complex structures of the latter type whose chemistry on the molecular level is difficult to characterize. Yet transition metal oxides constitute an important class of heterogeneous catalysts which display a remarkable variety of behavior toward organic substrate molecules [2]. Metal oxide catalysts are effective in transformations as diverse as partial oxidation of methanol, selective hydrocarbon oxidations, olefin metathesis, and ammoxidation [3].

Since solid metal oxide catalysts are of such significant practical importance and yet are notoriously difficult to characterize with respect to surface-bound intermediates, there is considerable interest in the chemistry of soluble metal oxides, or polyoxometalates [4], with simple organic subunits, such as carboxyl, carbonyl, alkoxy and organonitrogen groups. Many of the early transition elements form large polynuclear metal-oxoanions, $M_xO_y^{n-}$, where M = V(V), Nb(V), Ta(V), Mo(VI) or W(VI), which contain up to 200 atoms or more. The unusually large size of the early transition metal polyoxoanions places their solution chemistry in a region intermedi-

---

[1] To whom correspondence should be addressed.

0010-8545/92/$15.00

ate between small molecule chemistry and infinite lattice solid-state chemistry [5]. More significantly, the structural and bonding properties of the polyoxoanions suggest that these species may be described as fragments of the solid lattice structures.

Although these polyoxoanions have been investigated for more than a century, their coordination chemistry with simple organic ligands has received significant attention only in the last decade. This renewed interest in the chemistry of polyoxometalates is a consequence, in large measure, of the development of reactive polyoxometalate precursors soluble in organic solvents suited to coordination of organic ligands, a viewpoint most elegantly presented by Day and Klemperer in their seminal publication of 1985 [5]. Although polyoxometalates containing covalently attached organic groups were reported by Miolati in 1908 [6] and by Rosenheim and Bilecki in 1913 [7], the structures of these complexes were not established until quite recently. Furthermore, as illustrated by Table 1, the coordination chemistry of polyoxometalates was represented by a handful of examples prior to the 1985 publication of Day and Klemperer. The significant growth in the coordination chemistry of polyoxometalates since 1985 is amply demonstrated by Table 2, which does not claim to be an exhaustive compilation of polyoxometalate coordination compounds.

For the purposes of this review, the scope of the discussion has been limited generally to complexes of polyoxomolybdates and polyoxovanadates with simple organic ligands. Complexes containing polyoxometalates supporting organometallic subunits, whether of the transition metal or main group types, have been excluded, as has the vast literature on heteropolyoxoanions [4]. We have also chosen not to discuss complexes of nuclearity less than three or species with trinuclear cores which possess reduced metal sites and fewer oxo-groups than metal centers, such as the triangular Mo(IV) and V(III) carboxylate clusters.

B. STRUCTURAL CHEMISTRY OF POLYOXOMOLYBDATE COORDINATION COMPLEXES

(i) General considerations

As pointed out by Pope [4], the formation of polyoxoanions depends both on the appropriate relationship of coulombic factors of ionic radius and charge and on

TABLE 1

Polyoxomolybdate coordination complexes structurally characterized prior to 1985

Complex	Ref.
$[Mo_8O_{28}(HCO)_2]^{6-}$	8
$[CH_2Mo_4O_{15}H]^{3-}$	9
$[M_8O_{26}(C_5H_5N)_2]^{4-}$	10
$[Mo_8O_{24}(OCH_3)_4]^{4-}$	11

TABLE 2

Polyoxomolybdate and polyoxovanadate coordination complexes

Complex	Organic ligand(s)	Ref.
1 Polyoxomolybdates		
(a) Trinuclear core		
$[Mo_3O_8(OCH_3)(C_4O_4)_2]^{3-}$	$^-OCH_3$, $C_4O_4^{2-}$	12
$[Mo_3O_8(\text{pinacolate})_2]^{2-}$	$^-OC(Me_2)C(Me_2)O^-$	13
$[Mo_3O_7\{RC(CH_2O)_3\}_2]^{2-}$	$RC(CH_2O)_3^{3-}$	14
$[Mo_3O_6(OCH_3)\{RC(CH_2O)_3\}_2]^-$	$^-OCH_3$, $RC(CH_2O)_3^{3-}$	14
$[Mo_3O_9(DMSO)_4]$	$(CH_3)_2SO$	15
(b) Tetranuclear core		
$[Mo_4O_{10}(OCH_3)_6]^{2-}$	$^-OCH_3$	16,17
$[Mo_4O_{10}Cl_2(OCH_3)_4]^{2-}$	$^-OCH_3$	16,17
$[Mo_4O_{10}(C_6H_2O_4)_2]^{3-}$	$C_6H_2O_4^{3-}$	18,19
$[Mo_4O_8(OC_2H_5)_2\{RC(CH_2O)_3\}_2]$	$^-OC_2H_5$, $RC(CH_2O)_3^{3-}$	20
$[Mo_4O_{10}(OCH_3)_4(OC_6H_4O)_2]^{2-}$	$^-OCH_3$ catecholate	17
$[Mo_4O_8(OCH_3)_2(HOCH_3)_2Cl_4]^{2-}$	$^-OCH_3$, $HOCH_3$	17
$[Mo_4O_8(OC_2H_5)_2(HOC_2H_5)_2Cl_4]^{2-}$	$^-OC_2H_5$, HOC_2H_5	21
$[Mo_4O_6(OPr)_4(HOPr)_2Cl_4]$	^-OPr, HOPr	22
$[Mo_4O_8(OPr)_4(py)_4]$	^-OPr, C_5H_5N	23
$[Mo_4O_{11}(LH_2)(LH)(L)]^-$	Benzamidoxime, $CH_3C_6H_4C(NH)NO^{2-}$	24
$[Mo_4O_{12}\{CH_3C(NH_2)NO\}_2]^{2-}$	Acetamidoximate, $CH_3C(NH_2)NO^-$	25
$[Mo_4O_{12}(C_{12}H_{30}N_4S_2)_2]$	$(Me_2NCH_2NHCH_2CH_2S)_2$	26
$[Mo_4O_8(OCH_3)_2(NNPh)_4]^{2-}$	$^-OCH_3$, $-NNC_6H_5$	27,28
$[Mo_4O_6(OCH_3)_2(O_2C_6H_4)_2$-$(NNPh)_4]^{2-}$	$^-OCH_3$, $-NNC_6H_5$, $(O_2C_6H_4)^{2-}$	29,30
$[Mo_4O_{11}(dhphH_2)]^{2-}$	Dihdrazinophthalazine(4−)	31
$[Mo_4O_{12}(hphH)]^{2-}$	Hydrazinophthalazine(2−)	32
$[Mo_4O_{10}(OCH_3)_2(NNR_2)_2]^{2-}$	$^-OCH_3$, $-NNMePh$	33
$[Mo_4O_{11}(\text{malate})_2]^{2-}$	$\{O_2CCH_2CH(OH)CO_2\}^{2-}$	34,35
$[Mo_4O_{11}(\text{citrate})_2]^{4-}$	$\{O_2CCH_2C(OH)(CO_2)CH_2CO_2\}^{3-}$	36,37
$[Mo_4O_6Cl_2(O_2CR)_6]$	RCO_2^-	38,39
$[Mo_4O_{10}(OCH_3)_2(C_6H_4CONO)_2]^{2-}$	$^-OCH_3$, $C_6H_4CONO^{2-}$	40
$[Mo_4O_{10}(OCH_3)_2(NNPh)_2]^{2-}$	$^-OCH_3$, $-NNC_6H_5$	41
$[CH_2Mo_4O_{15}H]^{3-}$	$H_2CO_2^{2-}$	9
$[(HCCH)Mo_4O_{15}X]^{3-}$	$(O_2CHCHO_2)^{4-}$	42
$[(C_9H_4O)Mo_4O_{15}(OCH_3)]^{3-}$	$^-OCH_3$, $(C_9H_4O_4)^{4-}$	43
$[(C_{14}H_{10})Mo_4O_{15}(C_6H_5CO_2)]^{3-}$	$(C_{14}H_{10}O_4)^{4-}$, $C_6H_5CO_2^-$	43
$[(C_{14}H_8)Mo_4O_{15}(OH)]^{3-}$	$(C_{14}H_8O_4)^{4-}$	43
$[Mo_4O_8(OCH_3)_2(C_4O_4)_2$-$(C_4O_4H)_2]^{4-}$	$^-OCH_3$, $C_4O_4^{2-}$, $HC_4O_4^-$	44
$[Mo_4O_6(OH)_4(CO_3)(CO)_2(PMe_3)_6]$	CO_3^{2-}, CO, PMe_3	45
$[Mo_4O_6(SCH_2CH_2O)_5]^{2-}$	$(SCH_2CH_2O)^{2-}$	46
$[Mo_4O_4\{HB(pz)_3\}_2(HOCH_3)_2(OCH_3)_2]$	$^-OCH_3$, $-HOCH_3$, pyrazoylborate	47

TABLE 2 (*continued*)

Complex	Organic ligand(s)	Ref.
(c) Pentanuclear core		
$[Mo_5O_{16}(OCH_3)]^{3-}$	$^{-}OCH_3$	12
$[Mo_5Na(NO)O_{13}(OCH_3)_4]^{2-}$	$^{-}OCH_3$, NO	48
(d) Hexanuclear core		
$[Mo_6O_{18}(NNPh)]^{3-}$	$^{-}NNC_6H_5$	49
$[Mo_6O_{18}(NNMePh)]^{2-}$	$^{-}NNMePh$	50
$[Mo_6O_{18}(NO)]^{3-}$	$-NO$	48
$[Mo_6O_{10}(OPr)_{12}]$	^{-}OPr	51
(e) Octanuclear core		
$[(HCO)_2Mo_8O_{26}]^{6-}$	HCO_2^-	8
$[Mo_8O_{26}(py)_2]^{4-}$	C_5H_5N	10
$[Mo_8O_{26}(NCS)_2]^{4-}$	NCS^-	52
$[Mo_8O_{24}(OH)_4(sal)_2]^{2-}$	$PrN{=}CHC_6H_4O^-$	53
$[Mo_8O_{24}(OH)_2(met)_2]^{4-}$	$CH_3SCH_2CH_2CH(NH_2)CO_2^-$	53
$[Mo_8O_{24}(OCH_3)_4]^{4-}$	$^{-}OCH_3$	11
$[Mo_8O_{20}(OCH_3)_4\{RC(CH_2O)_3\}_2]^{2-}$	$^{-}OCH_3$, $RC(CH_2O)_3^{3-}$	54
$[Mo_8O_{20}(NNPh)_6]^{4-}$	$^{-}OCH_3$, $-NNC_6H_5$	55,56
$[Mo_8O_{16}(OCH_3)_6(NNMePh)_6]^{2-}$	$^{-}OCH_3$, $-NNC_6H_5$	33
$[H_2Mo_8O_{24}(OCH_3)_2]^{4-}$	$^{-}OCH_3$	57
$[Mg_2Mo_8O_{22}(OCH_3)_6(HOCH_3)_4]^{2-}$	$^{-}OCH_3$, $HOCH_3$	58
$[Mo_8O_{12}(OCH_3)_4(SCH_2CH_2O)_8]^{4-}$	$^{-}OCH_3$, $(SCH_2CH_2O)^{2-}$	59
$[Mo_8O_{16}(OCH_3)_8(C_2O_4)]^{2-}$	$^{-}OCH_3$, $C_2O_4^{2-}$	60
$[Mo_8O_{16}(OCH_3)_8(PR_3)_4]$	$^{-}OCH_3$, PR_3	61
(f) Decanuclear and dodecanuclear cores		
$[Mo_{10}O_{28}(SCH_2CH_2O)_2(HOCH_3)_2]^{4-}$	$HOCH_3$, $(SCH_2CH_2O)^{2-}$	46
$[Mo_{10}O_{24}(OMe)_7(NO)]^{2-}$	^{-}OMe, $-NO$	
$[Mo_{12}O_{36}(C_4O_4H)_4]^{4-}$	$HC_4O_4^-$	62
2 Polyoxovanadates		
(a) Trinuclear core		
$[VO(sal)(CH_3OH)]_3$	CH_3OH, salicylhydroximate	63
$[V_3O_3(THF)(C_6H_5CO_2)_6]$	THF, $C_6H_5CO_2^-$	64
(b) Tetranuclear and pentanuclear cores		
$[V_4O_8(NO_3)(\text{thiophene-2-carboxylate})_4]^{2-}$	Thiophene-2-carboxylate	65
$[V_4O_8(C_2O_4)_4(H_2O)_2]^{4-}$	$C_2O_4^{2-}$	66
$[V_5O_9Cl(\text{thiophene-2-carboxylate})_4]^{4-}$	Thiophene-2-carboxylate	65

(c) Hexanuclear core		
$[V_6O_{10}(PhCO_2)_9]$	$C_6H_5CO_2^-$	67
$[V_6O_{13}\{RC(CH_2O)_3\}_2]^{2-}$	$RC(CH_2O)_3^{3-}$	68
$[V_6O_9(OH)_4\{RC(CH_2O)_3\}_2]^{2-}$	$RC(CH_2O)_3^{3-}$	69
$[V_6O_7(OH)_6\{RC(CH_2O)_3\}_2]^{2-}$	$RC(CH_2O)_3^{3-}$	69
(d) Octanuclear to quindecanuclear cores		
$[V_8O_8(OCH_3)_{16}(C_2O_4)]^{2-}$	$^-OCH_3$, $C_2O_4^{2-}$	70
$[V_9O_{16}(bdta)_4]^{7-}$	Butanediaminetetraacetate	71
$[V_{10}O_{13}\{CH_3C(CH_2O)_3\}_5]^-$	$CH_3C(CH_2O)_3^-$	
$[V_{12}O_{32}(CH_3CN)]^{4-}$	CH_3CN	72
$[V_{15}O_{36}(CO_3)]^{7-}$	CO_3^{2-}	73

the accessibility of empty d orbitals for metal–oxygen bonding. Polyanion structures can often be represented as clusters of edge-shearing MO_6 octahedra in which the metal ions are displaced as a consequence of M—O π-bonding toward the vertices at the surface of the structure [74]. In addition, it has been noted that polyanion structures that contain three or more terminal oxo-groups are not observed [75], a restriction which has been explained in terms of the strong trans influence of terminal M—O bonds facilitating dissociation of the cluster [4]. This restriction, the "Lipscomb principle," is not absolute in the case of polyoxoanion coordination complexes where ligand influences often modify the general principles associated with the underivatized or parent polyoxometalates.

The fundamental structural motif for polyoxomolybdate structures is the pair of edge-sharing octahedra, illustrated in Fig. 1. No simple polymolybdate anion with the $[Mo_2O_{10}]$ core has been identified, as this clearly violates the Lipscomb restriction. However, several examples of coordination complexes with this core have been identified [76,77], and a representative structure is illustrated in Fig. 2. The shapes of polyanions can be predicted by adding additional octahedra in an edge-sharing fashion to this structural motif. Thus, a third octahedron may be added in any of

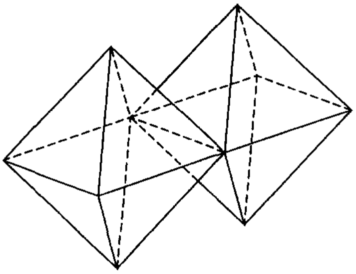

Fig. 1. Polyhedral representation of two edge-sharing octahedra producing the type II core.

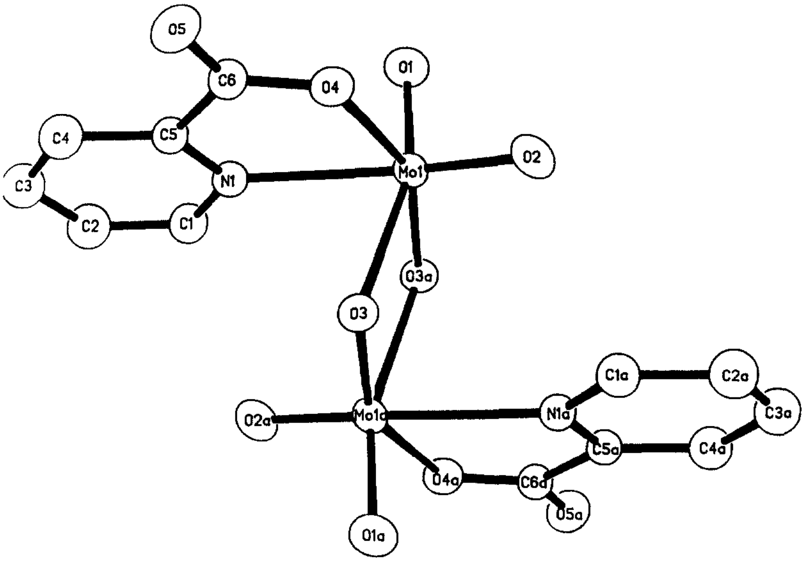

Fig. 2. The structure of $[Mo_2O_6(\text{pyridinecarboxylate})_2]^{2-}$.

four ways to generate possible trinuclear core structures, as illustrated in Fig. 3. In coulombic terms, structure **IIIa** is the most favorable; it is also the most compact.

In fact, further expansion of the aggregates may be accomplished by the "rule of compactness" [78], which requires that each octahedron share two edges on the same face. The polynuclear structures illustrated in Fig. 4 are constructed by following this principle [79]. Of these potential structural prototypes, only the hexanuclear and the octanuclear structures have been structurally characterized for the underivatized polyoxomolybdates. In non-aqueous solvents, $[Mo_6O_{19}]^{2-}$ [80] and β-$[Mo_8O_{26}]^{4-}$ [81] may be isolated, while the heptamolybdate $[Mo_7O_{24}]^{6-}$ [82] has been confirmed as the predominant species in aqueous solution at pH 3–5.5. The tetranuclear core **IVa** is known only in the solid phase $Li_{14}(WO_4)_3\ W_4O_{16}\cdot 4H_2O$ [83]. However, the introduction of common organic ligands expands the structural chemistry of the polyoxomolybdates to include not only the prototypes shown in Figs. 3 and 4 but a variety of novel geometries constructed from corner-sharing and face-sharing of octahedra, in addition to the more common edge-sharing, and from tetrahedral and square-pyramidal units, as well as the more common octahedral motifs.

(ii) Brief survey of the structural chemistry of polyoxomolybdate coordination complexes

(a) Trinuclear species

Although the trinuclear core **IIIa** is a constituent of numerous polyoxometalates such as $[PMo_{12}O_{40}]^{3-}$, the isolated core has been identified only recently. The

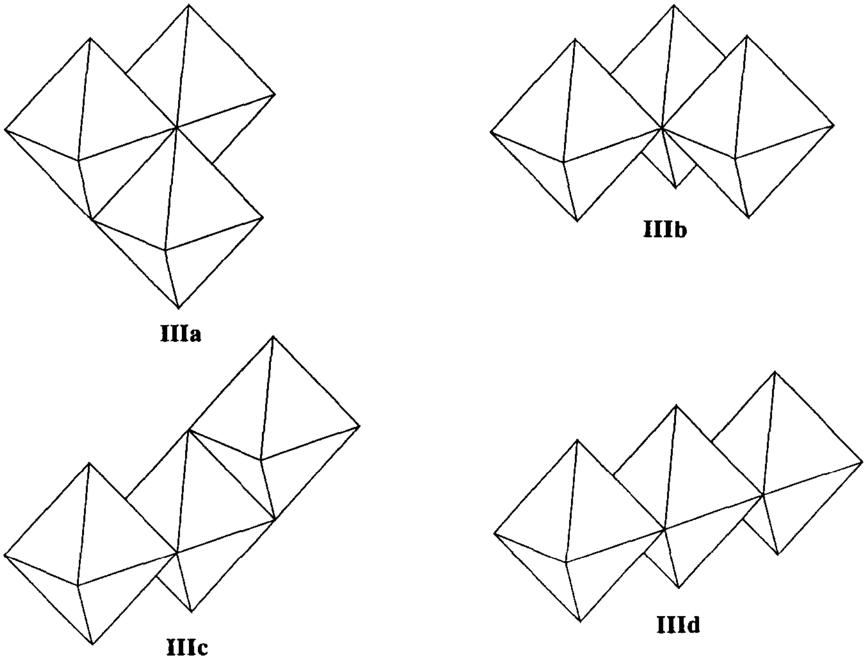

Fig. 3. Four ways of constructing a trinuclear core from three edge-sharing octahedra.

squarate complex $[Mo_3O_8(OCH_3)(C_4O_4)_2]^{3-}$, shown in Fig. 5, may be synthesized from $[Mo_5O_{16}(OCH_3)]^{3-}$ by direct displacement of two $[MoO_4]^{2-}$ units by the squarate ligands [12]. The trinuclear core $[Mo_3O_8(OCH_3)]^+$ is reminiscent of the general class of oxo-capped Mo(IV) triangulo clusters [84,85] but with an expanded $[Mo_3O]$ central fragment to accommodate the oxidized Mo(VI) centers.

While the squarate ligand effects direct displacement of $[MoO_4]^{2-}$ groups with concomitant retention of the central triangular core, reaction of $[Mo_5O_{16}(OCH_3)]^{3-}$ with dialcohols results in structural reorganization, as illustrated by the pinacolate derivative $[Mo_3O_8(\text{pinacolate})_2]^{2-}$, which adopts the structural type **IIIc** shown in Fig. 6. While the steric and bonding requirements of the ligand preclude adoption of structure **IIIa**, the most favorable geometry on purely electrostatic considerations, the observed structure is the most favorable of the three remaining prototypes, **IIIb–IIId**.

The influence of ligand geometry on structure is illustrated by the polyoxomolybdate chemistry of the trisalkoxy ligands of the 2-(hydroxymethyl)-2-methyl-1,3-propanediol class, $RC(CH_2OH)_3$, whose chelate geometry requires some degree of bridging of metal centers. The structure of the trinuclear polyoxomolybdate $[Mo_3O_7\{CH_3C(CH_2O)_3\}_2]^{2-}$, shown in Fig. 7, exhibits the triangulo core **IIIa** [14]. Mo(1) and Mo(2) are each bound to two terminal oxo groups and complete their coordination requirements through ligation to bridging and terminal alkoxy groups,

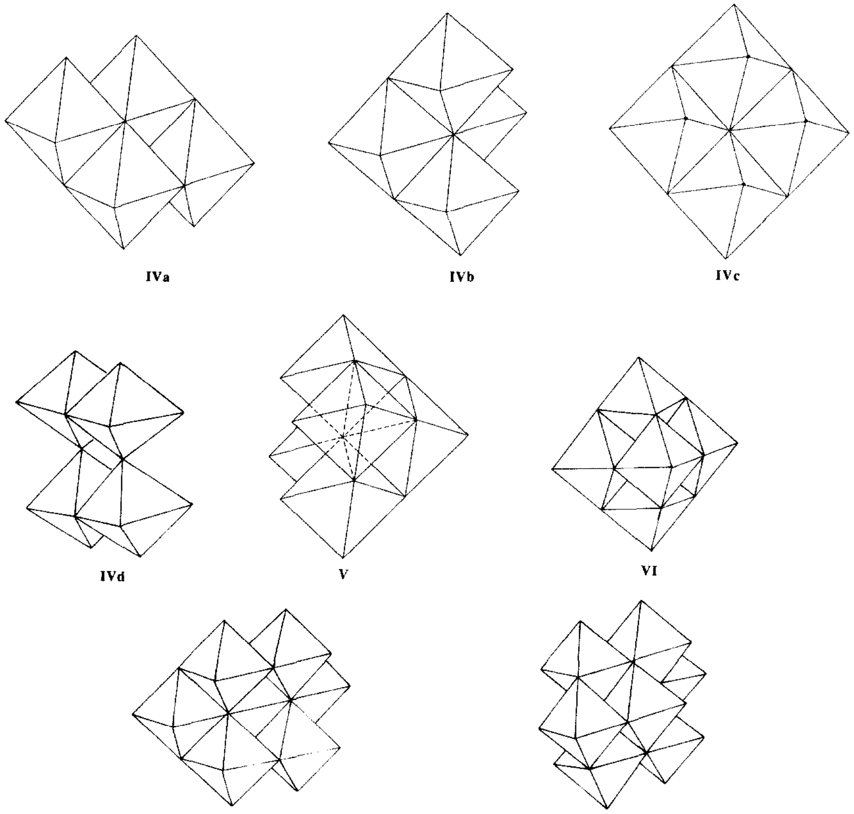

IVa IVb IVc

IVd V VI

VII VIII

Fig. 4. Several possible arrangements of four edge-sharing octahedra (**IVa**–**IVd**). Arrangements of five, six, seven and eight edge-sharing octahedra, **V**–**VIII**, respectively.

while the Mo(3) center coordinates to three bridging alkoxy units and completes its coordination by ligation to three terminal oxo groups, in clear violation of Lipscomb's restriction. As expected, there are relatively few examples of this structural unit, and these are largely limited to mononuclear species which are invariably unstable in solution [86–89] and to the binuclear $[Mo_2O_7]^{2-}$ [90]. When present in polynuclear species, such as $[M_{10}O_{34}]^{8-}$ [91] and $[Mo_8O_{24}(OCH_3)_2]^{4-}$ [57] the $[MoO_3]$ unit is associated with the cluster as part of a corner-sharing $[MoO_4]^{2-}$ tetrahedron and readily dissociates in solution. The terminal oxygen atoms of the *fac*-trioxomolybdate are basic/nucleophilic and provide a site for further reaction, such that $[Mo_3O_6(OCH_3)\{CH_3C(CH_2O)_3\}_2]^-$ may be prepared directly from $[Mo_3O_7\text{-}\{CH_3C(CH_2O)_3\}_2]^{2-}$ by reaction with methanol. The Mo(3) also provides a site for further oligomerization, a feature shared with mononuclear *fac*-trioxo complexes [7].

A trinuclear repeat unit is observed in the structure of the unusual adduct

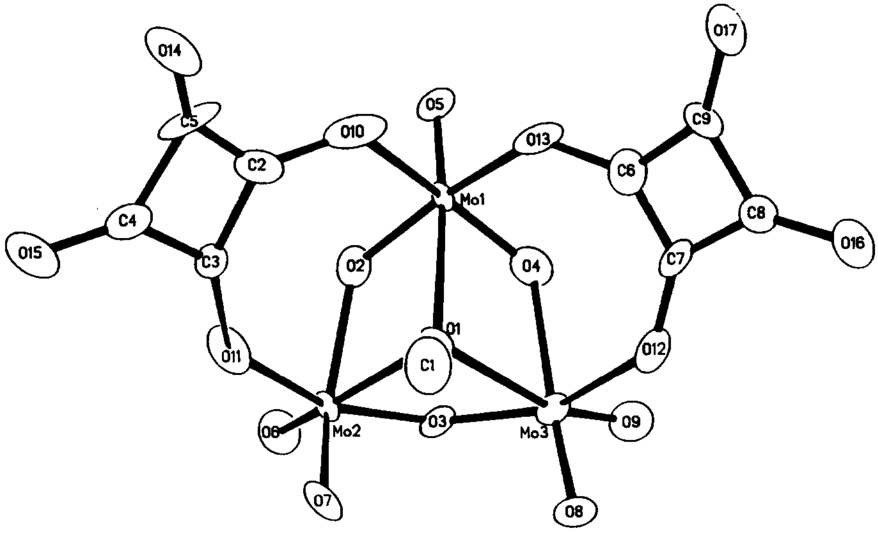

Fig. 5. The structure of $[Mo_3O_8(OCH_3)(C_4O_4)_2]^{3-}$.

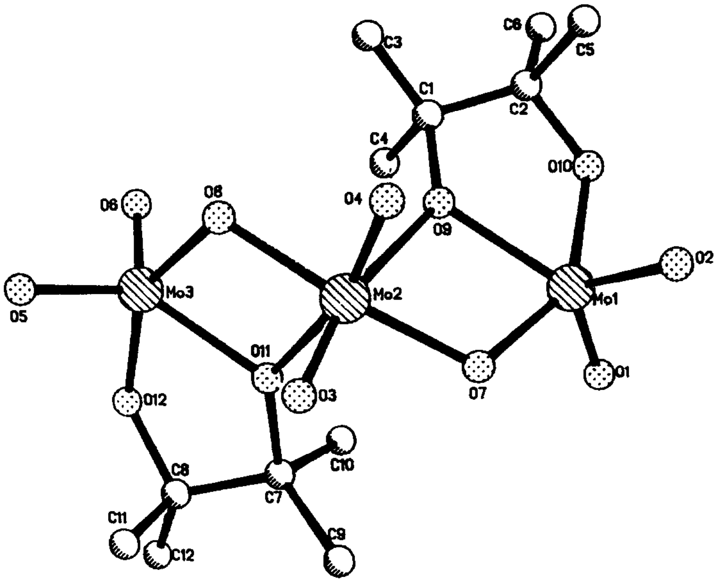

Fig. 6. The structure of $[Mo_3O_8(\text{pinacolate})_2]^{2-}$.

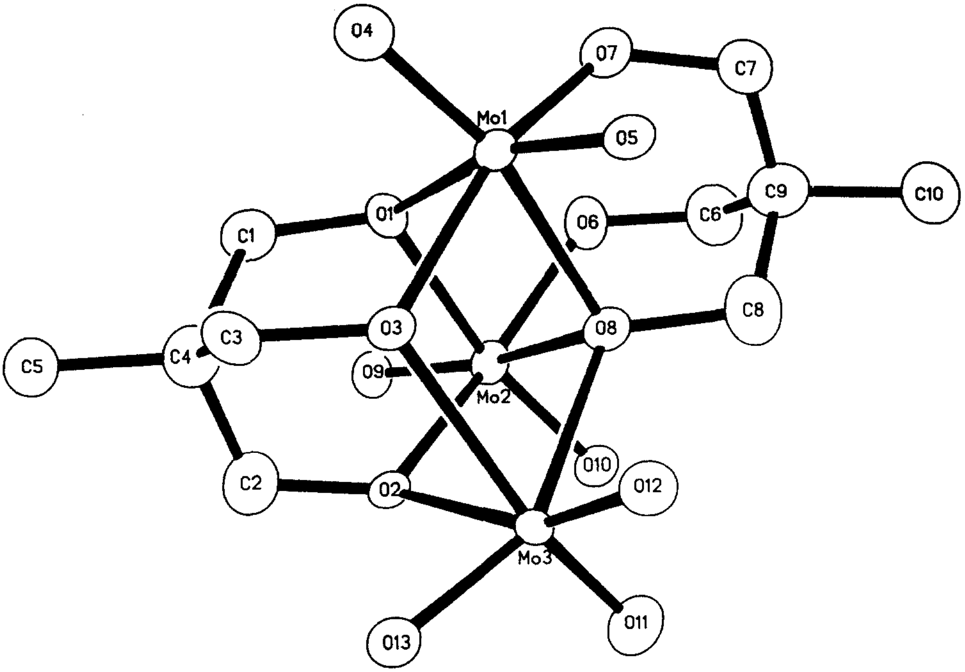

Fig. 7. The structure of $[Mo_3O_7\{CH_3C(CH_2O)_3\}_2]^{2-}$.

$[Mo_3O_9(DMSO)_4]$ [15], illustrated in Fig. 8. The structure consists of infinite chains of both octahedral and tetrahedral Mo sites repeating in a (-oct-tet-oct-oct-tet-oct-)$_n$ motif. The one-dimensional nature of the structure is unique for polyoxomolybdate coordination complexes and is most closely related to the inorganic structures $Na_2Mo_2O_7$ [92] and $K_2Mo_2O_7$ [93], which contain infinite chains of $[MoO_4]$ tetrahedra and $[MoO_6]$ octahedra, albeit in different arrangements.

(b) Tetranuclear species

The tetranuclear unit is by far the most common compositional motif in the coordination chemistry of polyoxomolybdates. The most common arrangement is that adopted by $[Mo_4O_{10}(OMe)_6]^{2-}$ [16,17] with four edge-sharing octahedra in the compact cluster of type **IVa**. As illustrated in Fig. 9, the structure displays two unique molybdenum centers, one displaying $[MoO_2(\mu\text{-}O)(OCH_3)(\mu\text{-}OCH_3)(\mu_3\text{-}OCH_3)]$ coordination and the second $[MoO_2(\mu\text{-}O)(\mu\text{-}OCH_3)(\mu_3\text{-}OCH_3)_2]$ geometry.

The structure illustrates a common feature of the chemistry of polymolybdates in alcoholic solvents: the incorporation of alkoxy groups into the cluster. Formation of the underivatized polyoxomolybdate parent structure, $[Mo_4O_{16}]^{8-}$, is most likely precluded by the high negative charge. Replacement of bridging oxo groups by alkoxy ligands serves to reduce the overall cluster charge and hence to stabilize the

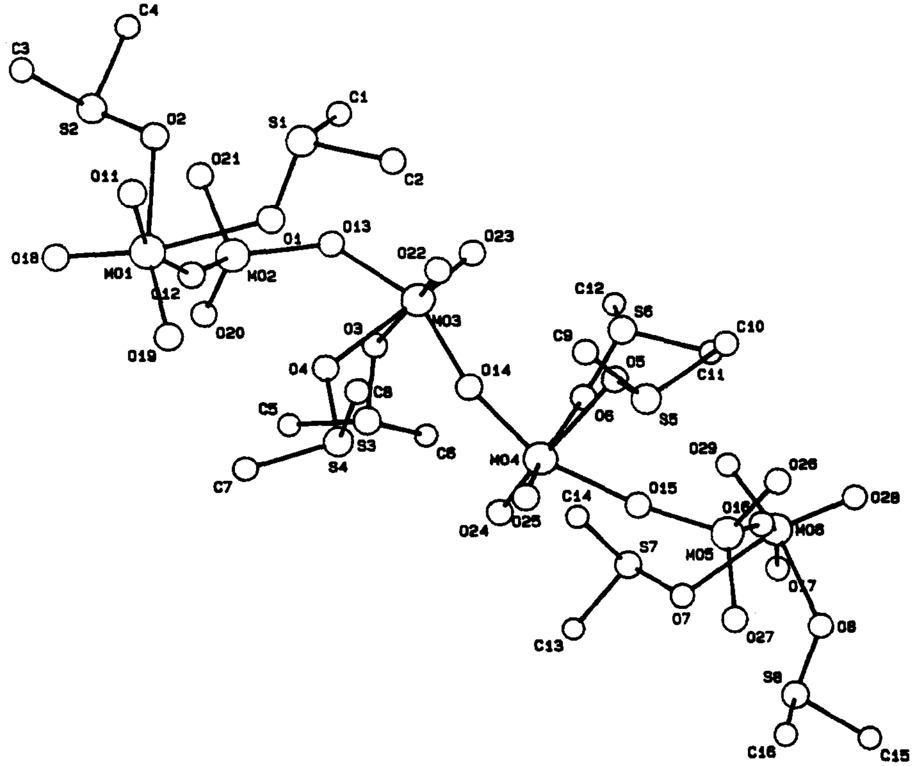

Fig. 8. The structure of $[Mo_3O_9(DMSO)_4]$.

unit in alcoholic solvents. Thus, the same core structure with replacement of peripheral and/or doubly bridging alkoxy groups or oxo groups is common to the structures of $[Mo_4O_{10}(OCH_3)_4Cl_2]^{2-}$ [17], $[Mo_4O_{10}(OCH_3)_2(OC_6H_4O)_2]^{2-}$ [17], $[Mo_4O_8(OC_2H_5)_2\{RC(CH_2O)_3\}_2]$ [20] and $[Mo_4O_{10}(OCH_3)_2(C_6H_4CONO)_2]^{2-}$ [40].

In the presence of appropriate reducing agents, $[Mo_4O_{10}(OCH_3)_4Cl_2]^{2-}$ may be reduced to the Mo(V) cluster $[Mo_4O_8(OCH_3)_2Cl_4(HOCH_3)_2]^{2-}$, which is shown in Fig. 10. While cluster geometry **IVa** is retained, the structural consequences of reduction are manifest in the shortening of the Mo(1)–Mo(2) distance to 2.595(1) Å, a bond length consistent with a significant degree of metal–metal bonding and with distances observed for other Mo(V) d^1 binuclear and tetranuclear species. The complex $[Mo_4O_8(OCH_3)_2Cl_4(HOCH_3)_2]^{2-}$ is a member of a class of reduced oxo-alkoxychloromolybdates structurally related by the tetranuclear core of edge-sharing octahedra $[MoO_5Cl]$, as shown schematically in Fig. 11. Other examples of this structural class include $[Mo_4O_8(OC_2H_5)_2(HOC_2H_5)_2Cl_4]^{2-}$ [21] and $[Mo_4O_6(OPr)_4(HOPr)_2Cl_4]$ [22]. Although both of these latter complexes were originally described as mixed valence Mo(V)/Mo(VI) species, the need to reformulate

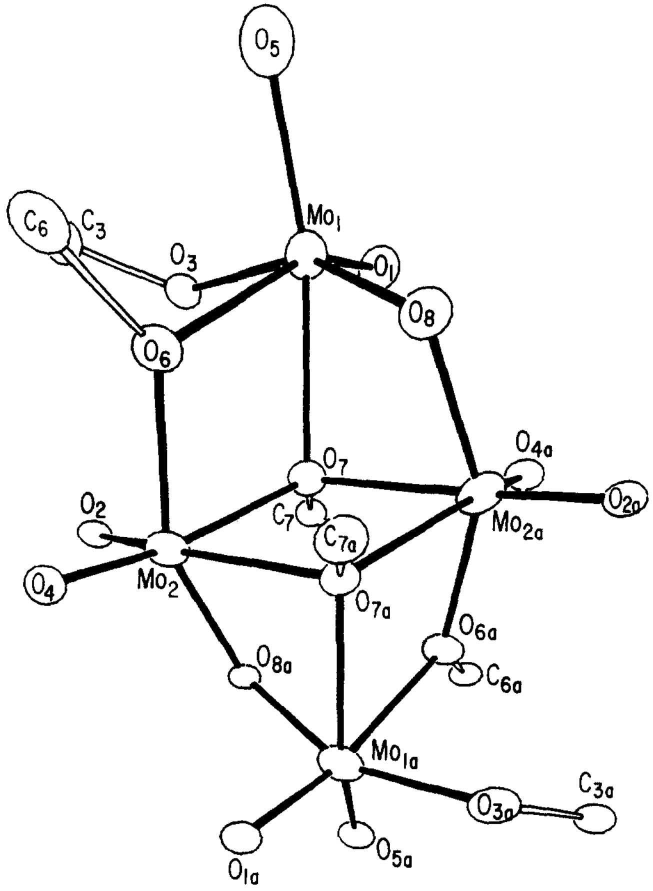

Fig. 9. The structure of $[Mo_4O_{10}(OMe)_6]^{2-}$.

these complexes as Mo(V) species is most convincingly presented by Lincoln and Koch [47]. Each of these structures exhibits a long bond length for the Mo—O bond to the terminally coordinated alcohol ligand (Mo—O > 2.10 Å) which reveals this ligand to be an alcohol, since these distances are far outside the range for terminal alkoxide ligands bound to Mo(V) (1.81–1.98 Å) [94,95].

A characteristic feature of this reduced core is the presence of easily displaced alcohol and chloride ligands as peripheral groups of the cluster. Appropriate ligands may be introduced to substitute for these groups to give clusters which do, however, retain the $[Mo_4O_8(OCH_3)_2]^{2+}$ core. The persistence of this robust unit is illustrated by the structures of the octanuclear Mo(IV)/Mo(V) mixed-valence cluster $[H_2Mo_8O_{24}(OCH_3)_2]^{4-}$ [57] and the squarate complex $[Mo_4O_8(OCH_3)_2(C_4O_4)_2(C_4O_4H)_2]^{4-}$ [44], which are illustrated schematically in Fig. 12.

While tetranuclear compositions are persistent in the structural chemistry of

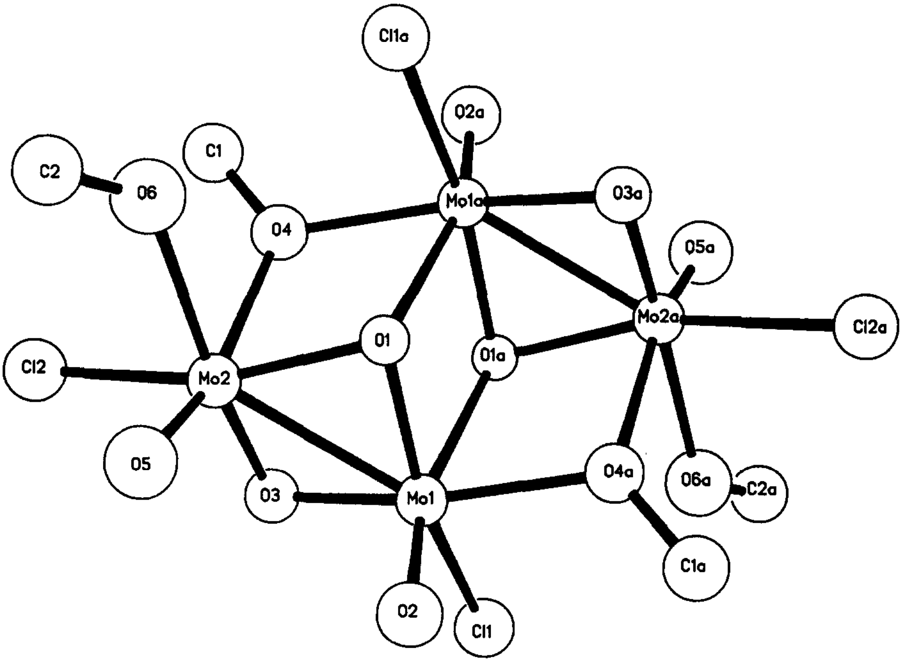

Fig. 10. The structure of $[Mo_4O_8(OCH_3)_2Cl_4(HOCH_3)_2]^{2-}$.

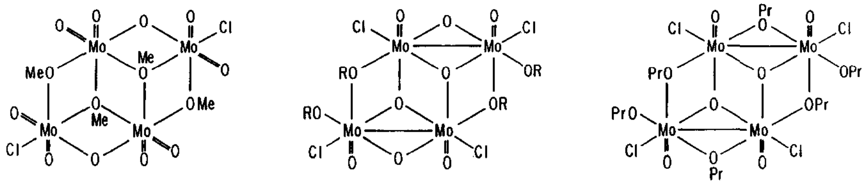

$[Mo_4O_{10}(OMe)_4Cl_2]^{2-}$

$[Mo_4O_8(OR)_4Cl_4]^{2-}$
R= -Me, -Et

$[Mo_4O_6(OPr)_6Cl_4]$

Fig. 11. Shematic representation of the structures of the Mo(VI) cluster $[Mo_4O_{10}(OCH_3)_4Cl_2]^{2-}$ and of the Mo(V) cluster $[Mo_4O_8(OCH_3)_2(HOCH_3)_2Cl_4]^{2-}$, and $[Mo_4O_6(OPr)_4(HOPr)_2Cl_4]$, showing the common tetranuclear core.

polyoxomolybdates, the arrangements of the constituent polyhedra of the clusters exhibit considerable variation. Although structural type **IVa** is the most common arrangement in conformity with "the principle of compactness" [78,79], ligand bonding and geometrical constraints play a critical role in determining the cluster geometry. Just as Lipscomb's principle is violated in coordination complexes of polyoxometalates, so too are a variety of polyhedral connectivities adopted by these

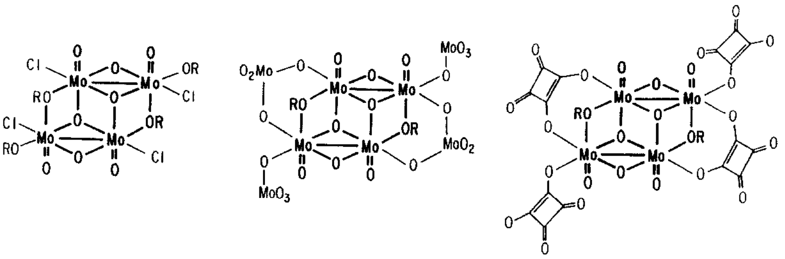

Fig. 12. Schematic representations of the structures of $[H_2Mo_8O_{24}(OCH_3)_4]^{4-}$ and $[Mo_4O_8(OCH_3)_2(C_4O_4)_2(C_4O_4H)_2]^{4-}$.

complexes. While there are approximately 20 ways of combining four edge-sharing octahedra and many more combinations if corner-sharing and face-sharing are considered, relatively few of these structural types have been realized. Several characteristic polyhedral geometries are illustrated in Figs. 13 and 14.

A variety of carbomolybdate clusters have been synthesized by substitutive intramolecular carbonyl insertion [9]. The structural prototype, $[(H_2CO_2)Mo_4O_{12}(OH)]^{3-}$, shown in Fig. 15, adopts a structure which may be viewed as a ring of oxo-bridged *cis*-dioxomolybdate units, $[MoO_2(\mu\text{-}O)]_4$, capped above and below by an acetal and a hydroxide, respectively. Since the OH^- group provides a common vertex, the structure may be described as two pairs of face-sharing octahedra, fused by corner-sharing. The molybdoarsinate complexes $[(R_2As)Mo_4O_{15}H]^{2-}$ [96–98] exhibit an identical core structure.

Since the formation of acetal and ketal derivatives of polyoxomolybdates is quite general, several related structures with different capping ligands have been determined. The structures of the formylated and fluoride derivatives, $[(HCCH)Mo_4O_{15}(HCO_2)]^{3-}$ and $[(HCCH)Mo_4O_{15}F]^{3-}$ [42] are illustrated schematically in Fig. 13. The most pronounced structural consequences of introducing the diacetal moiety on the prototype $[Mo_4O_{12}]^{2+}$ ring structure are the incorporation of one of the bridging oxo groups of the Mo_4O_4 heterocycle into the diacetal linkage with a concomitant increase in the Mo···Mo distances and replacement of the quadruply bridging OH^- group by the doubly bridging F^- or HCO_2^- unit. Consequently, the structures exhibit non-equivalent molybdenum centers: two are pentacoordinate with distorted trigonal bipyramidal geometry, while the remaining two sites display the usual distorted octahedral geometry.

Several organic substrates containing the α-diketone subunit are also incorporated into this tetramolybdate framework to yield diketal derivatives of the same structural type, $[RMo_4O_{15}X]^{3-}$. Thus, 1,2,3-indantrione (ninhydrin), benzil and phenanthraquinone are incorporated to yield $[(C_9H_4O)Mo_4O_{15}(OCH_3)]^{3-}$, $[(C_{14}H_{10})Mo_4O_{15}(C_7H_5O_2)]^{3-}$ and $[(C_{14}H_8)Mo_4O_{15}(OH)]^{3-}$, respectively [43,99], shown schematically in Fig. 13. The methoxy derivative $[(C_9H_4O)Mo_4O_{15}(OCH_3)]^{3-}$ is structurally analogous to $[(HCCH)Mo_4O_{15}F]^{3-}$ with F^- replaced

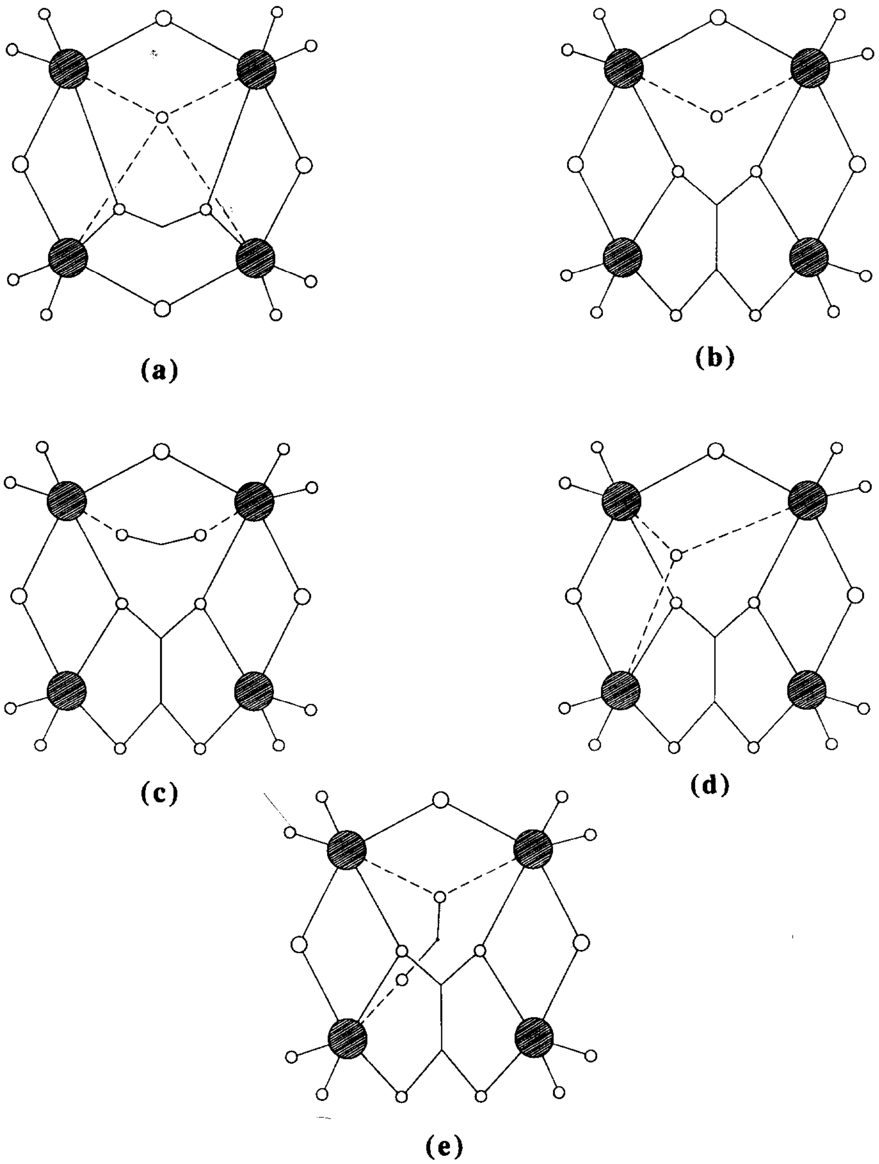

(a) (b) (c) (d) (e)

Fig. 13. Schematic representations of the structures of (a) $[(CH_2)Mo_4O_{15}H]^{3-}$, (b) $[(HCCH)Mo_4O_{15}F]^{3-}$, (c) $[(HCCH)Mo_4O_{15}(HCO_2)]^{3-}$, (d) $[(C_{14}H_8)Mo_4O_{15}(OH)]^{3-}$, (e) $[(C_{14}H_{10})Mo_4O_{15}(C_7H_5O_2)]^{3-}$.

by OCH_3^- and the [HCCH] moiety by $[C_9H_4O]$. In contrast, the latter two structures demonstrate the remarkable flexibility of the structural core. The phenanthraquinone derivative $[(C_{14}H_8)Mo_4O_{15}(OH)]^{3-}$ exhibits a triply bridging OH^- group, which results in three structurally distinct molybdenum sites: a pentacoordinate

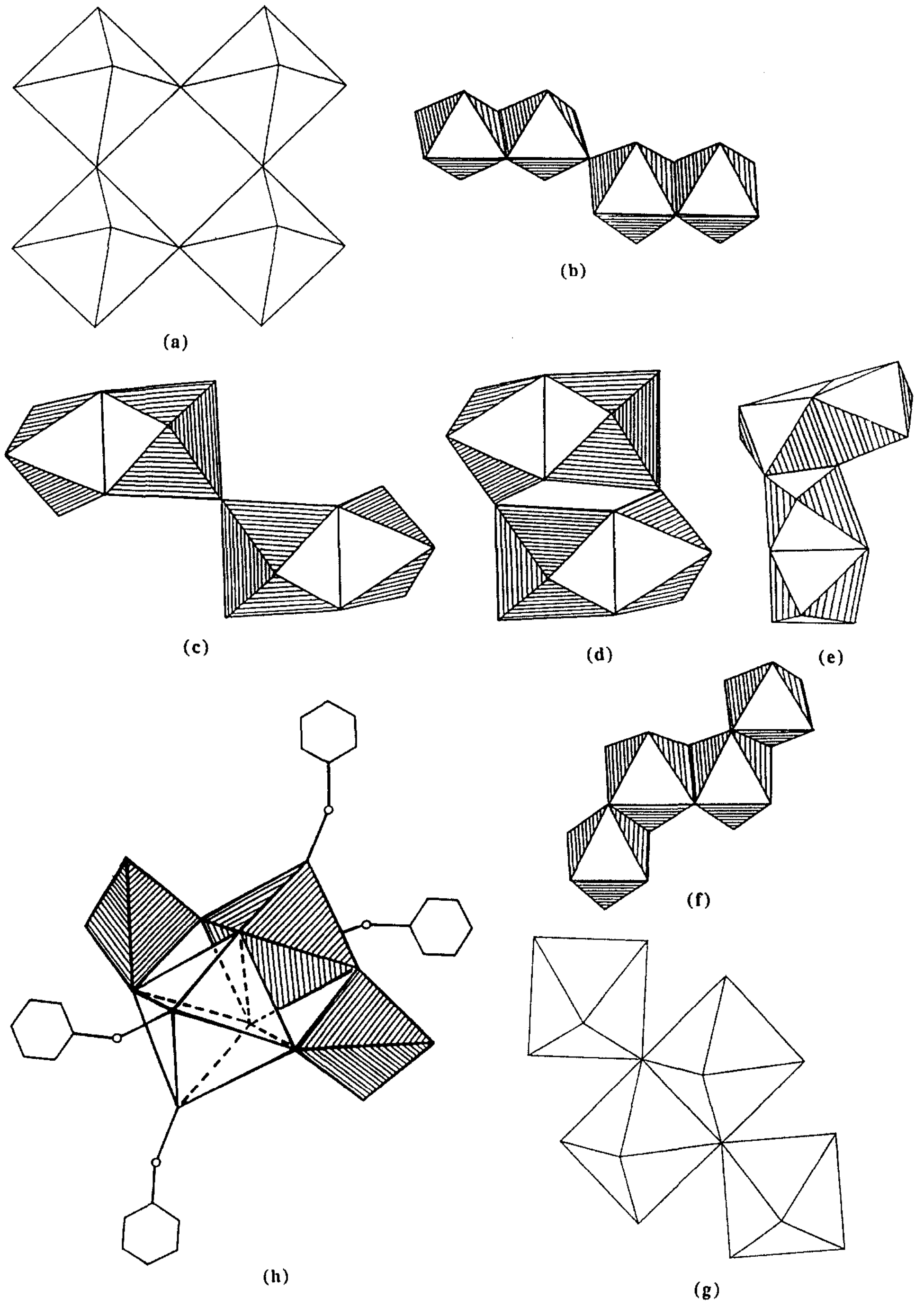

Fig. 14. Polyhedral representations of tetranuclear polyoxometalate coordination complexes. (a) $[Mo_4O_{12}(C_{12}H_{30}N_4S_2)_2]$, (b) $[Mo_4O_{11}(malate)_2]^{2-}$, (c) $[Mo_4O_{11}(LH_2)(LH)(L)]^-$ ($L = CH_3C_6H_4C(NH)NO^{2-}$), (d) $[Mo_4O_{12}\{H_3C(NH_2)NO\}_2]^{2-}$, (e) $[Mo_4O_6(SCH_2CH_2O)_5]^{2-}$, (f) $[Mo_4\{HB(pz)_3\}_2O_4(OCH_3)_2(HOCH_3)_2]$, (g) $[Mo_4O_6Cl_2(O_2CR)_6]$, (h) $[Mo_4O_8(OCH_3)_2(NNC_6H_5)_4]^{2-}$.

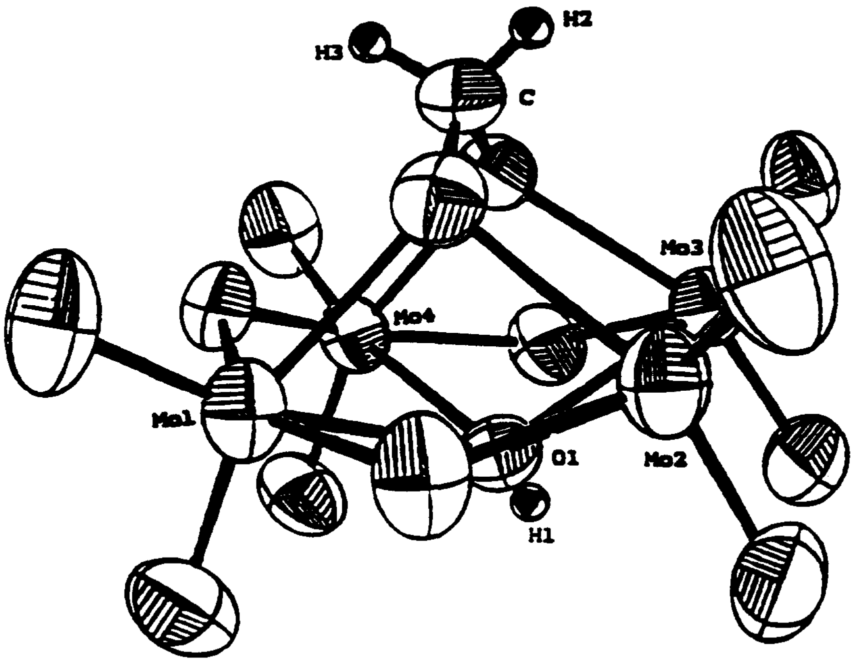

Fig. 15. The structure of $[(H_2CO_2)Mo_4O_{12}(OH)]^{3-}$.

center, the octahedral centers bonded to two μ-oxo groups, and the third octahedral center at the open edge of the $[Mo_4(\mu\text{-}O)_3]$ core. The bridging benzoate group of $[(C_{14}H_{10})Mo_4O_{15}(C_7H_5O)]^{3-}$ also adopts an unsymmetrical bidentate bridging mode, but bridges two molybdenum centers through one carboxylate oxygen and bonds to a third molybdenum through the second carboxylate oxygen in a weak interaction (Mo—O, 2.62 Å).

The geometries illustrated in Fig. 14 often represent structural singularities, an observation which may reflect the relatively undeveloped state of polyoxometalate coordination chemistry. It is clear, however, that both the geometric constraints of the ligand and the oxidation states of the molybdenum centers are important factors in determining the structure. The cluster $[Mo_4O_{12}(C_{12}H_{30}N_4S_2)_2]$ [26,100] represents the single example of a polyoxomolybdate species with amine ligands. The overall structure consists of an $[Mo_4O_4]$ ring of edge sharing $[MoO_4N_2]$ octahedra (Fig. 14(a)), with the tetradentate amine ligands each spanning two molybdenum centers.

Figure 14(b) illustrates the tetranuclear framework adopted by $[Mo_4O_{11}\text{-}(malate)_2]^{2-}$ [34,35] and $[Mo_4O_{11}(citrate)_2]^{4-}$ [36,37]. The structure consists of distorted $[MoO_6]$ octahedra, pairs of which share an edge and which are then linked by vertex-sharing interactions. The citrate groups are each terdentate, bonding through the central hydroxy unit, both oxygen donors of one carboxylato group, and a single oxygen of a second carboxylate. The third carboxylate arm is pendant, extending away from the metal ions and hydrogen bonding to water of crystallization. The malate derivative exhibits similar anion cluster geometry.

The consequences of introducing ambidentate ligands with different donor groups are illustrated in Fig. 14(c) and (d). The structure of $[Mo_4O_{11}(LH_2)(LH)(L)]^-$, $L=(CH_3C_6H_4C(NH)NO)^{2-}$, consists of non-symmetrical extended tetranuclear anions, constructed from two dinuclear units $[Mo_2O_5(H_2L)(L)]$ and $[Mo_2O_5(H_2L)]^+$ linked by one slightly bent μ-oxo bridge. In both units the H_2L ligand is present in the zwitterionic form with protonation occurring at the nitrogen. Within each dinuclear unit, the molybdenum atoms are linked by three oxygen bridges, one μ-oxo and two amidoximes, one of which chelates one molybdenum center [24]. In contrast, the structure of the acetamidoximato complex $[Mo_4O_{12}\{H_3C(NH_2)NO\}_2]^{2-}$ [25] is based upon two pairs of face-sharing octahedra connected by two corner-sharing μ-oxo groups to form a ring, structurally similar to the $[(H_2CO)Mo_4O_{15}H]^{3-}$ prototype discussed previously and to the peroxo species $[Mo_4O_{12}(O_2)_2]^{4-}$ [101]. The oxime oxygen and nitrogen donors of both oxime ligands assume bridging coordination modes to produce $[MoO_5N]$ coordination at each of the four molybdenum centers.

In addition to the Mo(V) clusters of the type $[Mo_4O_8(OR)_2(HOR)_2Cl_4]^{2-}$ discussed previously, several examples of tetranuclear polyoxomolybdates with reduced metal centers have been described recently. The Mo(V) cluster $[Mo_4O_6(SCH_2CH_2O)_5]^{2-}$ [46], shown in Fig. 14(e) exhibits a structure consisting of two triply bridged $[Mo_2O_3(SCH_2CH_2O)_2]^0$ units, sharing an edge defined by an oxygen donor of a mercaptoethanolate ligand and a triply bridging oxo group. The tetranuclear core adopted by this complex may be constructed by condensation of the binuclear cores previously reported for $[Mo_2O_2(SCH_2CH_2O)_2Cl_3]^-$ and $[Mo_2O_2(SCH_2CH_2O)_3Cl]^-$ [102]. In fact, reaction of the two binuclear species in wet methylene chloride produces $[Mo_4O_6(SCH_2CH_2O)_5]^{2-}$ in good yield [59].

The pyrazolylborate ligated cluster $[Mo_4\{HB(pz)_3\}_2O_4(OCH_3)_2(CH_3OH)_2]$ represents another example of a Mo(V) cluster [47]. The structure, illustrated in Fig. 14(f), consists of two pairs of edge-sharing octahedra fused along an edge defined by two methoxy oxygen donors. The face-capping pyrazolylborate groups prevent further aggregation and constrain the outermost molybdenum centers from forming additional edge-sharing interactions to give a more compact structure.

Reduced polyoxomolybdate(V)–carboxylate derivatives have also been described. Both $[Mo_4O_6Cl_2(O_2CCH_3)_6]$ [38] and $[Mo_4O_6Cl_2(O_2C_6H_4CH_3)_6]$ [39] exhibit the tetranuclear core shown in Figure 14(g). Two $[MoO_6]$ octahedra share an edge and exhibit a short Mo–Mo distance consistent with two interacting Mo(V) centers, while the two remaining $[MoO_5Cl]$ units each share a vertex of the $[Mo_2O_2]$ rhombus of this binuclear fragment. The six carboxylate ligands adopt the bridging bidentate mode to complete the coordination about the Mo centers. The arrangement of Mo octahedra is distinct from that observed for Mo(VI)–carboxylate clusters and is less compact as a consequence of adopting vertex-sharing rather the more common edge-sharing motif.

The introduction of ligands capable of π-bonding to the molybdenum centers would be expected to produce significant structural rearrangement of the cluster cores. Phenylhydrazine reacts with polymolybdates in alcoholic solution to give complexes of the type $[Mo_4O_8(OCH_3)_2(NNC_6H_5)_4]^{2-}$ [27,28]. The structure of the tetranuclear polyanion, shown in Fig. 14(h), consists of a binuclear unit of edge-sharing octahedra, bridged by two $[MoO_4]^{2-}$ tetrahedra, each sharing two corners with the binuclear core. A significant feature of the structure is the short Mo–N distance which, together with the short N–N distance and the linearity of the Mo–N–N unit, is a common feature of metal–diazenido bonding [103–107] and is consistent with the description of the diazenido ligand as a three-electron donor, RN_2^+. Using this formalism, the average molybdenum oxidation in the cluster is +3. Since the $[MoO_4]^{2-}$ units exhibit unexceptional metrical parameters for a tetraoxomolybdate(VI) moiety, the octahedral molybdenum sites of the $[Mo_2(OCH_3)_2(NNPh)_4]^{2+}$ core may be considered formally to be in the Mo(0) oxidation state.

Several variants of this structure have been isolated in reactions under modified conditions or with functionalized organohydrazines or diorganohydrazines. Thus, reaction of molybdates with 1,1-diphenylhydrazine yields the tetranuclear species $[Mo_4O_{10}(OCH_3)_2(NNR_2)_2]^{2-}$ [33]. The overall geometry is similar to that described above for $[Mo_4O_8(OCH_3)_2(NNR)_4]^{2-}$, except that in the core of edge-sharing octahedra, $[Mo_2O_2(OCH_3)_2(NNR_2)_2]^{2+}$, each molybdenum center possesses one terminal oxo group and one hydrazido(2−) ligand rather than the *cis*-bisdiazenido grouping $[Mo(NNR)_2]^{2+}$ associated with the prototype. The organohydrazine ligand in $[Mo_4O_{10}(OCH_3)_2(NNR_2)_2]^{2-}$ is formally described as a hydrazido(2−), four-electron donor, electronically analogous to an oxo group [108]. The $[MoO(NNR_2)]^{2+}$ unit is common in the chemistry of mononuclear Mo(VI) complexes [109–111], as is the $[Mo(NNR_2)_2]^{2+}$ unit [112,113], which does not appear, however, to be present in the polyoxomolybdate chemistry.

The complex $[Mo_4O_{10}(OCH_3)_2(NNPh)_2]^{2-}$ [41] also adopts the tetranuclear core common to this class of compounds, but with the $[Mo_2O_2(OCH_3)_2(NNPh)_2]^{2+}$ binuclear core consisting of a *cis*-dioxomolybdate center $[MoO_2]$ and a *cis*-bisdiazenidomolybdenum site $[Mo(NNPh)_2]$. Upon introduction of functionalized hydrazines, such as hydrazinophthalazine, $H_2NNH(C_8H_5N_2)$, (hphH$_2$), and dihydrazinophthalazine, $(H_2NNH)_2(C_8H_4N_2)$, (dhphH$_6$), the tetranuclear core (Fig. 14(h)) is again retained with some modification of the central binuclear unit. The structure of $[Mo_4O_{11}(dhphH_2)]^{2-}$ [31] exhibits a $[Mo_2O_3(dhphH_2)]^{2+}$ core. Each molybdenum center is ligated by one terminal oxo group and one terminal hydrazido(2−) moiety of the $(dphpH_2)^{4-}$ ligand, which also provides the nitrogen donors from the bridging phthalazine group. The two molybdenum centers are also bridged by a single oxo group, such that the central core may be described as two $[MoO_4N_2]$

octahedra sharing a corner defined by the oxo group. The structure of $[Mo_4O_{12}(hphH)]^{2-}$ [114], shown in Fig. 16, contains the $[Mo_2O_4(hphH)]^{2+}$ core, wherein one molybdenum displays the *cis*-dioxo $[MoO_2]$ geometry as a consequence of the ligand possessing a single hydrazine arm.

Structural modification of this class of compounds is not limited to the terminal and bridging groups of the edge-shared binuclear core, but may be extended to the bridging molybdenum sites. In this fashion, reactions of $[Mo_4O_8(OR)_2(NNPh)_4]^{2-}$ with catechols or *o*-aminophenol yield the complexes $[Mo_4O_6(OCH_3)_2(OC_6H_4O)_2(NNC_6H_5)_4]^{2-}$ and $[Mo_4O_6(OCH_3)_2(OC_6H_4NH)_2(NNC_6H_5)_4]^{2-}$, respectively [29,30]. The structures are related to the $[Mo_4O_8(OR)_2(NNPh)_4]^{2-}$ prototype through substitution of a single oxo group of each bridging $[MoO_4]^{2-}$ unit by a catecholate or *o*-amidophenolate ligand, as illustrated in Fig. 17. The resultant square pyramidal geometry at the bridging molybdenum sites, $[MoO_3(catecholate)]^{2-}$, is relatively unusual and may reflect the geometric and electronic requirements of the $[Mo_2(OR)_2(NNPh)_4]^{2+}$ core.

This brief introduction to the structural chemistry of tetranuclear Mo(V) and mixed-valence clusters suggests that clusters with reduced molybdenum sites may

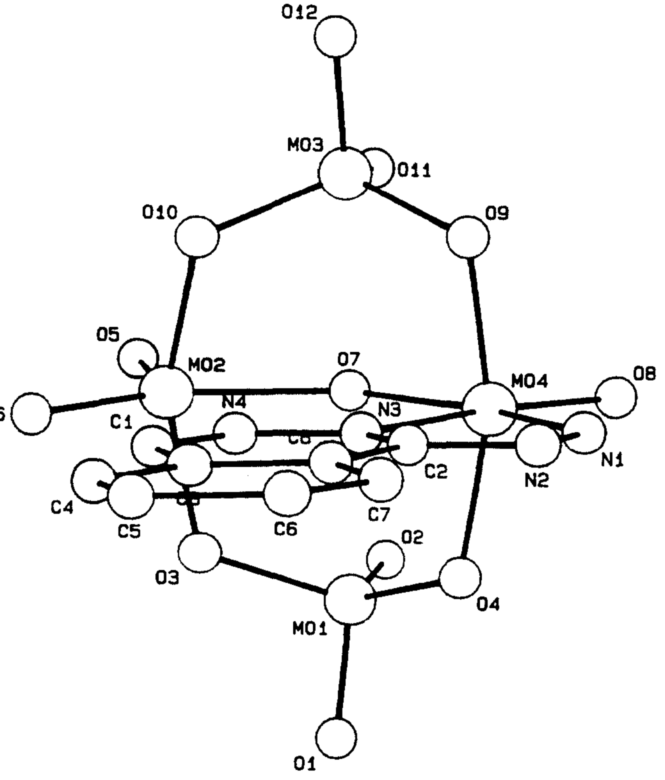

Fig. 16. The structure of $[Mo_4O_{12}(hphH)]^{2-}$.

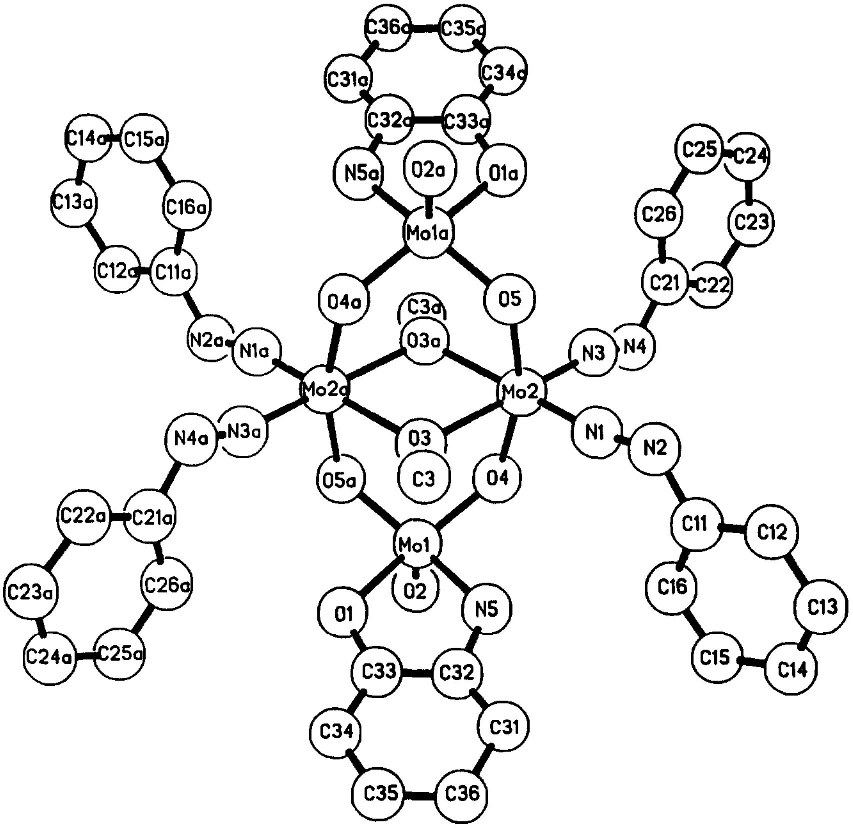

Fig. 17. The structure of $[Mo_4O_6(OCH_3)_2(O_2C_6H_4)_2(NNC_6H_5)_4]^{2-}$.

represent an area largely unexplored and potentially fruitful. Certainly, some unusual structural types have emerged, often serendipitously. As a final example, the polyoxomolybdate–triorganophosphine complex, $[Mo_4O_6(OH)_4(CO)_2(CO_3)(PMe_3)_6]$ [45], is illustrated diagrammatically in Fig. 18. The structure exhibits a binuclear $(\mu\text{-}O)_2$ bridged Mo(V) core, $[Mo_2O_4]$, bridged by hydroxy groups to the seven-coordinate Mo(II) sites. The carbonate groups assumes an unusual η^2, μ_4-coordination mode to bridge all four Mo sites. The edge-sharing binuclear core of $[Mo_4O_6(OH)_4(CO)_2(CO_3)(PMe_3)_6]$ appears to provide a template for further aggregation of the reduced Mo centers. Since a common feature of the structural chemistry of tetranuclear complexes with reduced metal sites is the presence of a binuclear core of edge-sharing octahedra, it is tempting to speculate that the aggregation process involves addition of molybdenum polyhedra to such robust cores.

(c) Pentanuclear species

Pentanuclear geometries are represented by only two clusters, $[Mo_5O_{16}(OCH_3)]^{3-}$ [12] and $[Mo_5O_{13}Na(NO)(OCH_3)_4]^{2-}$ [48]. The relative pau-

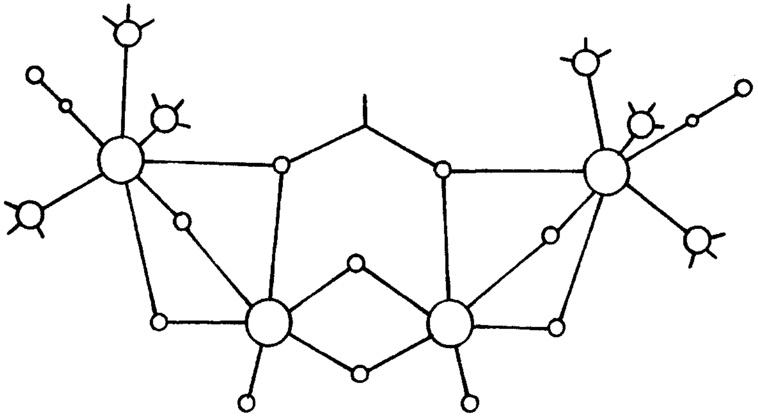

Fig. 18. Schematic representation of the structure of $[Mo_4O_6(OH)_4(CO)_2(CO)_3(PMe_3)_6]$.

city of examples may reflect the tendency of polymetalates to assume approximately spherical structures, so that addition of an additional [Mo=O] unit via condensation of a molybdate group to the pentanuclear core to generate the hexametalate structure **VI** is favored.

The pentanuclear $[Mo_5O_{16}(OCH_3)]^{3-}$ may be isolated from solutions of $Mo_2O_7^{2-}$ in methanol in the presence of Lewis bases [12]. Curiously, the structure does not conform to the "rule of compactness" to give a cluster of type **V**, but rather exhibits a structure similar to that previously described for $[Mo_3O_8(OCH_3)(C_4O_4)_2]^{3-}$. Thus, the structure consists of a trinuclear core $[Mo_3O_8(OCH_3)]^+$ coordinated to two bridging $(MoO_4)^{2-}$ groups. There are three distinct Mo coordination environments: two molybdenums display pseudo-tetrahedral coordination, while the remaining sites adopt distorted octahedral geometries, with two exhibiting the common *cis*-dioxo unit and the third possessing a single terminal oxo group. The analogous $[Mo_5O_{16}(OH)]^{3-}$ [13] appears to be structurally isomorphous.

In contrast, the nitrosyl-containing cluster $[Mo_5Na(NO)O_{13}(OCH_3)_4]^{2-}$ [48], shown in Fig. 19 adopts a structure derived from the Lindquist structure, or hexametalate $[M_6O_{19}]$ core, by removal of one MO group and replacement by the sodium cation. The linear $[Mo(NO)]^{3+}$ subunit is bridged by four methoxy ligands to the four Mo(VI) neighbors. The formal oxidation state of the Mo(1) center is inferred to be +2 from the net polyanion charge. This complex represents the only example of a lacunary Lindquist structure and, as expected, readily adds a $[MoO]^{4+}$ unit to complete the hexametalate core.

(d) *Hexanuclear species*

Not unexpectedly, most examples of hexanuclear polyoxomolybdate complexes adopt structures based on the hexametalate or "superoctahedral" framework

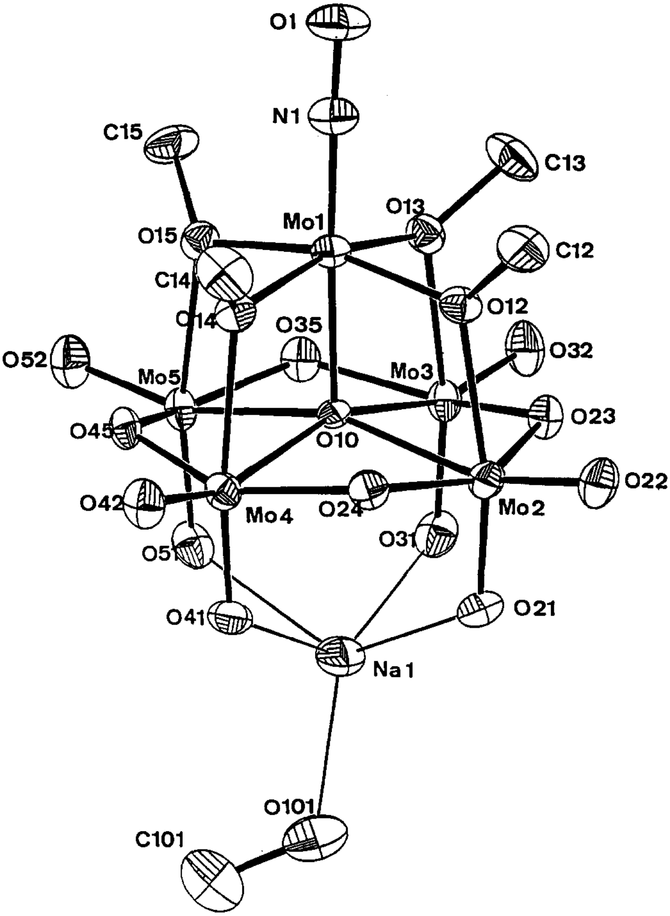

Fig. 19. The structure of $[Mo_5Na(NO)O_{13}(OCH_3)_4]^{2-}$.

$[M_6O_{19}]^{n-}$ [115–118] and their derivatives [119], illustrated in Fig. 4 and classified as structural type VI. The clusters $[Mo_6O_{18}(NNPh)]^{3-}$ [49], $[Mo_6O_{18}(NNMePh)]^{2-}$ [50], $[MoO_{18}(NO)]^{3-}$ [48] and $[Mo_6O_{18}(NC_6H_4CH_3)]^{2-}$ [80] exhibit the hexametalate structure with one terminal oxo group replaced by the π-bonding diazenido, hydrazido(2−), nitrosyl or imido ligand, respectively. However, it should be noted that, while the molybdenum centers of $[Mo_6O_{18}(NNMePh)]^{2-}$ and $[Mo_6O_{18}(NC_6H_4CH_3)]^{2-}$ are all formally in the +6 oxidation state, the ligand bound molybdenum sites of $[Mo_6O_{18}(NNPh)]^{3-}$ and $[Mo_6O_{18}(NO)]^{3-}$ are in the +2 oxidation state. We return to this point in the discussion of the electrochemical properties of these species.

In contrast to these pseudo-spherical structures, $[Mo_6O_{10}(OPr)_{12}]$ [51] adopts the extended structure shown in Fig. 20, consisting of two distorted octahedral $[MoO(OR)_5]$ units terminating either end of a chain of fused square-based pyramidal

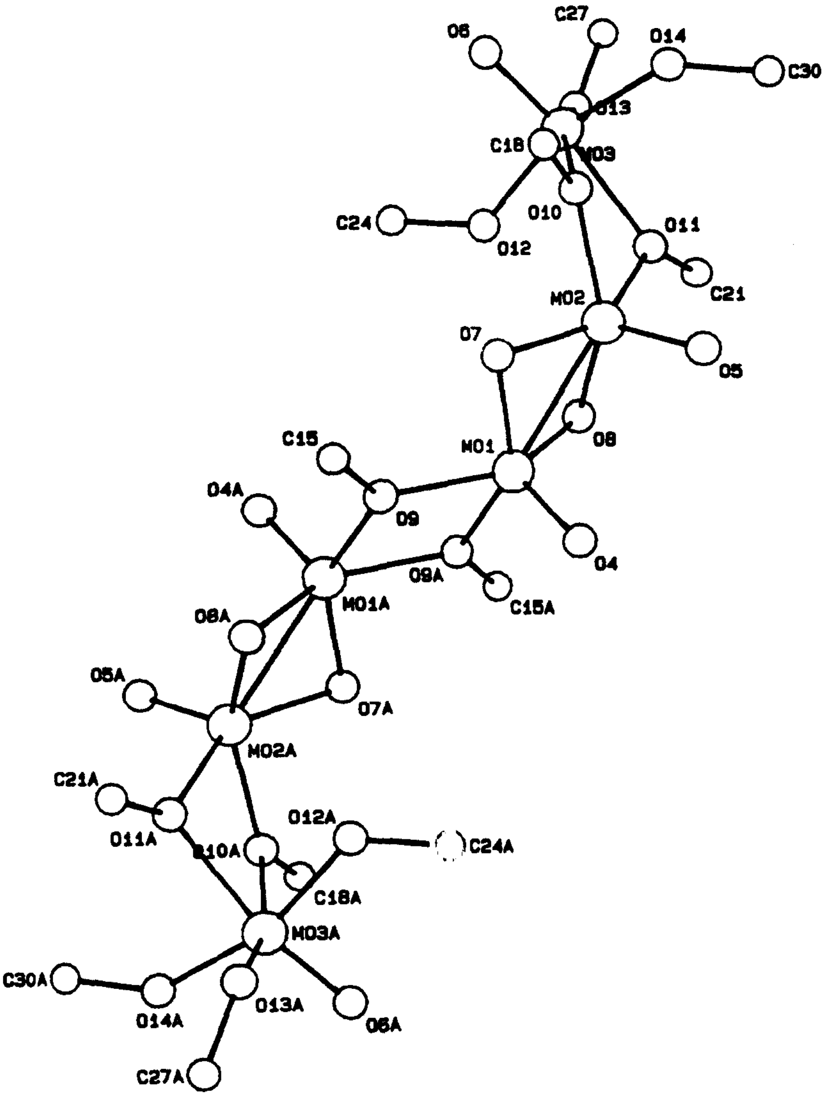

Fig. 20. The structure of $[Mo_6O_{10}(OPr)_{12}]$.

units $[Mo_2O_4(OPr)_2]$, with alternating $(\mu\text{-}OR)_2$ and $(\mu\text{-}O)_2$ bridges. As shown in Fig. 20, the coupling of $[Mo_2O_4(OR)_2]$ units produces a zigzag chain of edge-sharing polyhedra. Curiously, the complex is a mixed-valence species with the terminal Mo centers best described as Mo(VI) and the four central Mo sites as Mo(V).

(e) Octanuclear species

The persistence of certain structural motifs in the polyoxometalate chemistry is again apparent in the cluster geometries adopted by octanuclear polyoxomolybdate coordination compounds. Thus, both the β-$[Mo_8O_{26}]^{4-}$ [120,121] and the $[Mo_4O_{24}(OCH_3)_4]^{4-}$ [11] structures may be described in terms of the class **IVa** structure of $[Mo_4O_{10}(OCH_3)_6]^{2-}$, as illustrated in Fig. 21. Condensation of two $[Mo_4O_{10}(OCH_3)_6]^{2-}$ units by sharing of four edges of each unit and loss of CH_3OH produces the β-$[Mo_8O_{26}]^{4-}$ structure, while the $[Mo_8O_{24}(OCH_3)_4]^{4-}$ structure results either from shearing of $[Mo_4O_{13}]^{2-}$ asymmetric units of β-$[Mo_8O_{26}]^{4-}$ parallel to one another or from condensation of two $[Mo_4O_{10}(OCH_3)_6]^{2-}$ units along two edges of each unit and partial loss of CH_3OH.

Two common substitution patterns based on this octanuclear core are observed. The first is based on the structure of $[Mo_8O_{26}(OH)_2]^{6-}$ [122], where only the two **A** sites of the $[Mo_8O_{26}]$ core are occupied by ligands, while the second is that adopted by $[Mo_8O_{24}(OCH_3)_4]^{4-}$, where the four **B** sites are occupied by the methoxy groups (Fig. 22). The first of these structural prototypes is adopted by the formylated octamolybdate cluster $[(HCO_2)_2Mo_8O_{26}]^{6-}$ [8], $[Mo_8O_{26}(py)_2]^{4-}$ [10] and $[Mo_8O_{26}(NCS)_2]^{4-}$ [52]. On the other hand, $[Mo_8O_{24}(OH)_4(sal)_2]^{2-}$ (sal = salicylidenepropyliminato, $PrN{=}CHC_6H_4O^-$) and $[Mo_8O_{24}(OH)_2(met)_4]^{4-}$ (met = methionato, $CH_3SCH_2CH_2CH(NH_2)CO_2^-$) [53] provide a variant of this structural type. The methionine derivative exhibits the $[Mo_8O_{26}(OH)_2]^{6-}$ structure, with carboxylate oxygen donors replacing the OH^- groups of the prototype, and with two bridging oxo groups now protonated. The analogous silicylideneiminato structures has un-

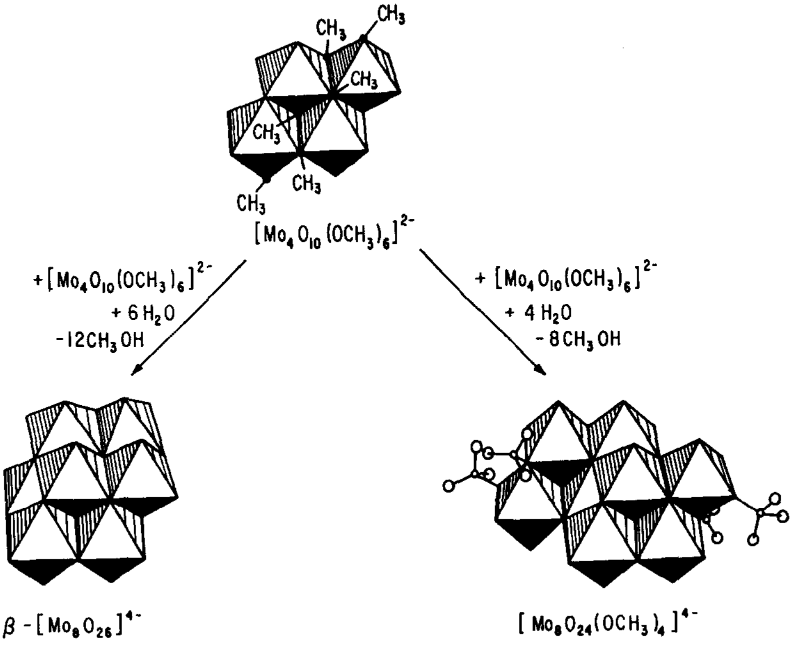

Fig. 21. Idealized polyhedral models illustrating the structural relationship of $[Mo_4O_{10}(OCH_3)_6]^{2-}$ to β-$[Mo_8O_{26}]^{4-}$ and to $[Mo_8O_{24}(OCH_3)_4]^{4-}$.

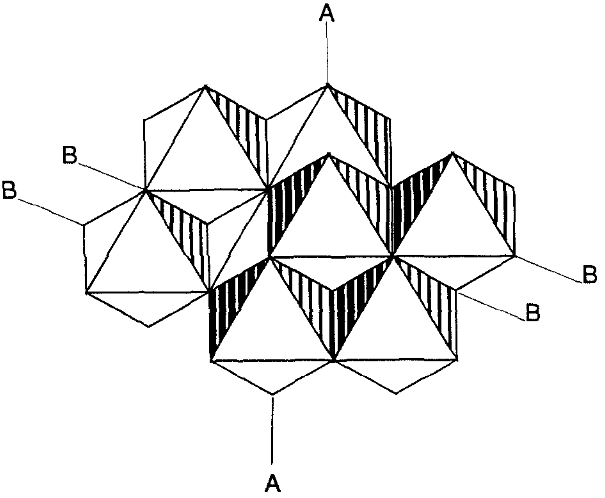

Fig. 22. Schematic representation of the structures of $[Mo_8O_{26}(OH)_2]^{6-}$ and $[Mo_8O_{24}(OCH_3)_4]^{4-}$.

dergone protonation at two additional bridging oxo sites. Unfortunately, the protonation positions could not be discerned in either case.

The structure of $[Mo_8O_{16}(OCH_3)_6(NNR_2)_6]^{2-}$, formed from the hydrolysis of $[Mo_4O_{10}(OCH_3)_2(NNR_2)_2]^{2-}$, may also be described in terms of two fused tetranuclear cores of type **IVa**, as shown in Fig. 21. The structure exhibits two centrosymmetrically related $[Mo_4O_8(OCH_3)_3(NNR)_3]^-$, units connected through doubly bridging and quadruply bridging oxo groups. Of the six methoxy groups, two are terminal and four are doubly bridging. Six terminal hydrazido(2−) groups ligated to each of six molybdenum centers, together with doubly and triply bridging oxo groups, complete the distorted octahedral coordination adopted by the molybdenum sites. The linkage of octahedra in this complex is unique, but clearly related to that observed in β-$[Mo_8O_{26}]^{4-}$ and in the derived structures $[Mo_8O_{26}(L)_2]^{2n-4}$. The latter species are related to the β-$[Mo_8O_{26}]^{4-}$ structure by translation of one set of one type **IVa** unit one octahedral edge length parallel to the second type **IVa** unit. A second translation in the perpendicular direction produces the framework for $[Mo_8O_{16}(OCH_3)_6(NNR_2)_6]^{2-}$.

The polyoxoalkoxy complex $[Mo_8O_{20}(OCH_3)_4\{CH_3C(CH_2O)_3\}_2]^{2-}$ [54] exhibits yet another variation in the joining of two type **IVa** cores. The structure consists of edge and corner sharing $[MoO_6]$ octahedra. There are two tetranuclear $[Mo_4O_{10}(OMe)_2\{CH_3C(CH_2O)_3\}]^-$ moieties related by a center of symmetry, and each Mo center of this tetranuclear core is structurally unique. As illustrated in Fig. 23, the two tetranuclear units adopt a corner-sharing geometry with relatively weak bridging interactions.

The oxoalkoxide cluster $[Mg_2Mo_8O_{22}(OCH_3)_6(HOCH_3)_4]^{2-}$ [58] provides an unusual example of a heterometallic, Mo(V)/Mo(VI) mixed valence species. The

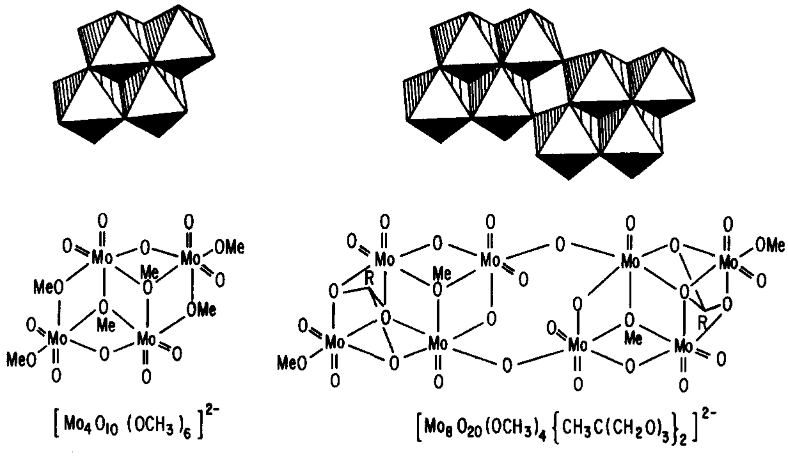

$[Mo_4O_{10}(OCH_3)_6]^{2-}$

$[Mo_8O_{20}(OCH_3)_4\{CH_3C(CH_2O)_3\}_2]^{2-}$

Fig. 23. Idealized polyhedral models and bond representations of the structures of $[Mo_4O_{10}(OCH_3)_6]^{2-}$ and $[Mo_8O_{20}(OCH_3)_4\{CH_3C(CH_2O)_3\}_2]^{2-}$.

structure, illustrated in Fig. 24, consists of two class **IVa** edge-sharing tetranuclear cores fused along the two AA edges (Fig. 4). The central core consists of two pairs of two edge-sharing Mo(V) octahedra joined by two corner-sharing interactions. The short Mo–Mo distances for the edge-sharing metal centers of this core identify these as the Mo(V) sites. The localization of these sites indicates that the complex may be classified as a class I mixed-valence compound with coupled binuclear Mo(V) centers [123]. The two $[Mg(OCH_3)_2]$ units fill the two cavities formed by the unusual stacking of Mo octahedra.

The Mo(V) cluster $[Mo_8O_{12}(OCH_3)_4(SCH_2CH_2O)_8]^{4-}$ adopts an extended structure consisting of two tetranuclear $[Mo_4O_6(OCH_3)_2(SCH_2CH_2O)_3]^0$ units bridged by two mercaptoethanolate groups. The structure has a precedent in the binuclear $[Mo_2O_2(SCH_2CH_2O)_3(SCH_2OH)]^-$ [102], which exhibits one mercaptoethanol ligand bound only through the sulfur and hence providing a pendant arm. The structural relationship to the tetranuclear $[Mo_4O_6(SCH_2CH_2O)_5]^{2-}$ is also evident. Displacement of one mercaptoethanolate oxygen donor by a methoxy group at one molybdenum site of this latter species and of one mercaptoethanolate sulfur donor by methoxy at a second site provides the coordination geometry observed at the tetranuclear moieties of $[Mo_8O_{12}(OCH_3)_4(SCH_2CH_2O)_8]^{4-}$.

The reduction of polyoxomolybdates by rhodizonic acid in alcohols yields the octanuclear Mo(V) species $[Mo_8O_{16}(OR)_8(C_2O_4)]^{2-}$, shown in Fig. 25. The structure exhibits an octagonal array of Mo atoms, alternately bridged by two methoxy groups and two oxo groups, producing a "tiara" framework $[Mo_8O_{16}(OCH_3)_8]^0$. The Mo–Mo distances display a short–long alternation around the ring, with average values of 2.578 and 3.282 Å, respectively. The short Mo–Mo distance, which is associated with the oxo-bridged Mo_2O_2 rhombi, is characteristic of Mo–Mo bonding distances for Mo(V) d^1 centers in bridged binuclear systems [124,125]. The cavity produced

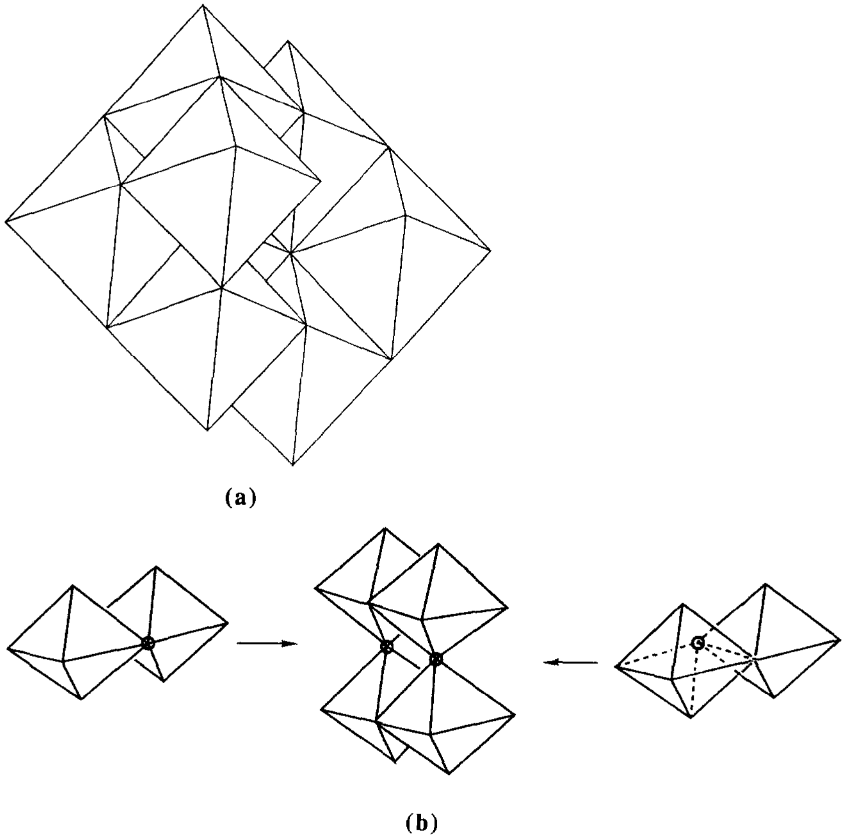

Fig. 24. (a) Polyhedral representation of the structure of $[Mg_2Mo_8O_{22}(OCH_3)_6(HOCH_3)_4]^{2-}$. (b) The structure viewed as a central type **IVd** core fused to two type **II** binuclear units, with the circles indicating the common vertices of each of the two resultant type **IVb** subunits.

by the cyclic $[Mo_8O_{16}(OCH_3)_8]$ unit is occupied by an oxalate moiety $[C_2O_4]^{2-}$. Each of the oxalate oxygen donors bridges two Mo centers to produce an arrangement of alternating face-sharing and edge-sharing $[MoO_6]$ octahedra. The structure may be alternatively described as an alkoxyoxomolybdate cluster $[Mo_8O_{20}(OCH_3)_8]$ encapsulating an acetylide C_2^{2-} unit. Although the mechanism of formation of the oxalate unit is not understood in detail, the process requires a succession of two-electron transfers and cationic intermediates.

The cyclic $[Mo_8O_{16}(OCH_3)_8]^0$ framework has also been observed in the structure of $[Mo_8O_{16}(OCH_3)_8(PR_3)_4]$ [61], illustrated in Fig. 26. Two features of this structure are noteworthy: the cavity is vacant and the ring is puckered rather than planar as is the case for $[Mo_8O_{16}(OCH_3)_8(C_2O_4)]^{2-}$. The short Mo–Mo distances are again localized to the oxo-bridged pairs of metal centers.

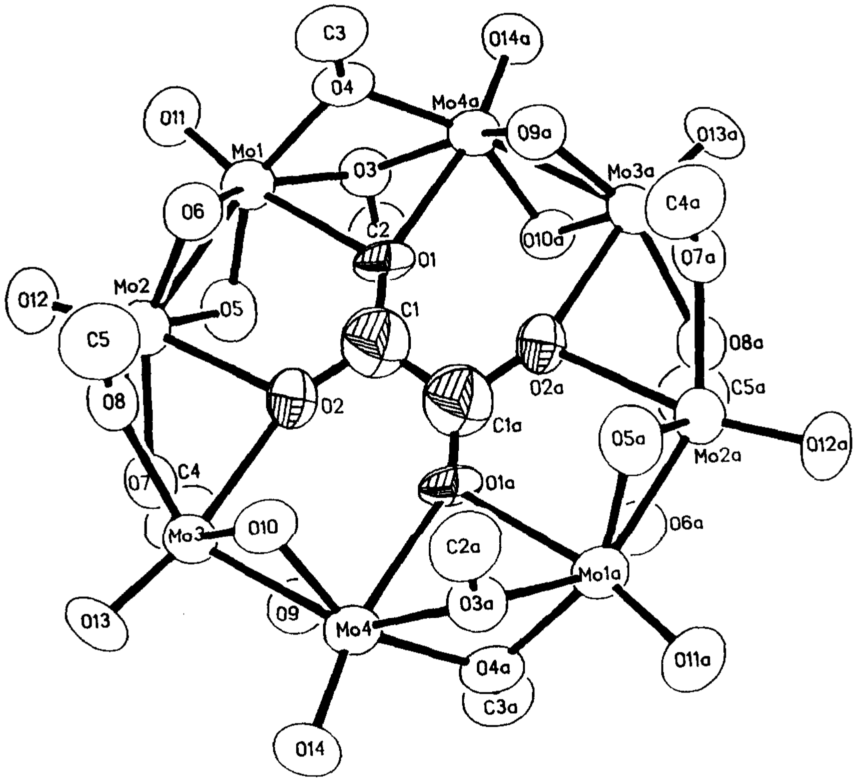

Fig. 25. The structure of $[Mo_8O_{16}(OR)_8(C_2O_4)]^{2-}$.

The structure of $[Mo_8O_{20}(NNPh)_6]^{4-}$ [55,56] is unique among the octanuclear species in possessing tetrahedral, as well as octahedral, building blocks. The overall geometry may be described as a crown of six oxo-bridged molybdenum centers alternating oxomolybdate units $[MoO_4]^{2-}$ and *cis*-bisdiazenido molybdenum sites $[Mo(NNPh)_2]^{2+}$, capped above and below by tetraoxomolybdate fragments. There are three structurally unique Mo centers: the tetrahedral $[MoO_4]^{2-}$ units bridging through two oxo groups and occupying positions in the $[Mo_6O_6]$ crown, distorted octahedral *cis*-bisdiazenidomolybdenum centers which alternate with the $[MoO_4]^{2-}$ groups in the crown, and the capping, triply bridging $[MoO_4]^{2-}$ tetrahedra. The structure is related to that of the parent polyanion α-$[Mo_8O_{26}]^{4-}$ [126–128] by replacement of two terminal oxo groups on each of three alternate molybdenum atoms in the Mo_6O_6 crown by two phenyldiazenido groups and rotation of the capping $[MoO_4]^{2-}$ unit so as to bridge to the *cis*-bisdiazenidomolybdenum units exclusively. The structural relationship of the octanuclear species is illustrated in Fig. 27.

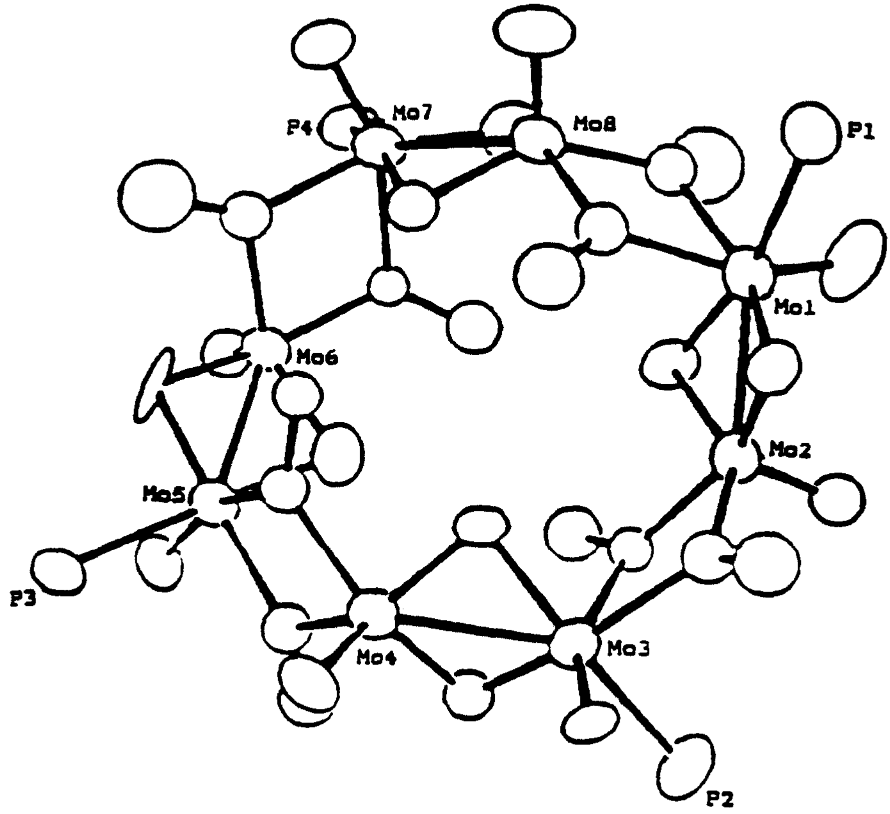

Fig. 26. The structure of $[Mo_8O_{16}(OCH_3)_8(PR_3)_4]$.

(f) Decanuclear and dodecanuclear species

Although clusters of nuclearity greater than eight are uncommon in the non-aqueous chemistry of oxomolybdates, several examples have been described recently.- Features which these larger aggregates share with the clusters discussed thus far are the presence of a simple core which provides a template for further accretion or the repetition of a simple structural motif.

The Mo(V)/Mo(VI) mixed valence cluster $[Mo_{10}O_{28}(SCH_2CH_2O)_2(HOCH_3)_2]^{4-}$, shown in Fig. 28, is isolated from the reaction of α-$[Mo_8O_{26}]^{4-}$ with 2-mercaptoethanol in methanol [46]. The structure consists of two $[Mo_5O_{14}(SCH_2CH_2O)(HOCH_3)]^{2-}$ units, bridged by two oxo-groups. The Mo centers coordinated to the mercaptoethanolate ligands are clearly identified as reduced Mo(V), exhibiting a short Mo–Mo distance of 2.693(1) Å and the triply bridged geometry through the mercaptoethanolate S and O donors and an oxo group, characteristic of binuclear Mo(V)–mercaptoethanol complexes [129,130]. A curious feature of the structure is the presence of five coordinate distorted square-pyramidal $[MoO_5]$ sites. Despite the apparent complexity of the structure, the structural core

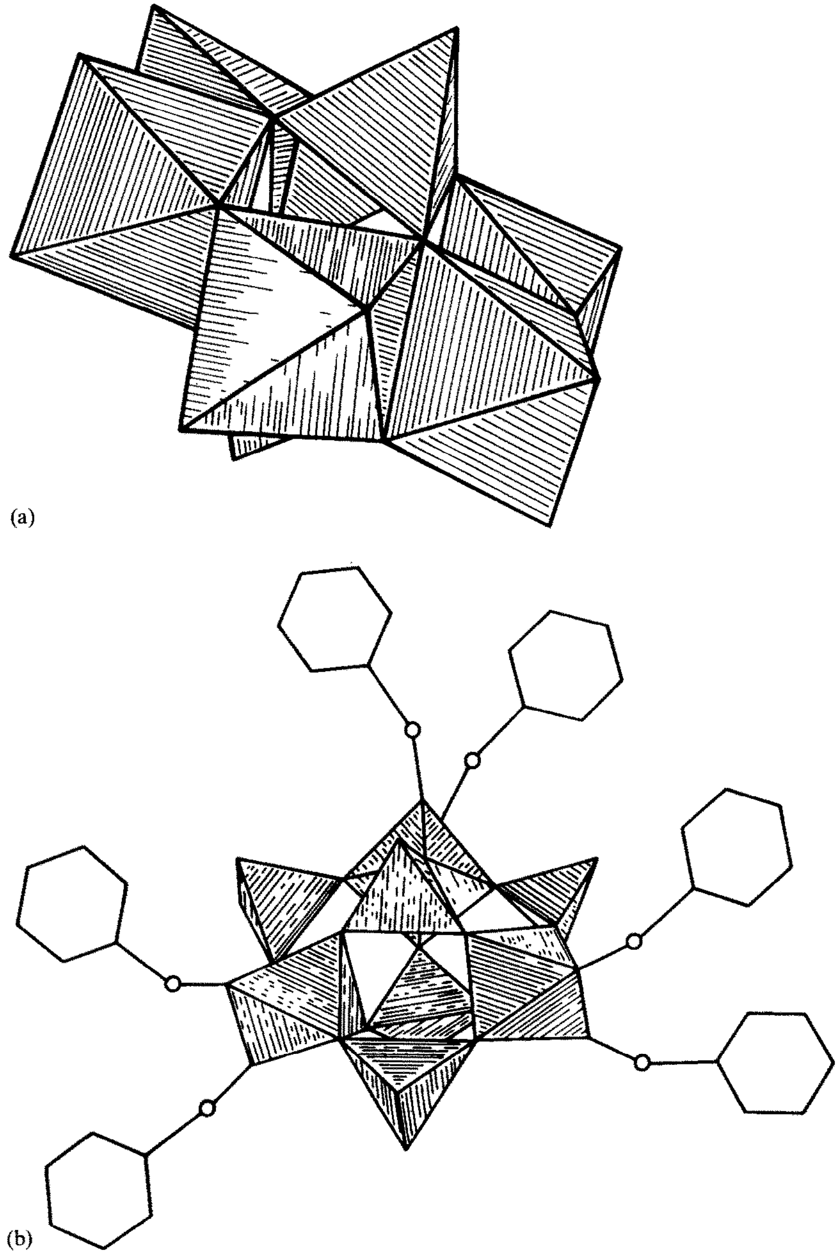

Fig. 27. Schematic representation of the relationship of the $[Mo_8O_{20}(NNPh)_6]^{4-}$ structure to the $[Mo_8O_{26}]^{4-}$ prototype.

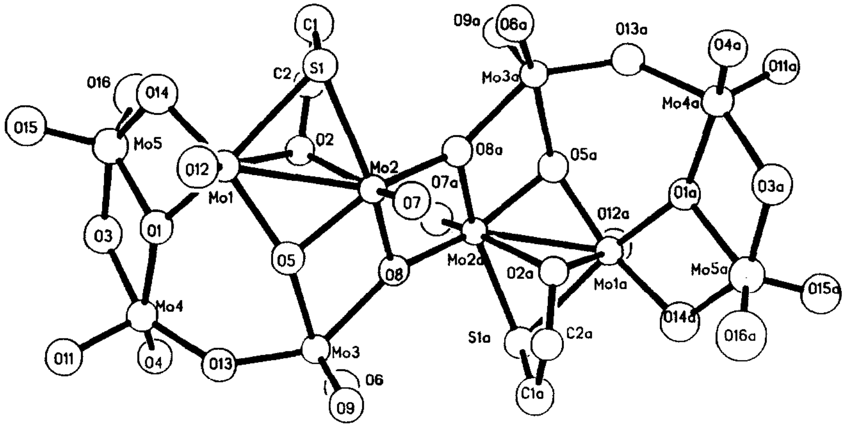

Fig. 28. The structure of $[Mo_{10}O_{28}(SCH_2CH_2O)_2(HOCH_3)_2]^{4-}$.

consists of binuclear Mo(V) thiolate species $[Mo_2O_7(SCH_2CH_2O)]^{4-}$ about which the pentacoordinate molybdate centers are disposed.

The nitrosyl-containing cluster $[Mo_{10}O_{24}(OCH_3)_7(NO)]^{2-}$ [131] provides an example of a decanuclear structure constructed from two lacunary Lindquist or type V cores joined by four corner-sharing interactions (Fig. 29), a polyhedral core also adopted by $[W_{10}O_{32}]^{4-}$ [132]. The average Mo oxidation state in the cluster is +5.2. If the nitrosyl bound molybdenum is assigned a formal oxidation state of +2, there are then five Mo(VI) and four Mo(V) sites. There is, however, no apparent localization of the d^1 centers to produce short Mo–Mo distances.

The cluster $[Mo_{12}O_{36}(C_4O_4H)_4]^{4-}$ consists of a dodecanuclear cage of Mo atoms, bridged by oxo groups to give a cyclic $[Mo_{12}O_{12}]$ framework. Each of the hydrogen squarate ligands bridges six Mo sites, such that two of the oxygen donors adopt bridging modes and two oxygens donors assume terminal monodentate coordination. The resultant $[MoO_6]$ octahedra form an edge- and corner-sharing framework which encapsulates the organic moieties, as illustrated in Fig. 30. The structural motif is clearly identified as the type **IIIb** trinuclear unit. Four of these subunits are connected through corner-sharing interactions to form the cyclic framework of the cluster.

C. STRUCTURAL CHEMISTRY OF POLYOXOVANADATE COORDINATION COMPLEXES

While the coordination chemistry of polyoxomolybdates has received considerable attention, the synthesis of analogous covalent polyoxovanadate derivatives remains relatively undeveloped. The growth of polyoxomolybdate coordination chemistry has paralleled the availability of soluble starting materials, such as $[(C_4H_9)_4N]_2[Mo_2O_7]$ and $[(C_4H_9)_4N]_4[Mo_8O_{26}]$ which are soluble in aprotic,

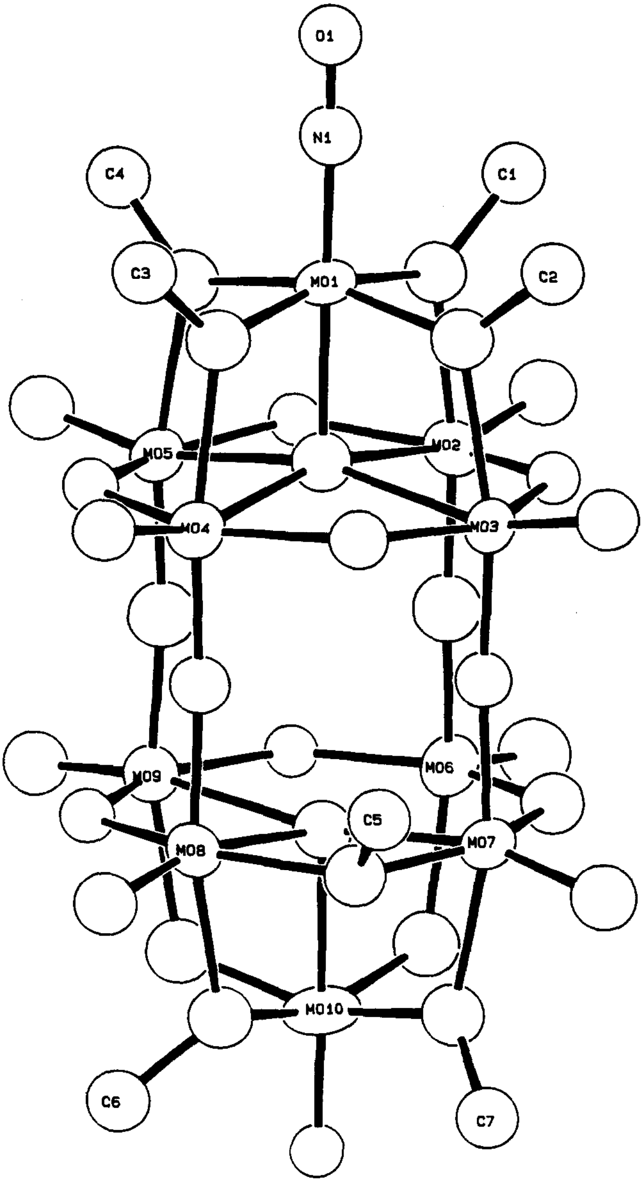

Fig. 29. The structure of $[Mo_{10}O_{24}(OCH_3)_7(NO)]^{2-}$.

polar solvents. Only recently have analogous polyoxovanadate salts, such as $[(C_4H_9)_4N]_3[V_5O_{14}]$ [133], $[(C_4H_9)_4N]_4[CH_3CN(V_{12}O_{32})]$ [72], and $[(C_4H_9)_4N]_3[H_3V_{10}O_{28}]$ [134–136], been described and employed in polyoxovanadate coordination chemistry.

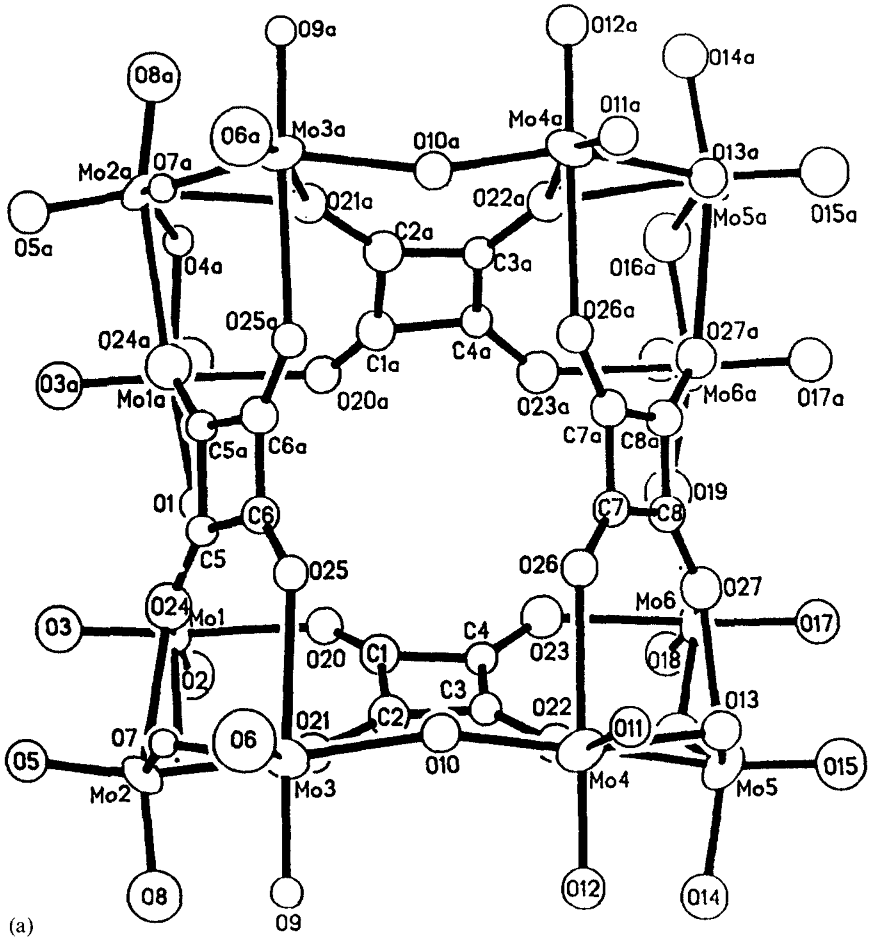

(i) *Trinuclear species*

The salicylhydroximato derivative [VO(sal)(CH_3OH)]$_3$ [63] exhibits a triangulo core of VO^{3+} units, bridged by the salicylhydroximato ligands which will employ all three oxygen donors and the nitrogen in ligation to the vanadium centers. The [VO_5N] coordination geometry at each V site is completed by the coordinated methanol molecule.

The vanadyl species [V_3O_3(THF)($C_6H_5CO_2$)$_6$] [64] also adopts a triangulo structure but with a central oxo group. Although the vanadium(IV) centers exhibit [VO_6] distorted octahedral coordination geometries, there are two distinct coordination types. Two of the vanadium centers are normal VO^{2+} vanadyl units, while the third exhibits a coordinated tetrahydrofuran molecule in place of the terminal oxo group. The structure belongs to the larger class of trinuclear, oxo-centered, basic

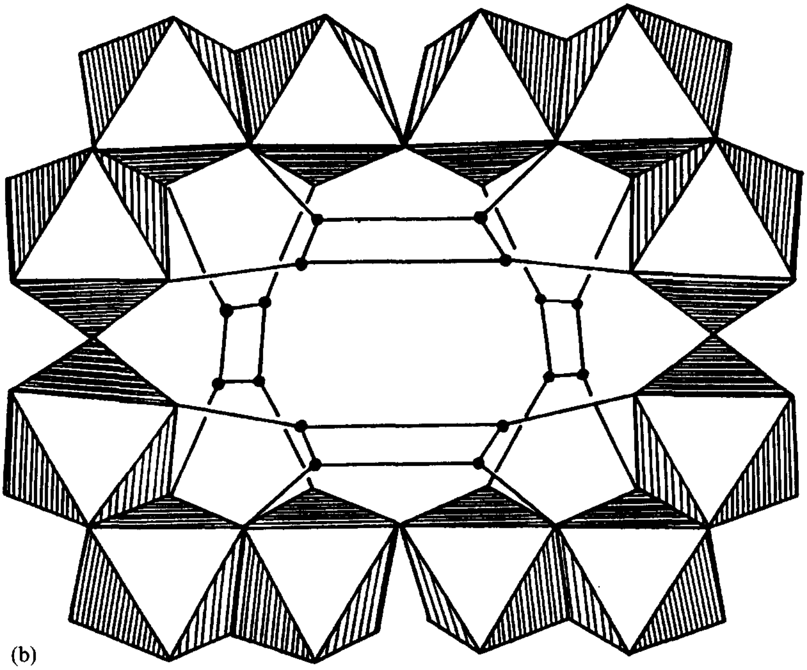

Fig. 30. The structure of $[Mo_{12}O_{36}(C_4O_4H)_4]^{4-}$.

carboxylates $[M_3O(RCO_2)_6L_3]$ [137–139], which fall beyond the scope of this review.

(ii) Tetranuclear and pentanuclear species

The tetranuclear $V^{IV}V^{V}_{3}$ complex $[V_4O_8(NO_3)(\text{thiophenecarboxylate})_4]^{2-}$ adopts the type **IVc** structure with an oxygen donor from the nitrate providing the common vertex, as shown in Fig. 31. The structure of $[V_5O_9Cl(\text{thiophenecarboxylate})_4]^{2-}$ is derived from that of $[V_4O_8(NO_3)(\text{thiophenecarboxylate})_4]^{2-}$ by replacement of the nitrate with chloride and capping the tetranuclear core by a [VO] unit. Since the apical vanadium is five-coordinate, the arrangement of metal centers is a modified form of the lacunary Lindquist or type **V** framework.

The V(V)-oxo-oxalate cluster $[V_4O_8(C_2O_4)_4(H_2O)_2]^{4-}$ [66] adopts a cyclic structure, in this instance based on a tetravanadate core with an eight-membered V_4O_4 ring. Each V(V) center coordinates to a terminal oxo group and a bidentate oxalato(2−) ligand, in addition to two bridging oxo groups and the oxygen donor of a bridging aquo ligand. Viewed as idealized octahedra, the structure may be described as two sets of two edge-sharing octahedra, joined by two corner-sharing interactions. The complex appears to provide a unique example of a type **IVd** core

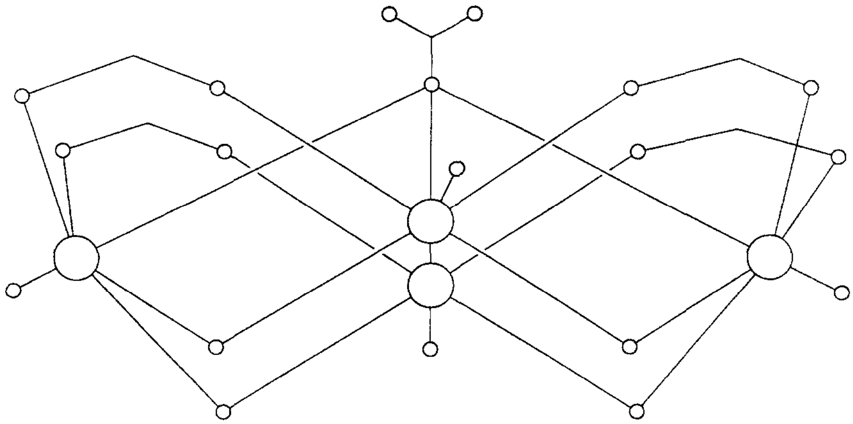

Fig. 31. The structure of $[V_4O_8(NO_3)(\text{thiophene-carboxylate})_4]^{2-}$.

(Fig. 4). The structure also illustrates the tendency of polyoxovanadates to form cyclic structures.

(iii) Hexanuclear species

The mixed-valence $V_5^VV^{IV}$ cluster $[V_6O_{10}(O_2CPh)_9]$ [67] also exhibits a cyclic structure, shown in Fig. 32. The framework consists of a binuclear $[V_2O_3(O_2CR)_2]$ moiety bridged by four carboxylate groups to a tetranuclear $[V_4O_7(O_2CR)_3]$ unit in which the vanadium centers are in square pyramidal geometries. The binuclear and tetranuclear fragments may be regarded as mixed anhydrides of benzoic acid with divanadic and linear tetravanadic acids, respectively [140].

Although the hexametalate core $[M_6O_{19}]^{n-}$ is represented for $M = Nb$, Ta, Mo and W, $[V_6O_{19}]^{8-}$ has not been isolated, possibly as a consequence of the high charge/volume ratio. However, the hexavanadate core may be stabilized in the presence of organic ligands or organometallic moieties. The structure of $[V_6O_{13}\{O_2NC(CH_2O)_3\}_2]^{2-}$ [68] exhibits a $[V_6O_{13}]^{4+}$ core binding two $[RC(CH_2O)_3]^{3-}$ subunits (Fig. 33). Alternatively, the structure may be described as a hexametalate core $[V_6O_{19}]^{8-}$ supporting two $[RC(CH_2)_3]^{3+}$ subunits. The structural core is similar to that reported for $[(C_5H_5)Rh]_4[V_6O_{19}]$ [141,142].

(iv) Octanuclear to quindecanuclear species

The structure of $[V_8O_8(OCH_3)_{16}(C_2O_4)]^{2-}$ [143] is similar to that previously described for $[Mo_8O_{16}(OCH_3)_8(C_2O_4)]^{2-}$ (Fig. 23) with the exception that there are no V(IV)–V(IV) interactions. This latter observation appears to be a common feature of the structural chemistry of reduced polyoxovanadates.

Another example of a polyoxovanadate complex with V(IV) sites is provided

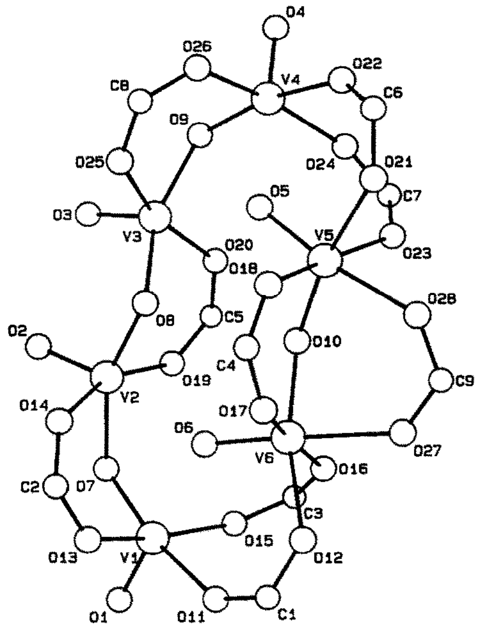

Fig. 32. The structure of $[V_6O_{10}(O_2CPh)_9]$.

by the nonanuclear $V_5^VV_4^{IV}$ cluster $[V_9O_{16}(bdta)_4]^{7+}$ (bdta = butanediaminetetracetate [71]), shown in Fig. 34. The structure contains a central tetrahedral VO_4^{3-} group linking four binuclear mixed valence moieties. The mixed-valence units are linked by the bdta ligands, acting as hepta-coordinating groups.

Although the decavanadate anion $[V_{10}O_{28}]^{6-}$ is well established in polyvanadate chemistry, replacement of peripheral oxo-groups by organic ligands with retention of the structural core has been achieved only recently [144]. The decanuclear complex $[V_{10}O_{13}\{CH_3C(CH_2O)_3\}_5]^-$ exhibits the decavanadate core, with 15 μ-oxo groups replaced by the alkoxy oxygen donors of the ligand, as shown in Fig. 35. The decavanadate core [134] consists of an efficiently packed cluster of edge-sharing octahedra, related to the structural type **VIII** of Fig. 4 by addition of two octahedra. Curious features of the polyanion are the presence of only V(IV) sites and the absence of any short V(IV)–V(IV) distances.

An unusual development in polyoxovanadate chemistry has been the recent description of soluble oxide inclusion complexes. The first of these to be reported is the dodecanuclear $[V_{12}O_{32}(CH_3CN)]^{4-}$ [72] whose structure, shown in Fig. 36, consists of an acetonitrile molecule suspended in the center of a basket-like $[V_{12}O_{32}]^{4-}$ cage. This *nido*-$[V_{12}O_{32}]^{4-}$ framework is derived from the *closo*-structures $[PV_{14}O_{42}]^{9-}$ [145] and $[V_{18}O_{42}]^{12-}$ [70] by removal of the appropriate number of [VO] vertices and the central PO_4^{3-} unit of the heteropoly-structure and by a small amount of reorganization of the vanadium polyhedra. Cages or "hollow

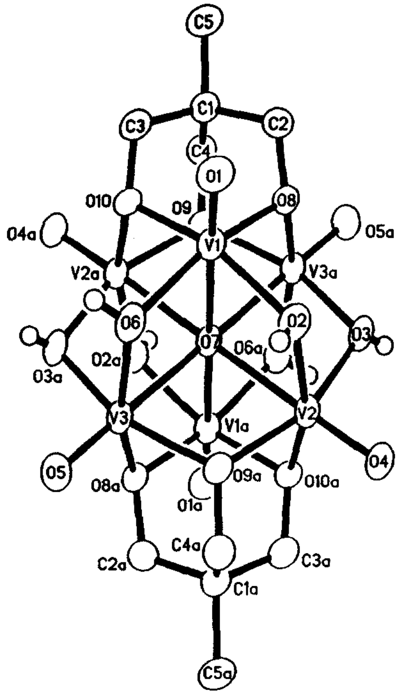

Fig. 33. The structure of $[V_6O_{13}\{CH_3C(CH_2O)_3\}_2]^{2-}$.

spheres" with "cryptand" properties have also been formed by exploiting the topological possibilities for linked VO_5 square pyramids. These spherical cluster shells, $[V_{18}O_{42}]$ and $[V_{15}O_{36}]$, are capable of encapsulating negatively charged ions to give complexes of the types $[H_4V_{18}O_{42}X]^{9-}$ (X = Br, I), $[V_{15}O_{36}Y]^{6-}$ (Y = Cl, Br) and $[V_{15}O_{36}(CO_3)]^{7-}$ [73]. The structure of the carbonate derivative, shown in Fig. 37, exhibits a spherical arrangement of edge-sharing $[VO_5]$ square pyramids surrounding a central $(CO_3)^{2-}$ group. These spherical cages are structurally related to their polyoxovanadate prototypes, the V(IV) cluster $[V_{18}O_{42}]^{12-}$ and the mixed-valence $V^{V}_{7}V^{IV}_{8}$ cluster $[V_{15}O_{36}]^{5-}$.

The common occurrence of vanadium(IV) centers in polyoxovanadate coordination complexes may reflect the relative oxidation and hydrolytic stability of the lower oxidation state isopolyoxovanadates and heteropolyoxovanadates. In addition to the examples cited above, heteropolyvanadate(IV) clusters, of which $[As_6V_{15}O_{42}(H_2O)]^{6-}$ [146] is an example, have also been described. Mixed-valence $V^{IV}V^{V}$ clusters include the $V^{V}_{8}V^{IV}_{2}$ cluster $[V_{10}O_{26}]^{4-}$ [147,148], the $V^{V}_{7}V^{IV}_{8}$ species $[V_{15}O_{36}]^{5-}$ [149], the $V^{V}_{13}V^{IV}_{6}$ aggregate $[V_{19}O_{40}H]^{8-}$ [150], and the heteropolyoxovanadate structure of the $V^{V}_{2}V^{IV}$ cluster $[P_2W_{15}V_3O_{62}]^{10-}$ [151].

The reduced vanadium polyanions exhibit a characteristic which is markedly

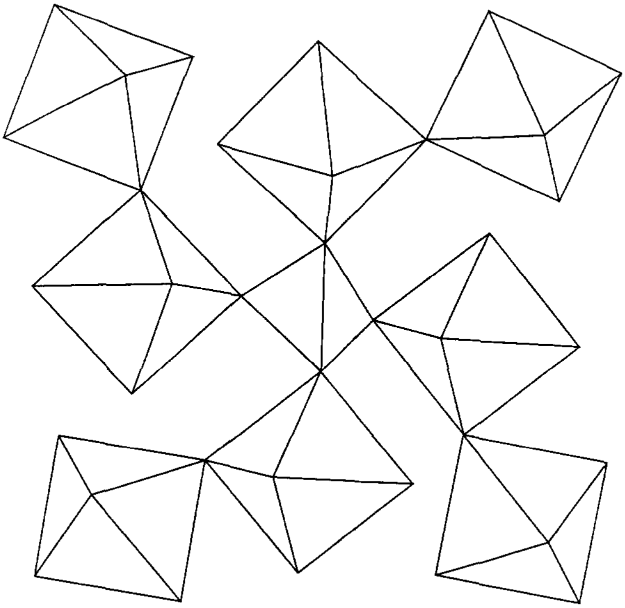

Fig. 34. Schematic representation of the structure of $[V_9O_{16}(bdta)_4]^{7-}$.

different from that observed for Mo and W species, namely, that metal–metal interactions are not pronounced for the V(IV)-containing complexes, in contrast to the Mo(V) and W(V) d^1 species which exhibit strong spin-pairing manifest in short M–M distances. As previously noted, the range of V^VV^{IV} mixed-valence structures is quite remarkable, including a single d^1 center in $[V^V_5V^{IV}O_{10}(O_2CPh)_9]$ [67] and $[V^V_3V^{IV}O_8(NO_3)(\text{thiophenecarboxylate})_4]^{2-}$ [65], two weakly ferromagnetically coupled d^1 centers in $[V^V_8V^{IV}_2O_{26}]^{4-}$ [147,148], and multi-vanadyl site clusters, exemplified by $[V^V_{13}V^{IV}_6O_{40}H]^{8-}$ [150], $[V^V_5V^{IV}_4O_{16}(bdta)_4]^{7+}$ [71], $[V^V_7V^{IV}_8O_{36}]^{5-}$ [149], and $[V^VV^{IV}_4Cl(\text{thiophene-2-carboxylate})_4]^{4-}$ [65]. In addition to the absence of short V(IV)–V(IV) distances in these structures, the vanadium coordination geometries are also observed to be variable, such that V(V) sites may adopt tetrahedral, square pyramidal, trigonal bipyramidal and octahedral geometries, while the V(IV) centers are observed in square pyramidal and octahedral coordination. This diversity of coordination type is reflected in the range of structures adopted by the polyvanadates.

D. SOLUTION CHEMISTRY: SELECTED EXAMPLES

The reaction chemistry of polyoxometalate anions in non-aqueous solvents has been characterized by the replacement of peripheral oxo groups by organometallic units [152–154], by a variety of simple organic ligands with oxygen, nitrogen and

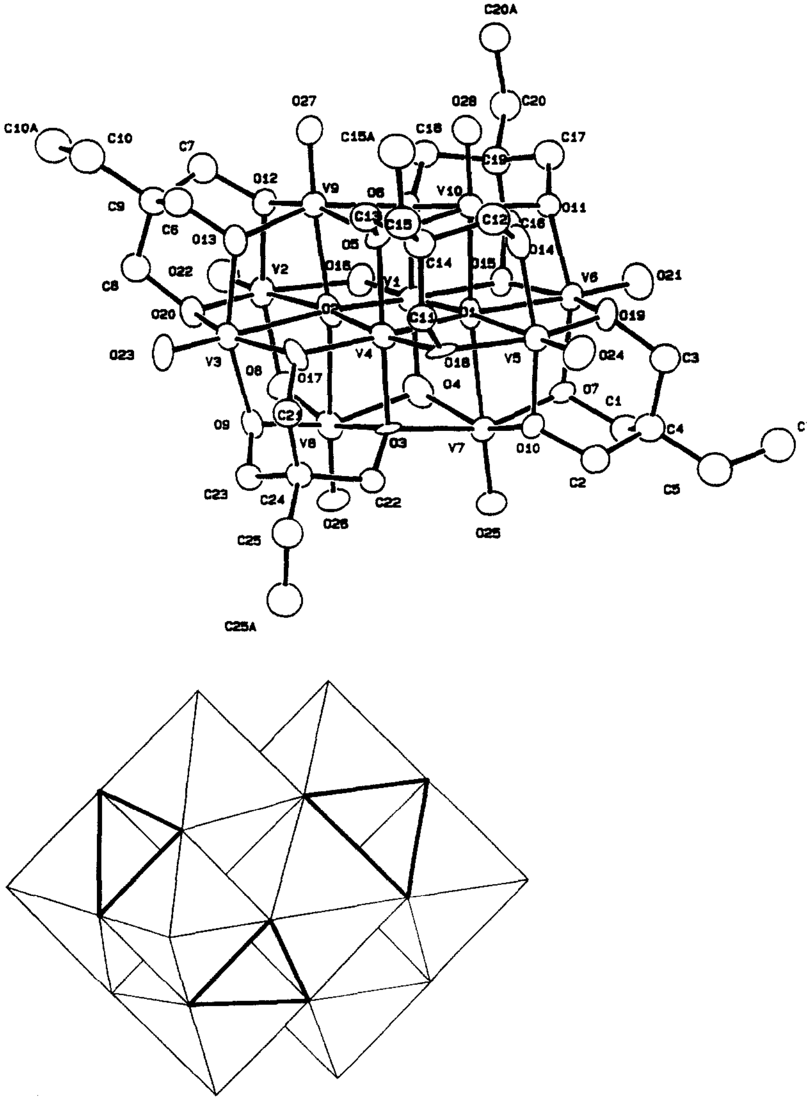

Fig. 35. The structure of $[V_{10}O_{13}\{CH_3C(CH_2O)_3\}_5]^-$ and a polyhedral representation of the structure.

sulfur donors, and by inorganic ligands such as halide and sulfide donors [155,156]. In addition, polyoxometalate coordination compounds exhibit electrochemical and chemical redox chemistry, oligomerization processes, and even transformations of organic substrate molecules.

The solution chemistry of polyoxoanions can be quite complicated. However, under carefully controlled conditions in organic solvents, a single polyoxoanion is formed in most cases, rather than a mixture of several oligomers. ^{17}O NMR spectro-

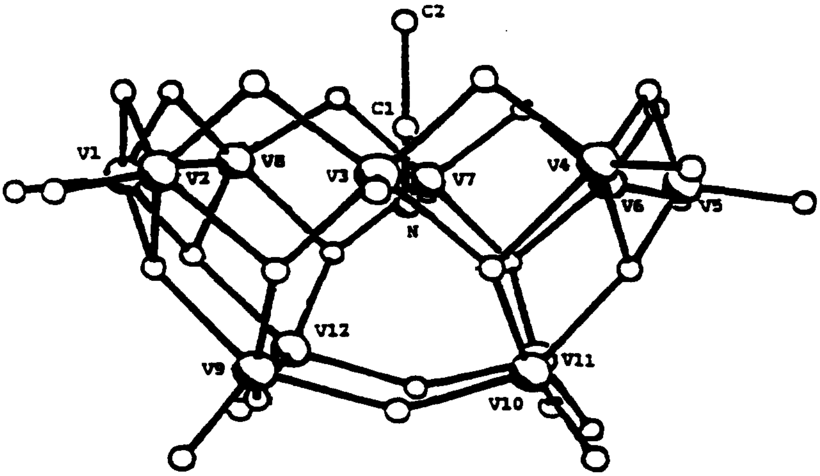

Fig. 36. The structure of $[V_{12}O_{32}(CH_3CN)]^{4-}$.

scopy has proved most useful in establishing the identity of these polyoxoanions in solution [157]. Chemical shift data provide the most readily interpreted structural information, and assignments can be made based on the general correlation between downfield chemical shift and oxygen π-bond order.

The chemistry of $[Mo_4O_{10}(OCH_3)_6]^{2-}$ in alcoholic solvents provides an example of the wide-ranging reaction chemistry associated with polyoxoanions in organic media and of the utility of ^{17}O NMR spectroscopy in identifying the species present in solution. Figure 38 presents a schematic summary of the chemistry of $[Mo_4O_{10}(OCH_3)_6]^{2-}$ and its derivative polyanion complexes.

Substitution chemistry of $[Mo_4O_{10}(OCH_3)_6]^{2-}$, involving peripheral oxo and methoxy groups, is readily effected by appropriate reagents. Thus, treatment with $(CH_3)_3SiCl$ results in displacement of the terminal methoxy groups, while reaction with catechols displaces both terminal and bridging methoxy groups.

$$[Mo_4O_{10}(OCH_3)_6]^{2-} + 2(CH_3)_3SiCl \rightarrow [Mo_4O_{10}(OCH_3)_4Cl_2]^{2-} + 2(CH_3)_3SiOCH_3$$

$$[Mo_4O_{10}(OCH_3)_6]^{2-} + HOC_6H_4OH \rightarrow [Mo_4O_{10}(OCH_3)_2(OC_6H_4O)_2]^{2-} + 4CH_3OH$$

The identity of the reactant and product in solution for this latter reaction are confirmed by ^{17}O NMR spectra, shown in Fig. 39.

The addition of reducing agents to $[Mo_4O_{10}(OCH_3)_4Cl_2]^{2-}$ results in reduction of Mo(VI) centers to Mo(V) sites in $[Mo_4O_8(OCH_3)_2Cl_4(HOCH_3)_2]^{2-}$. The

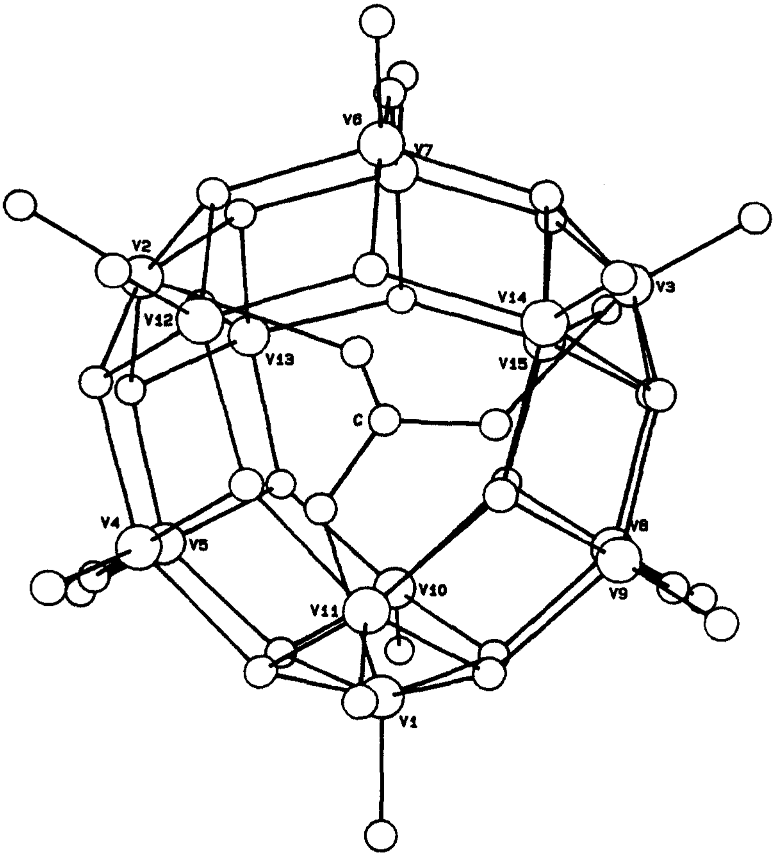

Fig. 37. The structure of $[V_{15}O_{36}(CO_3)]^{7-}$.

reduced core is also sufficiently stable to undergo substitution reactions at the terminal chloride and methanol sites

$$[Mo_4O_8(OCH_3)_2Cl_4(HOCH_3)_2]^{2-} + 4H_2C_4O_4 \rightarrow$$

$$[Mo_4O_8(OCH_3)_2(C_4O_4)_2(C_4O_4H)_2]^{4-} + 2HOCH_3 + 4HCl + 2H^+$$

$$[Mo_4O_8(OCH_3)_2Cl_4(HOCH_3)_2]^{2-} + 2Mo_2O_7^{2-} + 2H^+ + 2H_2O \rightarrow$$

$$[H_2Mo_4O_8(OCH_3)_2(MoO_4)_4]^{4-} + 4HCl + 2HOCH_3$$

The tetranuclear species $[Mo_4O_{10}(OCH_3)_6]^{2-}$ also reacts with monosubstituted hydrazines with displacement of terminal oxo-groups and with core rearrangement to give the complexes of the $[Mo_4O_8(NNR)_4(OCH_3)_2]^{2-}$ class. This latter complex reacts, in turn, with catechols by substitution of one terminal oxo-group at each tetrahedral $[MoO_4]$ unit of the parent to give $[Mo_4O_6(OCH_3)_2(NNPh)_4$-

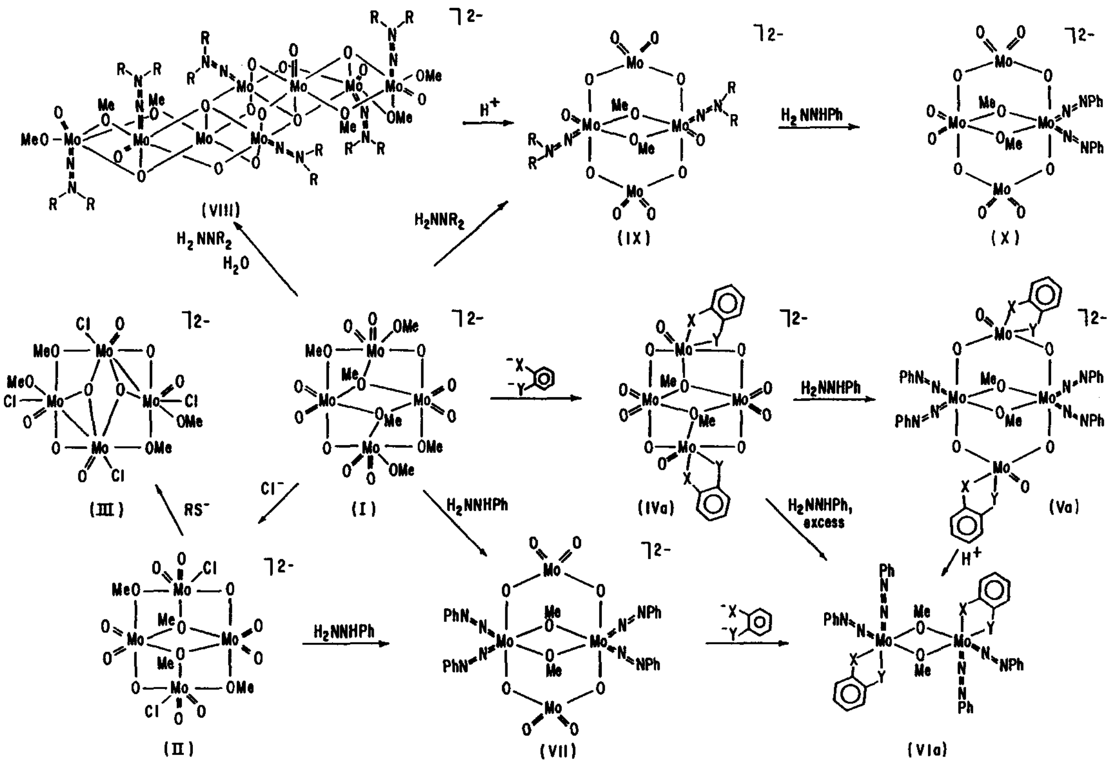

Fig. 38. Solution chemistry of $[Mo_4O_{10}(OCH_3)_6]^{2-}$.

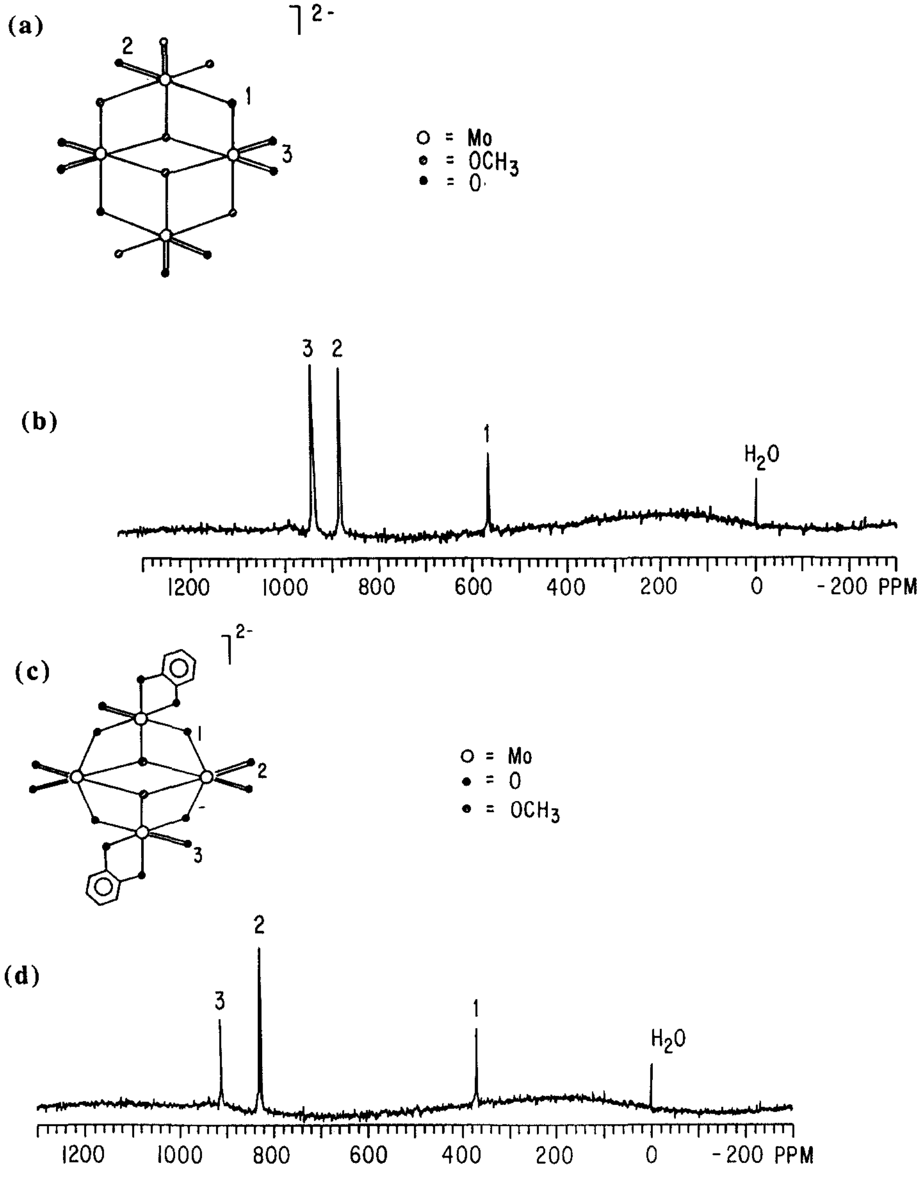

$(OC_6H_4O)_2]^{2-}$, whose structure is shown schematically in Fig. 39. The identity of this species in solution may again be confirmed by ^{17}O NMR as shown in Fig. 39(f).

In the presence of excess ligand, however, the weakly bonded $[MoO_4]^{2-}$ groups of $[Mo_4O_8(OCH_3)_2(NNPh)_4]^{2-}$ may be displaced by a variety of ligands, including squarate to give $[Mo_2(OCH_3)_2(C_4O_4)_2(NNPh)_4]^{2-}$ [44], catechols to give $[Mo_2(OCH_3)_2(OC_6H_4O)_2(NNPh)_4]^{2-}$, and neutral and monoanionic ligands to give the neutral binuclear series of complexes $[Mo_2(OR)_2(NNPh)_4(L_1)_2(L_2)_2]$ [158–160].

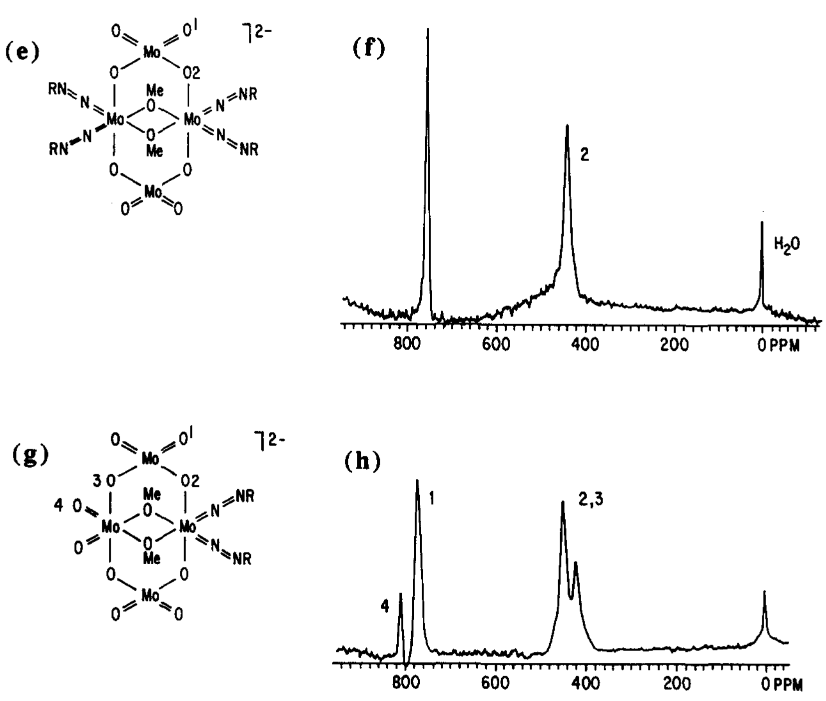

The displacement of tetrahedral units $[MoO_4]^{2-}$ from polyanions, particularly by dianionic ligands with similar geometric requirements, is quite general.

In contrast to the reactions with phenylhydrazine, $[Mo_4O_{10}(OCH_3)_6]^{2-}$ reacts with 1,1-disubstituted hydrazines to give complexes with the *cis*-$[MoO(NNR_2)]^{2+}$ core, rather than the *cis*-bisdiazenido core $[Mo(NNPh)_2]^{2+}$. The product of this reaction, $[Mo_4O_{10}(OCH_3)_2(NNR_2)_2]^{2-}$, reacts in controlled hydrolysis reactions to aggregate into a higher oligomer.

$$3[Mo_4O_{10}(OCH_3)_2(NNR_2)_2]^{2-} \xrightarrow{H_2O/MeOH} [Mo_8O_{16}(OCH_3)_6(NNR_2)_6]^{2-} + 2Mo_2O_7^{2-}$$

Although the principles underlying polyanion accretion are not understood in detail, condensation processes have been invoked [161,162]. The aggregation process is demonstrated most convincingly in the synthesis of higher oligomers from $[Mo_2O_4\{RC(CH_2O)_3\}_2]^{2-}$ [14,20,163–168]. The structural interrelationships of the bi-, tri-, and tetranuclear are shown in Fig. 40, which illustrates schematically the course of the aggregation process viewed as successive condensations of $[MoO_2(OR)]^+$ units.

$$[Mo_2O_7]^{2-} + 2H_3L \rightarrow [Mo_2O_4L_2]^{2-} + 3H_2O$$

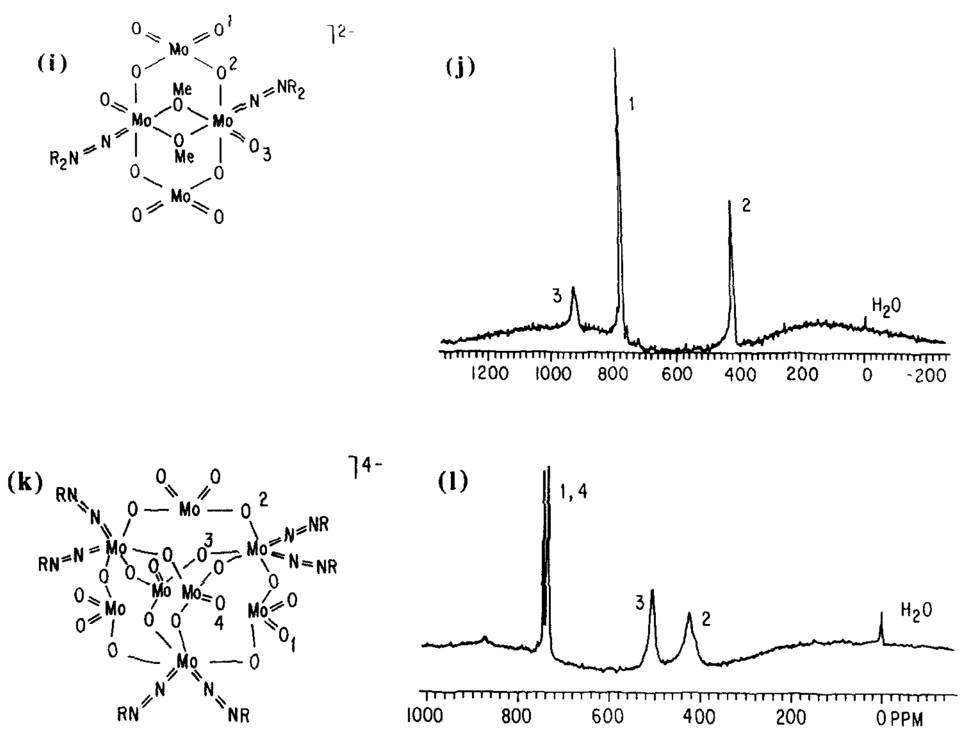

Fig. 39. (a) Schematic representation of the structure of $[Mo_4O_{10}(OCH_3)_6]^{2-}$, with oxygen environments labelled; (b) ^{17}O NMR spectrum of $[Mo_4O_{10}(OCH_3)_6]^{2-}$; (c) schematic representation of $[Mo_4O_8(OCH_3)_2(OC_6H_4O)_6]^{2-}$, indicating the different oxo-group environments; (d) ^{17}O NMR spectrum of $[Mo_4O_8(OCH_3)_2(OC_6H_4O)_2]^{2-}$; (e) schematic representation of the structure of $[Mo_4O_8(OCH_3)_2(NNR)_4]^{2-}$; (f) ^{17}O NMR spectrum of $[Mo_4O_8(OCH_3)_2(NNR)_4]^{2-}$; (g) schematic representation of the structure of $[Mo_4O_{10}(OCH_3)_2(NNR)_2]^{2-}$; (h) ^{17}O NMR spectrum of $[Mo_4O_{10}(OCH_3)_2(NNR)_2]^{2-}$; (i) schematic representation of the structure of $[Mo_4O_{10}(OCH_3)_2(NNR_2)_2]^{2-}$; (j) ^{17}O NMR spectrum of $[Mo_4O_{10}(OCH_3)_2(NNR_2)_2]^{2-}$; (k) schematic representation of the structure of $[Mo_8O_{16}(OCH_3)_6(NNR_2)_6]^{2-}$; (l) ^{17}O NMR spectrum of $[Mo_8O_{16}(OCH_3)_6(NNR_2)_6]^{2-}$.

$$2[Mo_2O_4L_2]^{2-} + [Mo_2O_7]^{2-} + H_3L + MeOH \rightarrow$$

$$[Mo_3O_6(OMe)L_2]^{-} + [Mo_3O_7L_2]^{2-} + 2H_2O + L^{3-}$$

$$2[Mo_3O_6(OMe)L_2]^{-} + [Mo_2O_7]^{2-} + 6MeOH \rightarrow$$

$$[Mo_4O_8(OMe)_2L_2] + [Mo_4O_{10}(OMe)_6]^{2-} + H_2O + 2H_2L^{-}$$

$$2[Mo_4O_8(OMe)_2L_2] + 4H_2O \rightarrow [H_2Mo_8O_{20}(OMe)_4L_2] + 2H_3L$$

New reaction pathways are available if the oxo groups of the polyoxoanions are sufficiently basic/nucleophilic. The $[MoO_3]$ unit of $[Mo_3O_7\{RC(CH_2O)_3\}_2]^{2-}$ offers a reactive site of this type, allowing protonation, alkylation and silylation reactions.

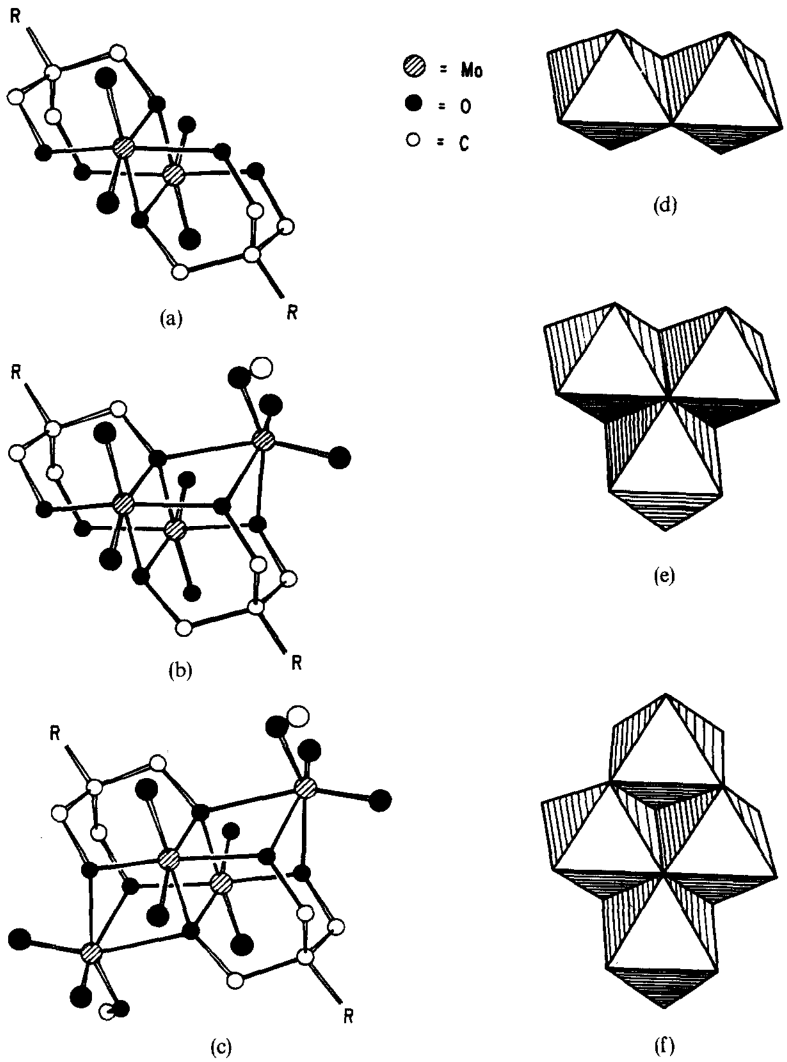

Fig. 40. Schematic representation of the structures of $[Mo_2O_4\{RC(CH_2O)_3\}_2]^{2-}$, $[Mo_3O_6(OCH_3)\{RC(CH_2O)_3\}_2]^{-}$ and $[Mo_4O_8(OCH_3)_2\{RC(CH_2O)_3\}_2]$.

This behavior may be compared with that of the $[WO_3]$ unit of [(1,4,7-triazocyclononane(WO_3]$\cdot 3H_2O$ [182].

$$2[Mo_3O_7L_2]^{1-} \xrightarrow{H+} 2[Mo_3O_6(OH)L_2]^{1-} \xrightarrow{-H_2O} [\{Mo_3O_6L_2\}_2O]^{2-}$$

$$[Mo_3O_7L_2]^{2-} \xrightarrow[-X]{+RX} [Mo_3O_6(OR)L_2]^{1-}$$

In addition to substitution reactions, oligomerizations, and alkylation-type processes, polyoxoanions often react with organic substrates to effect chemistry at the organic site. The most common reaction of this type is the carbonyl insertion reaction, which is quite general in converting aldehydes to acetals and dialdehydes to diacetals. The process may be illustrated by the reaction of dimolybdate with glyoxal to give the formylated methylenedioxymolybdate. The carbonyl group of this species inserts into an adjacent Mo—O bond upon replacement of OH^- with F^- or HCO_2^- [42]. This reaction is quite general and has been observed for ninhydrin, benzil and phenanthraquinone [43,99].

$$[Mo_2O_7]^{2-} + OHCCHO \rightarrow [OHCCHMo_4O_{15}H]^{3-}$$

$$[OHCCHMo_4O_{15}H]^{3-} + HX \rightarrow [(H_2C_2O_4)Mo_4O_{11}X]^{3-} + H_2O$$

On the other hand, rhodizonic acid, $C_6O_4(OH)_2$ [169] reacts with polyoxomolybdates with ligand dissociation to give $[Mo_8O_{16}(OCH_3)_8(C_2O_4)]^{2-}$ (Fig. 25). The synthesis of a Mo(V)–oxalate cluster from polyoxomolybdate(VI) and rhodizonic acid precursors implies that, in this instance, the well-documented carbonyl insertion reaction is coupled with ligand dissociation and redox processes. Although no mechanistic information is available, the process most likely involves a succession of two-electron transfers and cationic intermediates of the types illustrated in Fig. 41. Since multicenter Mo clusters are involved in the chemistry, the formally Mo(IV) sites produced in this sequence of electron transfer steps are in close proximity to oxidized Mo(VI) sites and rapid disproportionation is to be expected

$$\mathrm{Mo(IV)\cdots Mo(VI) \rightarrow Mo(V)\cdots Mo(V)}$$

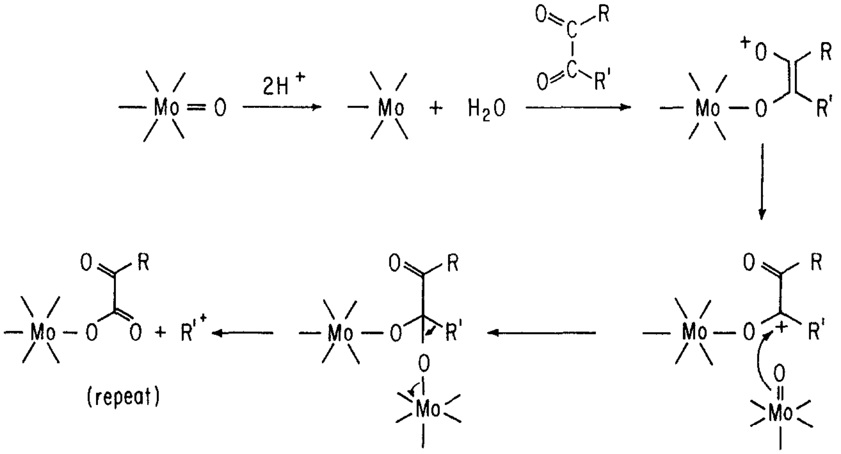

Fig. 41. Possible mechanism for the synthesis of $[Mo_8O_{16}(OCH_3)_8(C_2O_4)]^{2-}$ from $[Mo_2O_7]^{2-}$ and rhodizonic acid.

Under more forcing reaction conditions, polyoxoanion coordination compounds may effect dramatic organic transformations. For example, while thermal decomposition of $[Mo_3O_6(OEt)\{RC(CH_2O)_3\}_2]^-$ yields acetaldehyde and ethanol as organic products, photochemical degradation yields ethylene, as well as acetaldehyde and ethanol. Similar results have been observed in the degradation of $[(P_3O_9)MoO_3CH_2CH_3]^{2-}$ [2], and the photochemical process has been rationalized in terms of a carbonyl Norrish Type II intramolecular hydrogen transfer (Fig. 42). The production of ethylene would proceed by the six-membered intermediate shown while acetaldehyde production would result from a five-membered ring transition state.

Although the solution chemistry of polyoxoanion coordination complexes remains largely unexplored, the range of reactivity appears to encompass both organic molecule activation as well as substitution chemistry and accretion processes centered at the polyoxometalate core.

E. ELECTRONIC STRUCTURES: ELECTROCHEMISTRY, MIXED VALENCY SPECIES, AND REDUCED SPECIES

The electronic structures of oxidized (d^0) polyoxometalates have been discussed in terms of the properties of the individual MO_6 octahedra of the polynuclear framework. The MO_6 octahedra may be described in terms of two classes of idealized geometries: the "mono-oxo" (C_{4v}) class or type I which have one terminal oxo group and the "*cis*-dioxo" (C_{2v}) class or type II which exhibit two terminal oxo groups [170]. While the lowest unoccupied molecular orbital of the type I class is approximately non-bonding and metal-centered, the LUMO for the type II octahedra is strongly antibonding with respect to the M=O bonds. As a consequence of this difference in the characteristics of the LUMO, type I polymetalates may be reduced reversibly to mixed valence species while type II polymetalates exhibit irreversible reduction processes.

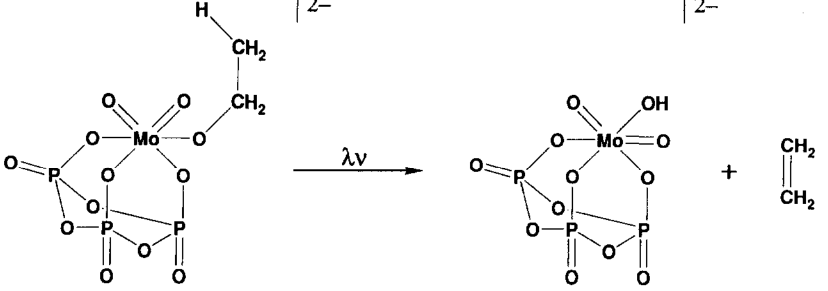

Fig. 42. The production of ethylene from coordinated ethoxide by a mechanism similar to the Norrish type II intramolecular hydrogen transfer.

These restrictions apply to the coordination compounds of polyoxometalate as well. Thus, all the polyoxomolybdate complexes of Table 2 constructed from octahedra with the *cis*-dioxo unit exhibit irreversible reductions in their electrochemistry with the exception of the "semiquinone" derivatives of which $(TBA)_2$-$[Mo_4O_{10}(C_6H_2O_4)_2]$, shown in Fig. 43, is characteristic [43,99]. However, careful analysis of the electrochemical and spectroscopic data indicates that the electrochemical processes are totally ligand-based rather than metal-based, such that the common $[Mo_2O_5]^{2+}$ units [171–176], which provide the framework for these structural types, are unaffected by the redox processes. Characteristic cyclic voltammograms are shown in Fig. 44.

The reduction process for $[Mo_4O_{10}(C_6H_2O_4)_2]^{2-}$ may be summarized by

$$[Mo_4O_{10}(C_6H_2O_4)_2]^{2-} \xrightleftharpoons{-0.208\ V} [Mo_4O_{10}(C_6H_2O_4)_2]^{3-} \xrightleftharpoons{-0.677\ V} [Mo_4O_{10}(C_6H_2O_4)_2]^{4-}$$

Such successive one-electron processes are characteristic of ligand-based redox, rather than metal-centered processes, a feature of the electrochemistry confirmed by the EPR spectrum of the one-electron reduced species $[Mo_4O_{10}(C_6H_2O_4)_2]^{3-}$. The sharp, single-line spectrum, centered at $g = 1.999$, is characteristic of an unpaired electron localized on the ligand orbitals. Addition of a second electron to give $[Mo_4O_{10}(C_6H_2O_4)_2]^{4-}$ results in a diamagnetic, EPR-silent species.

In contrast to this behavior, $[Mo_6O_{15}(C_6O_6)_2]^{3-}$ exhibits a reversible one-electron reduction *and* a reversible one-electron *oxidation.*

$$[Mo_6O_{15}(C_6O_6)_2]^{2-} \xrightleftharpoons{-0.428\ V} [Mo_6O_{15}(C_6O_6)_2]^{3-} \xrightleftharpoons{-0.024\ V} [Mo_6O_{15}(C_6O_6)_2]^{4-}$$

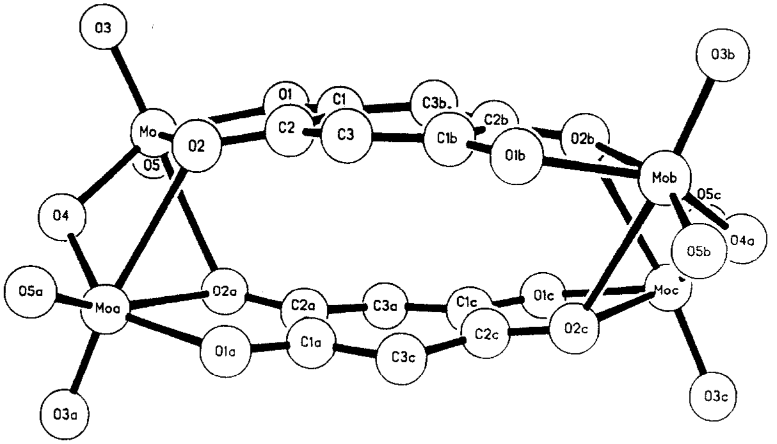

Fig. 43. The structure of $[Mo_4O_{10}(C_6H_2O_4)_2]^{2-}$.

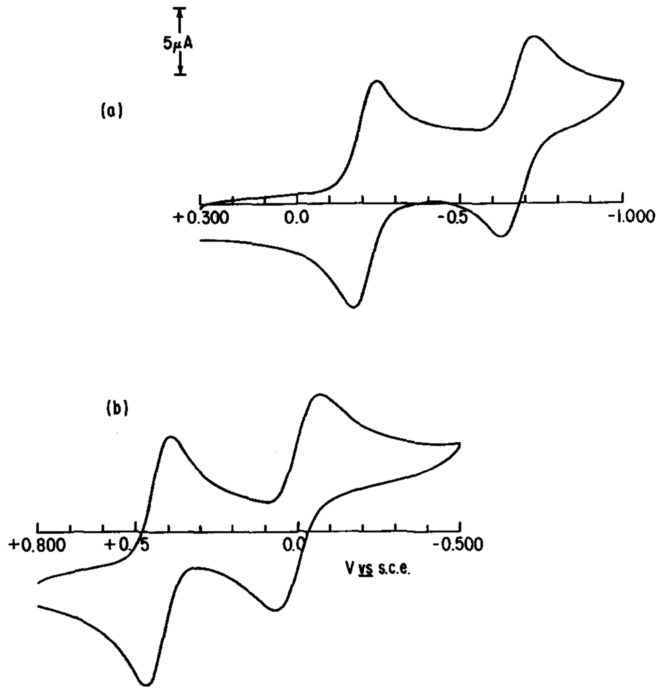

Fig. 44. Cyclic voltammograms for $[Mo_4O_{10}(C_6H_2O_4)_2]^{2-}$ and $[Mo_6O_{15}(C_6O_6)_2]^{3-}$.

Since the rest state for $[Mo_6O_{15}(C_6O_6)_2]^{3-}$ is one oxidation state negative of the stable form of $[Mo_4O_{10}(C_6H_2O_4)_2]^{2-}$, the complexes exhibit the identical redox levels but shifted ca. 0.65 V more positive in potential for $[Mo_6O_{15}(C_6O_6)_2]^{3-}$. Thus, one-electron oxidation of the paramagnetic $[Mo_6O_{15}(C_6O_6)_2]^{3-}$ removes an electron from the HOMO to give the diamagnetic $[Mo_6O_{15}(C_6O_6)_2]^{2-}$. Similarly, one-electron reduction of $[Mo_6O_{15}(C_6O_6)_2]^{3-}$ results in spin-pairing in the ligand-based HOMO to give the diamagnetic $[Mo_6O_{15}(C_6O_6)_2]^{4-}$.

Type I polymolybdate clusters are represented by the hexametalate series $[Mo_6O_{19}]^{2-}$, $[Mo_6O_{18}(NNPh)]^{3-}$ and $[Mo_6O_{18}(NNR_2)]^{2-}$. An unusual feature of the structure is the difference in the formal oxidation states of the Mo centers: in $[Mo_6O_{19}(NNR)]^{3-}$ the diazenido(1+) formalism results in the $Mo_5^{VI}Mo^{II}$ description while for $[Mo_6O_{18}(NNR_2)]^{2-}$ the hydrazido(2−) formalism requires that all six Mo centers be in the +6 oxidation state, as are the Mo centers of the parent complex $[Mo_6O_{19}]^{2-}$. Although such formal oxidation states should be viewed with caution, the differences in the cluster oxidation levels are apparent in the redox behavior of these complexes, illustrated in Fig. 45. The hydrazido(2−) species $[Mo_6O_{18}(NNR_2)]^{2-}$ exhibits electrochemical characteristics similar to those of $[Mo_6O_{19}]^{2-}$ but shifted to more positive potentials. Thus, there are two successive

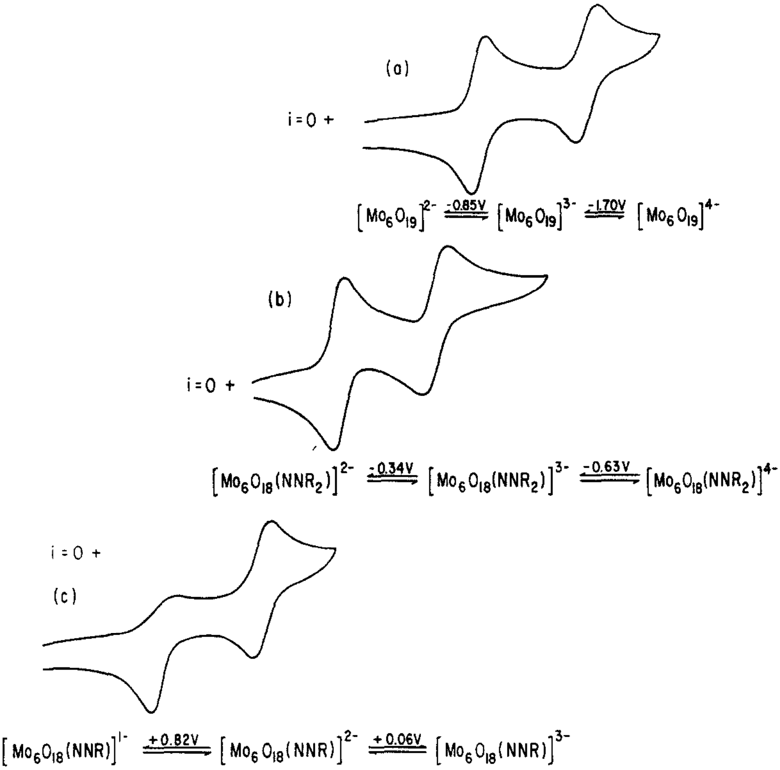

Fig. 45. Cyclic voltammograms for $[Mo_6O_{19}]^{2-}$, $[Mo_6O_{18}(NNR_2)]^{2-}$ and $[Mo_6O_{18}(NNPh)]^{3-}$.

one-electron reductions at −0.35 and −0.63 V, compared with −0.85 and −1.70 V for $[Mo_6O_{19}]^{2-}$. In contrast, $[Mo_6O_{18}(NNPh)]^{3-}$, exhibits successive one-electron *oxidations* at +0.08 and +0.84 V. These oxidative processes are consistent with the presence of a reduced molybdenum center, since polyoxomolybdate(VI) clusters would be expected to be thermodynamically resistant to oxidation [178].

Mixed-valence clusters were seen to be common in the polyvanadate chemistry, and a varied electrochemistry might be anticipated. This has been realized in the "hexavanadate" series of complexes which exhibit structurally identical cores with different electron populations. The red complex $[V_6O_{13}\{RC(CH_2O)_3\}_2]^{2-}$ exhibits reversible one-electron reduction to give the emerald green $V^V_5V^{IV}$ mixed-valence complex $[V_6O_{13}\{RC(CH_2O)_3\}_2]^{3-}$ whose EPR spectrum indicates charge localization at a single vanadium site at low temperatures and rapid intramolecular electron transfer or "hopping" at higher temperatures (Fig. 46).

The hexametalate $[V_6O_{13}\{RC(CH_2O)_3\}_2]^{2-}$ also undergoes coupled reduction and protonation reactions to give the mixed valence species $[V^V_4V^{IV}_2O_{11}(OH)_2\{RC(CH_2O)_3\}_2]^{2-}$, and $[V^V_2V^{IV}_4O_9(OH)_4\{RC(CH_2O)_3\}_2]^{2-}$ and the fully-reduced $[V^{IV}_6(OH)_6\{RC(CH_2O)_3\}_2]^{2-}$ (Fig. 47). Although the magnetic moments

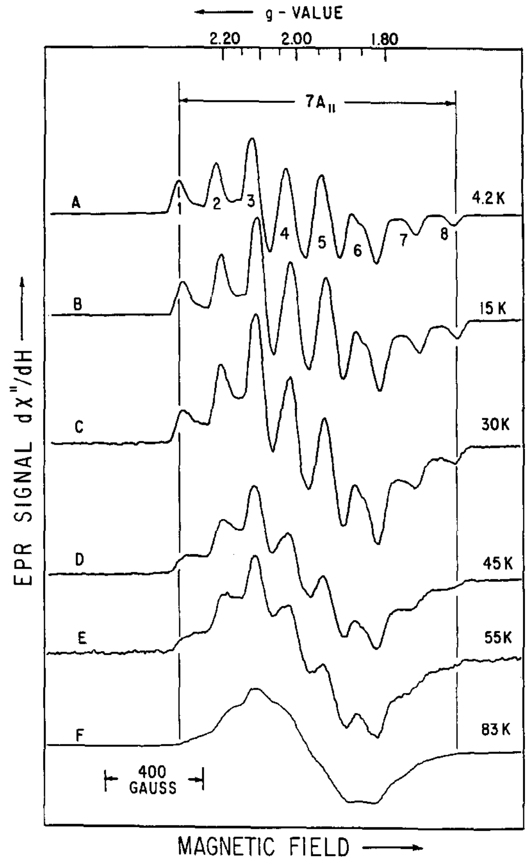

Fig. 46. EPR spectrum of $[V_6O_{13}\{RC(CH_2O)_3\}_2]^{3-}$.

of these complexes decrease with increasing number of V(IV) centers, the antiferromagnetic coupling occurs in the absence of V—V bonding, the maor consequences of reduction manifesting themselves in cluster expansion (Fig. 48).

F. CONCLUSIONS

Although systematic studies of polyoxometalate coordination chemistry are of recent origin, the growth of the field in the last decade, and particularly since 1985, has been significant. The field has been characterized by the varied structural chemistry associated with these aggregates and by a rich spectroscopy and electrochemistry for certain classes of complexes. The potential applications to catalysis and the value of these species as models for interactions of organic substrates with metal oxide surfaces have been discussed [2,4,5].

However, there are yet great opportunities for the realization of interesting

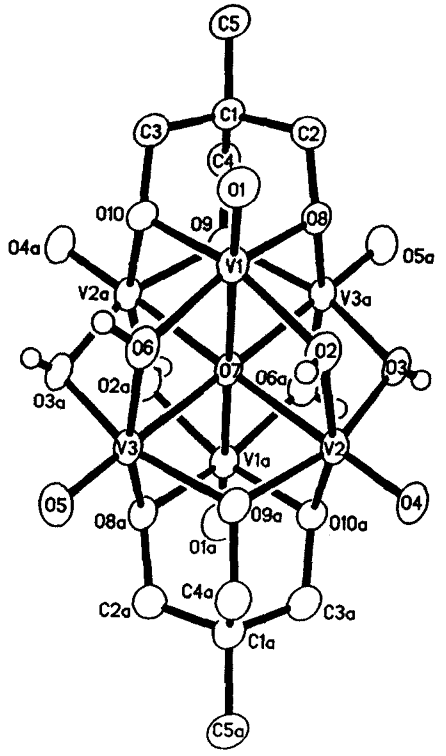

Fig. 47. The structure of $(TBA)_2[V_6^{IV}O_7(OH)_6\{RC(CH_2O)_3\}_2]$.

chemistry. Although a multitude of new structural types have been characterized, the mechanisms of accretion processes in solution remain elusive. Likewise, control of aggregation has not been achieved to allow the construction of clusters of a given nuclearity or molecular architecture. Perhaps the time is ripe for the design of ligands which may constrain the aggregation process or extend the nuclearity. Ligands developed from arboral technology [178,179], for example, may provide a starting point for molecular engineering of novel polyoxometalates.

The mixed-valence chemistry of polyoxometalate coordination complexes has also developed sporadically and requires a more systematic approach. The wide range of oxidation states available to vanadium and molybdenum and their variable coordination numbers and geometries provide an unusual potential for the existence of novel mixed-valence clusters. Similarly, few attempts have been documented to incorporate heterometal centers into polyoxometalate coordination complexes to provide species of the type $[M_xM'_yO_zL_n]$, although the precedent exists in the organometallic chemistry where species such as $[(C_4H_9)_4N]_3[Nb_2W_4O_{18}(OSiR_3)]$ [181] and $[(C_5H_5)TiW_5O_{18}]^{3-}$ [182], to name but two, have been described.

Only a decade ago, polyoxometalate coordination complexes were virtually

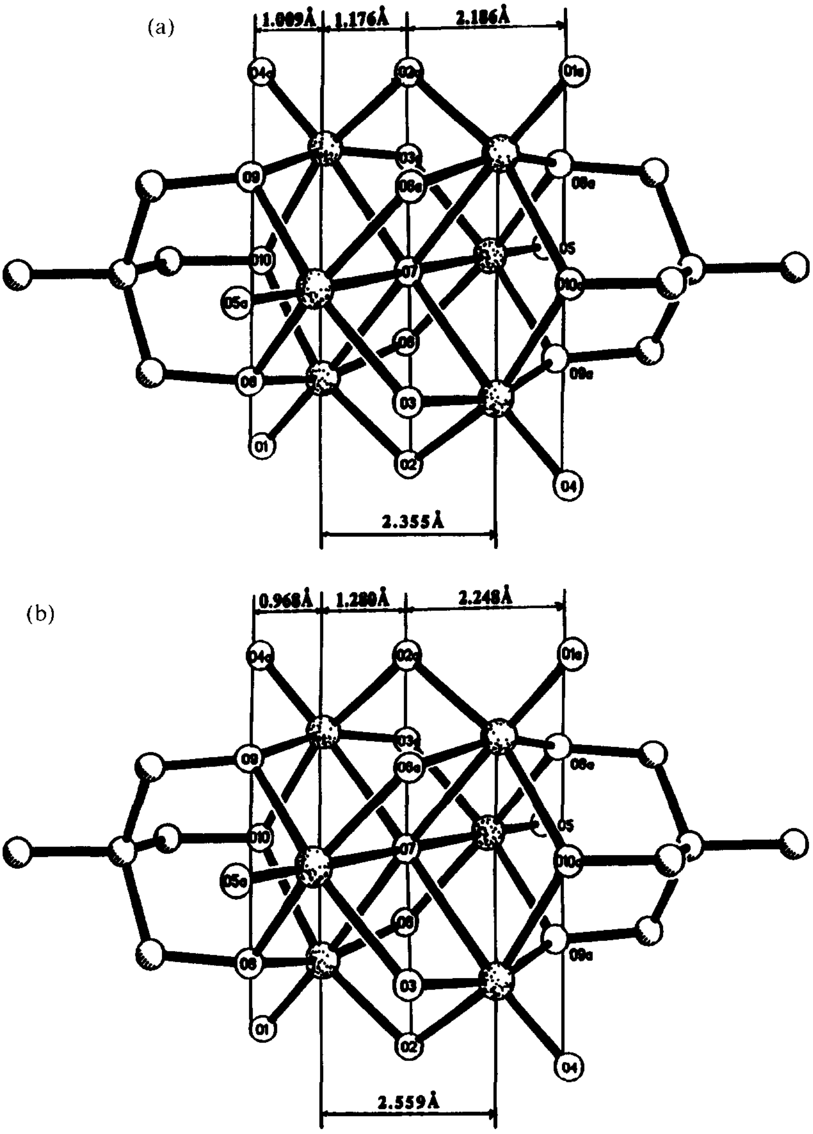

unknown. The first examples seemed to be chemical curiosities, exotic compounds prepared inadvertently or in the absence of rational synthetic design. This is no longer the case since the advent of a variety of synthetic precursors which provide a starting point for the study of covalent transformations of the type conventionally used in organic and organometallic chemistry [5]. As a consequence, rational synthesis and systematic studies of polyoxometalate coordination complexes are attracting growing interest. As more examples of this class of complexes are characterized, the structural interrelationships will evolve, as well as the understanding of reactivity

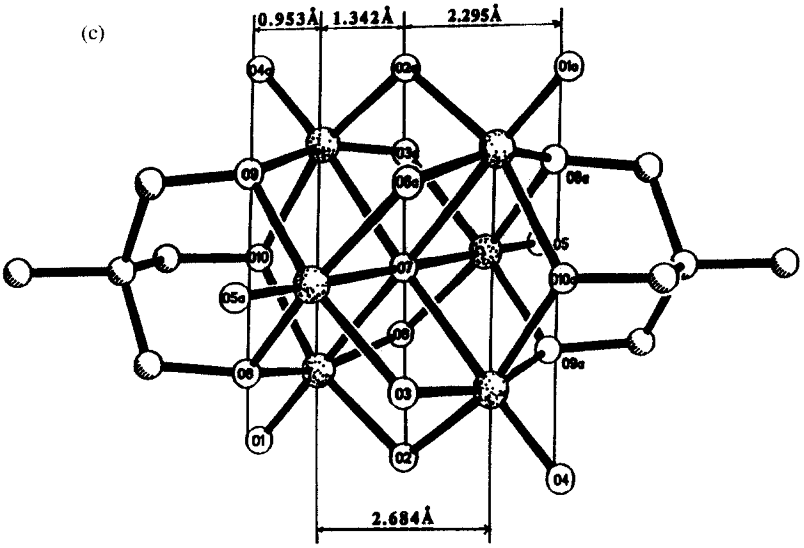

Fig. 48. Comparison of the structures of (a) $[V_6O_{13}\{RC(CH_2O)_3\}_2]^{2-}$, (b) $[V_6O_9(OH)_4\{RC(CH_2O)_3\}_2]^{2-}$ and (c) $[V_6O_7(OH)_6\{RC(CH_2O)_3\}_2]^{2-}$ viewed as planar layers of negatively charged close-packed oxygen atoms separated by layers of vanadium cations.

and mechanisms of polyoxoanion transformations. We hope that this review will stimulate the continuing growth of this area of chemistry.

REFERENCES

1 N.N. Greenwood and A. Earnshaw, Chemistry of the Elements, Pergamon Press, New York, 1984.
2 V.W. Day, W.G. Klemperer, C. Schwartz and R.-C. Wang, in J.M. Bassett and B. Gates (Eds.), Surface Organometallic Chemistry: Molecular Approaches to Surface Catalysis, NATO ASI Series C, Vol. 231, Kluwer, Dordrecht, 1988, p. 173.
3 I.M. Campbell, Catalysis at Surfaces, Chapman and Hall, New York, 1988.
4 M.T. Pope, Heteropoly and Isopolymetalates, Springer-Verlag, New York, 1983.
5 V.W. Day and W.G. Klemperer, Science, 228 (1985) 533.
6 A.J. Miolati, J. Prakt. Chem., 77 (1908) 439.
7 A. Rosenheim and R. Bilecki, Ber., 4 (1913) 543.
8 R.D. Adams, W.G. Klemperer and R.-S. Liu, J. Chem. Soc. Chem. Commun., (1979) 256.
9 V.W. Day, M.F. Fredrick, W.G. Klemperer and R.-S. Liu, J. Am. Chem. Soc., 101 (1979) 491.
10 E.M. McCarron III, J.F. Whitney and D.B. Chase, Inorg. Chem., 23 (1984) 3275.
11 E.M. McCarron III and R.L. Harlow, J. Am. Chem. Soc., 105 (1983) 6179.
12 Q. Chen, L. Ma, S. Liu and J. Zubieta, J. Am. Chem. Soc., 111 (1989) 5944.
13 M. Filowitz, W.G. Klemperer and W. Shum, J. Am. Chem. Soc., 100 (1978) 2580.
14 L. Ma, S. Liu and J. Zubieta, Inorg. Chem., 28 (1989) 175.
15 E.M. McCarron III and R.L. Harlow, J. Chem. Soc. Chem. Commun., (1983) 90.
16 S. Liu, S.N. Shaikh and J. Zubieta, Inorg. Chem., 26 (1987) 4305.

17 H. Kang, S. Liu, S.N. Shaikh, T. Nicholson and J. Zubieta, Inorg. Chem., 28 (1989) 920.
18 S. Liu, S.N. Shaikh and J. Zubieta, J. Chem. Soc. Chem. Commun., (1988) 1017.
19 S. Liu, S.N. Shaikh and J. Zubieta, Inorg. Chem., 28 (1989) 723.
20 A.J. Wilson, W.T. Robinson and C.J. Wilkins, Acta Crystallogr. Sect. C, 39 (1983) 54.
21 M.F. Belicchi, G.G. Fava and C. Pelizzi, J. Chem. Soc. Dalton Trans., (1983) 65.
22 J.A. Beaver and M.G.B. Drew, J. Chem. Soc. Dalton Trans., (1973) 1376.
23 M.H. Chisholm, J.C. Huffman, C.C. Kirkpatrick, J. Leonelli and K. Folting, J. Am. Chem. Soc., 103 (1981) 6093.
24 V. Chilou, P. Gouzerh, Y. Jeannin and F. Robert, J. Chem. Soc. Chem. Commun., (1989) 76.
25 V. Chilou, P. Gouzerh, Y. Jeannin and F. Robert, J. Chem. Soc. Chem. Commun., (1987) 1469.
26 M.B. Hursthouse, R.L. Short, B. Piggott, A. Tucker and S.F. Wong, Polyhedron, 5 (1986) 2121.
27 T.-C. Hsieh and J. Zubieta, Inorg. Chem., 24 (1985) 1287.
28 T.-C. Hsieh and J. Zubieta, Polyhedron, 5 (1986) 305.
29 S. Liu and J. Zubieta, Polyhedron, 7 (1988) 401.
30 H. Kang, S. Liu, S.N. Shaikh and J. Zubieta, Inorg. Chem., 28 (1989) 920.
31 D. Attanasio, V. Fares and P. Imperatori, J. Chem. Soc. Chem. Commun., (1986) 1476.
32 S. Bank, S. Liu, S.N. Shaikh, X. Sun, J. Zubieta and P.D. Ellis, Inorg. Chem., 27 (1988) 3535.
33 S.N. Shaikh and J. Zubieta, Inorg. Chem., 25 (1986) 4615.
34 M.A. Porai-Koshits, L.A. Aslanov, G.V. Ivanova and T.N. Polynova, J. Struct. Chem. (USSR), 9 (1968) 401.
35 C.B. Knobler, A.J. Wilson, R.N. Hilder, I.W. Jensen, B.R. Penfold, W.T. Robinson and C.J. Wilkins, J. Chem. Soc. Dalton Trans., (1983) 1299.
36 L.R. Nassimbeni, M.L. Niven, J.J. Cruywager and J.B.B. Heyns, J. Crystallogr. Spectrosc. Res., 17 (1987) 373.
37 N.W. Alcock, M. Dudik, R. Grybos, E. Hodorowicz, A. Kanas and A. Samotus, J. Chem. Soc. Dalton Trans., (1990) 707.
38 B. Kamenar, B. Korpar-Colig and M. Penavić, J. Chem. Soc. Dalton Trans., (1981) 311.
39 S. Chunting, G. Chunxiao, J. Yan, L. Tiejin, Y. Ling and F. Yuguo, Eur. J. Solid State Inorg. Chem., 26 (1989) 231.
40 P. Gouzerh and Y. Jeannin, personal communication, 1989.
41 S.N. Shaikh and J. Zubieta, Inorg. Chim. Acta, 121 (1986) 243.
42 V.W. Day, M.R. Thompson, C.S. Day, W.G. Klemperer and R.-S. Liu, J. Am. Chem. Soc., 102 (1980) 5973.
43 Q. Chen, S. Liu, H. Zhu and J. Zubieta, Polyhedron, 8 (1989) 2915.
44 Q. Chen, S. Liu and J. Zubieta, Inorg. Chim. Acta, 164 (1989) 115.
45 E. Carmona, F. Gonzalez, M.L. Povede, J.L. Atwood and R.D. Rogers, J. Am. Chem. Soc., 105 (1983) 3365.
46 S. Liu, X. Sun and J. Zubieta, J. Am. Chem. Soc., 110 (1988) 3324.
47 S. Lincoln and S.A. Koch, Inorg. Chem., 25 (1986) 1594.
48 P. Gouzerh, Y. Jeannin, A. Proust and F. Robert, Angew. Chem. Int. Ed. Engl., 28 (1989) 1364.
49 T.-C. Hsieh and J.A. Zubieta, Polyhedron, 5 (1986) 1655.
50 H. Kang and J. Zubieta, J. Chem. Soc. Chem. Commun., (1988) 1192.
51 M.H. Chisholm, K. Folting, J.C. Huffman and C.C. Kirkpatrick, Inorg. Chem., 23 (1984) 1021.

52 B. Kamenar, M. Penanvić and B. Marković, Acta Crystallogr. Sect. C, 44 (1988) 1521.
53 B. Kamenar, B. Korpar-Colig, M. Penavić and M. Cindrić, J. Chem. Soc. Dalton Trans., (1990) 1125.
54 L. Ma, S. Liu and J. Zubieta, J. Chem. Soc. Chem. Commun., (1989) 440.
55 T.-C. Hsieh and J. Zubieta, J. Chem. Soc. Chem. Commun., (1985) 1749.
56 T.-C. Hsieh, S.N. Shaikh and J. Zubieta, Inorg. Chem., 26 (1987) 4079.
57 S. Liu and J. Zubieta, Polylhedron, 8 (1989) 537.
58 M. Yu Antipin, L.P. Didenko, L.M. Kachapina, A.E. Shilov, A.K. Shilova and Y.T. Struchou, J. Chem. Soc. Chem. Commun., (1989) 1467.
59 S. Liu, X. Sun and J. Zubieta, unpublished results, 1990.
X. Sun, Masters Dissertation, State University of New York at Albany, Albany, 1988.
60 Q. Chen, S. Liu and J. Zubieta, Angew. Chem. Int. Ed. Engl., 27 (1988) 1724.
61 O.J. Darensbourg, R.L. Gray and T. Delord, Inorg. Chim. Acta, 98 (1985) 239.
62 Q. Chen, S. Liu and J. Zubieta, Angew. Chem. Int. Ed. Engl., 29 (1990) 70.
63 V.L. Pecoraro, Inorg. Chim. Acta, 155 (1989) 171.
64 F.A. Cotton, G.E. Lewis and G.N. Mott, Inorg. Chem., 21 (1982) 3127.
65 D.D. Heinrich, K. Folting, W.E. Streib, J.C. Huffmann and G. Christou, J. Chem. Soc. Chem. Commun., (1989) 1411.
66 H. Reiskamp, P. Gietz and R. Mattes, Chem. Ber., 109 (1976) 2090.
67 D. Rehder, W. Priebsch and M. von Oeynhausen, Angew. Chem. Int. Ed. Engl., 28 (1989) 1221.
68 Q. Chen and J. Zubieta, Inorg. Chem., 29 (1990) 1456.
69 Q. Chen, D.P. Goshorn, X.-L. Tan and J. Zubieta, J. Am. Chem. Soc., in press .
70 G.K. Johnson and E.O. Schlemper, J. Am. Chem. Soc., 100 (1978) 3645.
71 J.-P. Launay, Y. Jeannin and M. Daoudi, Inorg. Chem., 24 (1985) 1052.
72 V.W. Day, W.G. Klemperer and O.M. Yaghi, J. Am. Chem. Soc., 111 (1989) 5959.
73 A. Müller, M. Penk, R. Rohlbing, E. Krickemeyer and J. Döring, Angew. Chem. Int. Ed. Engl., 29 (1990) 926.
74 M.T. Pope and A. Miller, Angew. Chem. Int. Ed. Engl., 30 (1991) 34.
75 W.N. Lipscomb, Inorg. Chem., 4 (1965) 132.
76 Q. Chen, S. Liu and J. Zubieta, Inorg. Chim. Acta, 162 (1989) 163.
77 Q. Chen, S. Liu and J. Zubieta, Inorg. Chim. Acta, 162 (1989) 163.
78 A. Goiffen and B. Spinner, Rev. Chim. Miner., 12 (1975) 316.
79 D.L. Kepert, Inorg. Chem., 8 (1969) 1556.
80 Y. Du, A.L. Rheingold and E.A. Maatta, J. Am. Chem. Soc., 114 (1992) 345.
81 H. Vivier, J. Bernard and H. Djomaa, Rev. Chim. Miner., 14 (1977) 584.
82 H.T. Evans, Jr., J. Am. Chem. Soc., 90 (1968) 3275.
83 A. Hüllen, Angew. Chem., 76 (1964) 588.
84 A. Bino, F.A. Cotton and Z. Dori, J. Am. Chem. Soc., 100 (1978) 5252.
85 A. Bino, F.A. Cotton and Z. Dori, J. Am. Chem. Soc., 103 (1981) 243.
86 R.J. Butcher and B.R. Penfold, J. Cryst. Mol. Struct., 6 (1976) 13.
87 F.A. Cotton and R.C. Elder, Inorg. Chem., 3 (1964) 397.
88 J.J. Park, M.D. Glick and J.L. Hoard, J. Am. Chem. Soc., 91 (1969) 301.
89 W. Hermann and K. Wieghardt, Polyhedron, 5 (1986) 513.
90 V.W. Day, M.F. Fredrich, W.G. Klemperer and W. Shum, J. Am. Chem. Soc., 99 (1977) 6146.
91 J.L. Garin and J.A. Costamanga, Acta Crystallogr. Sect. C, 44 (1988) 799.
P.K. Bharadwaj, Y. Ohashi, Y. Sasada, Y. Sasaki and T. Yamase, Acta Crystallogr. Sect. C, 42 (1986) 545.

92 M. Seleborg, Acta Chem. Scand., 20 (1966) 2195.
93 S.A. Magarill and R.F. Klesetsova, Sov. Phys. Crystallogr., 16 (1972) 645.
94 M.H. Chisholm, Polyhedron, 2 (1983) 681.
95 M.H. Chisholm, Transition Met. Chem., 3 (1978) 321.
96 K.M. Barkigia, L.M. Rajkovic-Blazer, M.T. Pope and C.O. Quicksall, J. Am. Chem. Soc., 97 (1975) 4146.
97 K.M. Barkigia, L.M. Rajkovic-Blazer, M.T. Pope, E. Prince and C.O. Quichsall, Inorg. Chem., 19 (1980) 2531.
98 K.Y. Matsumoto, Bull. Chem. Soc. Jpn., 52 (1979) 3284.
99 S. Liu, S.N. Shaikh and J. Zubieta, Inorg. Chem., 27 (1988) 3064.
100 K. Gebreyes, S.N. Shaikh and J. Zubieta, Acta Crystallogr. Sect. C, 41 (1985) 871.
101 R. Stomberg, L. Trysberg and I. Larking, Acta Chem. Scand., 24 (1970) 2678.
102 I.W. Boyd, I.G. Dance, A.E. Landers and A.G. Wedd, Inorg. Chem., 18 (1979) 1875.
103 M. Cowie, B.L. Haymore and J.A. Ibers, Inorg. Chem., 14 (1975) 2617.
104 B.L. Haymore and J.A. Ibers, Inorg. Chem., 18 (1979) 2423.
105 A.P. Gaughan, R.L. Haymore, J.A. Ibens, W.H. Myers, T.E. Nappier and D.W. Meek, J. Am. Chem. Soc., 95 (1973) 6859.
106 P.L. Dahlstrom, S. Kumar, P.A. Vella and J. Zubieta, Inorg. Chem., 21 (1982) 908.
107 J.R. Dilworth, in G. Wilkinson, R.D. Gillard and J.A. McCleverty (Eds.), Comprehensive Coordination Chemistry, Pergamon Press, Oxford, 1987.
108 J.R. Dilworth, Coord. Chem. Rev., 21 (1976) 29.
109 M.W. Bishop, J. Chatt, J.R. Dilworth, M.R. Hursthouse and M. Motevalli, J. Chem. Soc. Dalton Trans., (1979) 1600.
110 B.J. Burt, J.R. Dilworth, G.J. Leigh and J.A. Zubieta, J. Chem. Soc. Dalton Trans., (1982) 2295.
111 J.R. Dilworth, J. Hutchinson, L. Throop and J. Zubieta, Inorg. Chim. Acta, 79 (1983) 208.
112 J. Chatt, B.A.L. Crichton, J.R. Dilworth, P. Dahlstrom, R. Gutkoska and J. Zubieta, Inorg. Chem., 21 (1982) 2383.
113 B.A.L. Crichton, J.R. Dilworth, P. Dahlstrom and J. Zubieta, Transition Met. Chem. (Weinheim, Ger.), 5 (1980) 316.
114 S.N. Shaikh and J. Zubieta, Inorg. Chem., 27 (1988) 1896.
115 O. Nagano and Y. Sasaki, Acta Crystallogr. Sect. B, 35 (1979) 2387.
116 H.R. Allcock, E.C. Brissell and E.T. Shaw, Inorg. Chem., 12 (1973) 2963.
117 C.D. Garner, N.C. Howlander, F.E. Mabbs, A.T. McPhail, R.W. Miller and K.D. Onan, J. Chem. Soc. Dalton Trans., (1978) 1582.
118 P. Dahlstrom, J. Zubieta, B. Neaves and J.R. Dilworth, Cryst. Struct. Commun., 11 (1982) 463.
119 T.M. Che, V.W. Day, L.C. Francesconi, M.F. Frederich, W.G. Klemperer and W. Shum, Inorg. Chem., 24 (1985) 4055.
120 I. Lindquist, Ark. Kemi, 2 (1950) 349.
121 L.O. Atovmyan and O.N. Kresochka, J. Struct. Chem. (USSR), 13 (1972) 319.
122 M. Isobe, F. Marumo, T. Yamase and T. Ikawa, Acta Crystallogr. Sect. B, 34 (1978) 2728.
123 M.B. Robin and P. Day, Adv. Inorg. Chem. Radiochem., 10 (1967) 247.
124 B. Spivack and Z. Dori, Coord. Chem. Rev., 17 (1975) 99.
125 E. Stiefel, Prog. Inorg. Chem., 22 (1977) 1.
126 J. Fuchs and H. Hartl, Angew. Chem. Int. Ed. Engl., 15 (1976) 375.
127 W.G. Klemperer and W. Shum, J. Am. Chem. Soc., 98 (1976) 8291.
128 K. Matsumoto, A. Kobayashi and Y. Sasaki, Bull. Chem. Soc. Jpn., 48 (1975) 1009.
129 T.-C. Hsieh, T. Nicholson and J. Zubieta, Inorg. Chem., 27 (1988) 241.

130 I. Buchanan, W. Clegg, C.D. Garner and G.M. Sheldrick, Inorg. Chem., 22 (1983) 3657.

131 A. Proust, P. Gouzerh, F. Robert, Y. Jeannin, Q. Chen and J. Zubieta, 4^e Congrès de la Société Française de Chimie, Strasbourg, 17–20 September 1991, AF. 304, pp. 136–137.

132 J. Fuchs, H. Harth, W. Schiller and U. Gerlach, Acta Crystallogr. Sect. B, 32 (1975) 740.

133 V.W. Day, W.G. Klemperer and O.M. Yaghi, J. Am. Chem. Soc., 111 (1989) 4519.

134 V.W. Day, W.G. Klemperer and D.J. Maltbie, J. Am. Chem. Soc., 109 (1987) 2991.

135 K.F. Jahr, J. Fuchs and R. Oberhausen, Chem. Ber., 101 (1968) 482.

136 J. Fuchs, S. Mahjour and R. Palm, Z. Naturforsch. Teil B, 31 (1976) 544.

137 F.A. Cotton, G.E. Lewis and G.N. Mott, Inorg. Chem., 21 (1982) 3316.

138 F.A. Cotton and W. Wang, Inorg. Chem., 21 (1982) 2675.

139 F.A. Cotton, M.W. Extine, L.R. Falvello, D.B. Lewis, G.E. Lewis, C.A. Murillo, W. Schwotzer, M. Tomas and J.M. Troup, Inorg. Chem., 25 (1986) 3505.

140 L. Pettersson, B. Hedman, I. Andersson and N. Ingri, Chem. Scr., 22 (1983) 254.

141 H. Chae, W.G. Klemperer and V.W. Day, Inorg. Chem., 28 (1989) 1423.

142 Y. Hayashi, Y. Ozawa and K. Isobe, Chem. Lett., (1989) 425.

143 Q. Chen, S. Liu and J. Zubieta, Inorg. Chem., 28 (1989) 4433.

144 M.I. Khan, Q. Chen, D.P. Goshorn, H. Hope, S. Parkin and J. Zubieta, J. Am. Chem. Soc., in press.

145 R. Kato, A. Kobayashi and Y. Sasaki, Inorg. Chem., 21 (1982) 240.

146 A. Müller and J. Doring, Angew. Chem. Int. Ed. Engl., 27 (1988) 1721.

147 A. Bino, S. Cohen and C. Heitner-Wirguin, Inorg. Chem., 21 (1982) 429.

148 S.M. Baxter and P.T. Wolczanski, Inorg. Chem., 28 (1989) 3263.

149 A. Müller, E. Krickemeyer, M. Penk, H.-J. Walberg and H. Bögge, Angew. Chem. Int. Ed. Engl., 26 (1987) 1045.

150 G.K. Johnson, Ph.D. Thesis, University of Missouri-Columbia, 1977; Diss Abstr. B, 38 (1978) 4801.

151 M.M. Mossoba, C.J. O'Connor, M.T. Pope, E. Sinn, G. Hervé and A. Tézé, J. Am. Chem. Soc., 102 (1980) 6864.

152 T.M. Che, V.W. Day, L.C. Francesconi, M.F. Fredrick, W.G. Klemperer and W. Shum, Inorg. Chem., 24 (1985) 4055.

153 C.J. Besecker, V.W. Day, W.G. Klemperer and M.R. Thompson, Inorg. Chem., 24 (1985) 44.

154 W.G. Klemperer and D.J. Main, Inorg. Chem., 29 (1990) 2355 and references cited therein.

155 Y. Do, E.D. Simhon and R.H. Hahn, Inorg. Chem., 24 (1985) 2827.

156 N. Buckholz and R. Mattes, Angew. Chem. Int. Ed. Engl., 25 (1986) 1104.

157 M. Filowitz, R.K.C. Ho, W.G. Klemperer and W. Shum, Inorg. Chem., 18 (1979) 93 and references cited therein.

158 V. Chilou, P. Gouzerh, T.-C. Hsieh, Y. Jeannin, G. Olivares, F. Robert and J. Zubieta, Polyhedron, 8 (1989) 29.

159 D. Carillo, P. Gouzerh and Y. Jeannin, Nouv. J. Chim., 9 (1985) 749.

160 T.-C. Hsieh and J. Zubieta, Inorg. Chim. Acta, 127 (1987) 231.

161 D.C. Kepert, Inorg. Chem., 8 (1969) 1556.

162 K.H. Tytko and O. Glemser, Adv. Inorg. Chem. Radiochem., 19 (1976) 239.

163 H. Schultheis, Ger. Pats. 1,022,205 (1985); 1,162,849 (1964); Chem. Abstr., 54 (1960) 4390; 60 (1964) 15909.

164 V. McKee and C.J. Wilkins, J. Chem. Soc. Dalton Trans., (1987) 523.

165 R.N. Hilder and C. Wilkins, J. Chem. Soc. Dalton Trans., (1984) 495.

166 C.B. Knobler, B.R. Penfold, W.T. Robinson, C.J. Wilkins and S.M. Yong, J. Chem. Soc. Dalton Trans., (1980) 284.

167 E. Gumaer, K. Lettko, L. Ma, D. Macherone and J. Zubieta, Inorg. Chim. Acta, in press.
168 S. Liu, L. Ma, D. McGowty and J. Zubieta, Polyhedron, 9 (1990) 1541.
169 R. West (Ed.), Oxocarbons, Academic Press, New York, 1980.
170 M.T. Pope, Inorg. Chem., 11 (1972) 1973.
171 C.G. Pierpont and R.M. Buchanan, J. Am. Chem. Soc., 97 (1975) 6450.
172 R.M. Buchanan and C.G. Pierpont, Inorg. Chem., 18 (1979) 1616.
173 C.G. Pierpont and H.M. Downs, J. Am. Chem. Soc., 97 (1975) 2123.
174 M.E. Cass and C.G. Pierpont, Inorg. Chem., 25 (1986) 122.
175 W.P. Griffith, C.A. Pumphrey and T.A. Rainey, J. Chem. Soc. Dalton Trans., (1986) 1125.
176 V.V. Tkachev and L.O. Atovmyan, Sov. J. Coord. Chem., 1 (1975) 715.
177 J.E. Toth, J.D. Melton, D. Cabelli, B.H.J. Bielski and F.C. Anson, Inorg.Chem., 29 (1990) 1952.
178 G.R. Newkome, Z. Yao, G.R. Baker and V.N. Cupta, J. Org. Chem., 50 (1985) 2004.
179 G.R. Newkome, G.R. Baker, M.J. Saunders, P.S. Russo, V.K. Gupta, Z. Yao, J.E. Miller and K. Bouillion, J. Chem. Soc. Chem. Commun., (1986) 752.
180 V.W. Day, W.G. Klemperer and C. Schwartz, J. Am. Chem. Soc., 109 (1987) 6030.
181 V.W. Day, C.W. Earley, W.G. Klemperer and D.J. Maltbie, J. Am. Chem. Soc., 107 (1985) 8261.
182 P. Schreiber, K. Weighardt, B. Nuber and J. Weiss, Polyhedron, 8 (1989) 1675.